X-ray Spectroscopy of O Supergiant Winds: Shock Physics, Clumping, and Mass-Loss Rates

David Cohen
Department of Physics & Astronomy
Swarthmore College

Maurice Leutenegger (GSFC), Véronique Petit, Stan Owocki, & Dylan Kee (Delaware), Jon Sundqvist (Delaware and Munich), Marc Gagné (West Chester), Asif ud-Doula (Penn St. Worthington-Scranton)
Emma Wollman (Caltech, Swarthmore '09), Jake Neely (Swarthmore '13),
Zack Li (Swarthmore '16), Kelley Langhans (Swarthmore '16)

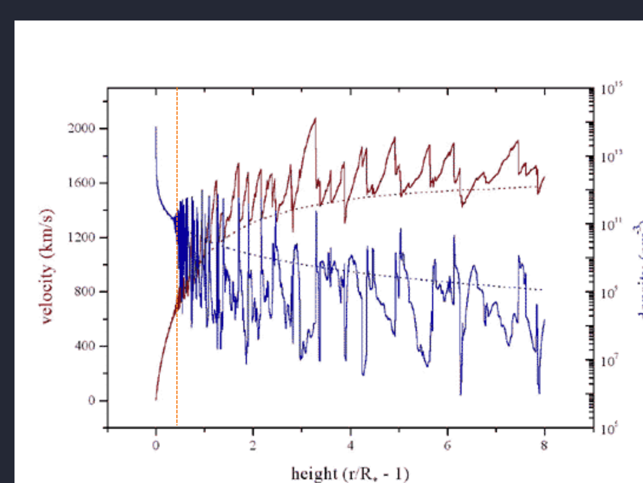

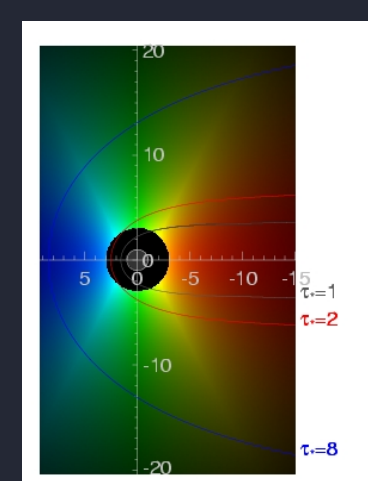

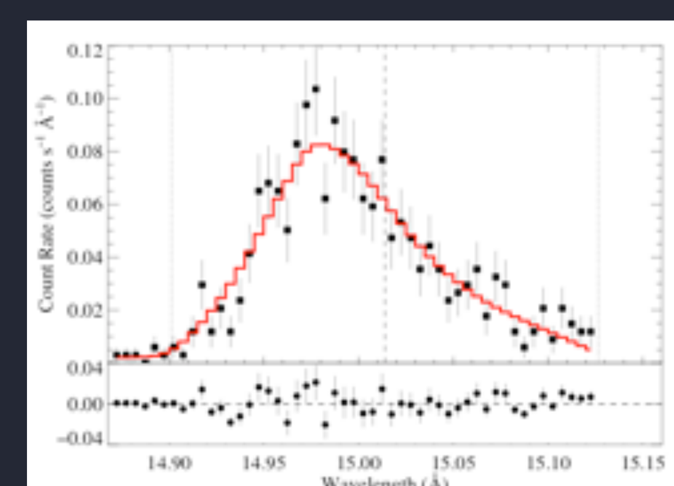

Talk Outline

Context of O star X-ray emission: wind shocks

(focus on effectively single O supergiants)

1. X-ray constraints on the shocked wind plasma
2. X-ray absorption as a mass-loss diagnostic
3. Clumping diagnostics from X-rays + Hα

Radiative vs. Adiabatic shocks

Open questions: very dense winds (WR stars); low density winds (B stars); magnetic OB stars

O stars are strong sources of soft X-ray emission

thermal emission from hot ($T > 10^6$ K) plasma

HD 93129A (O2 If*)

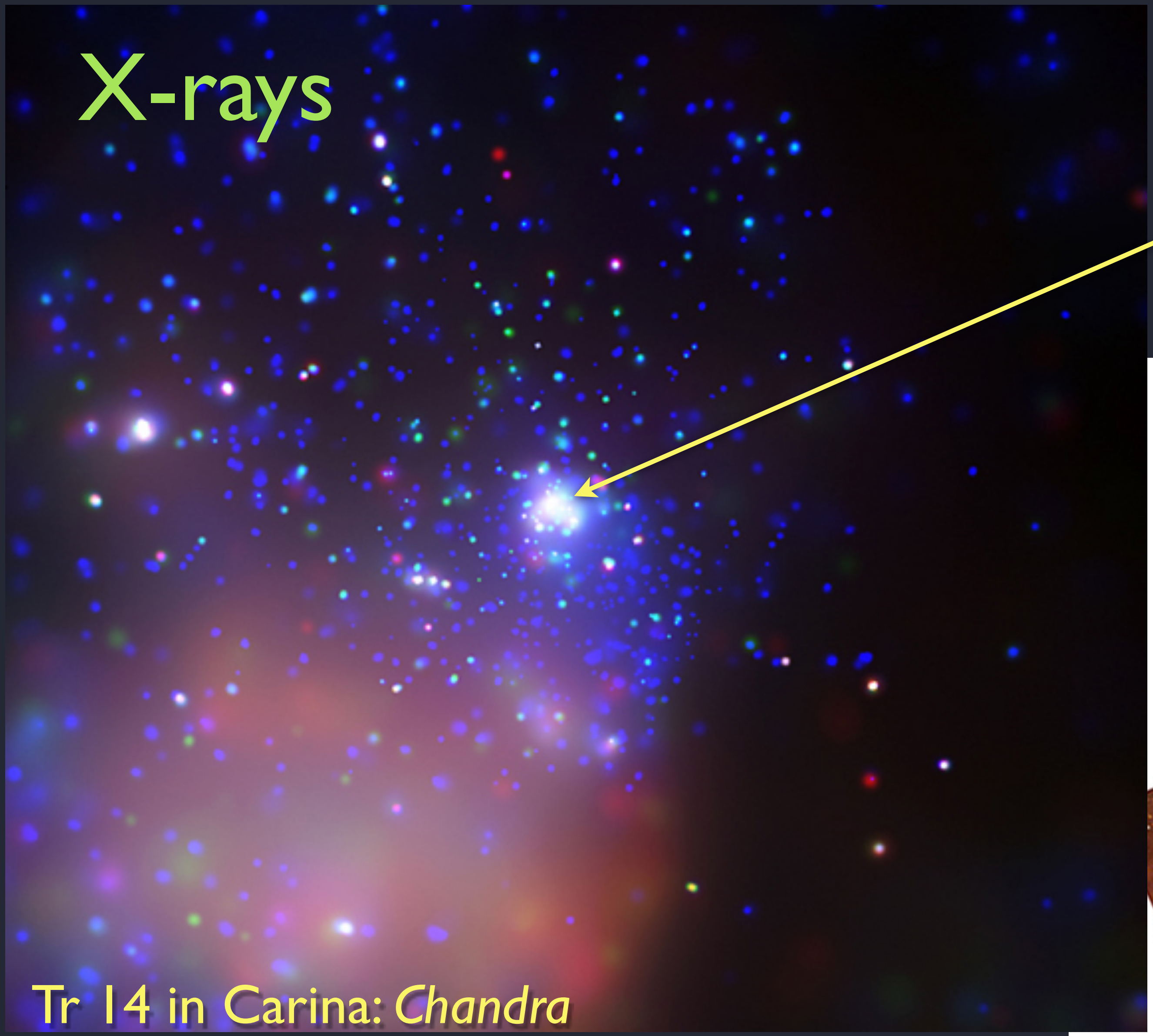

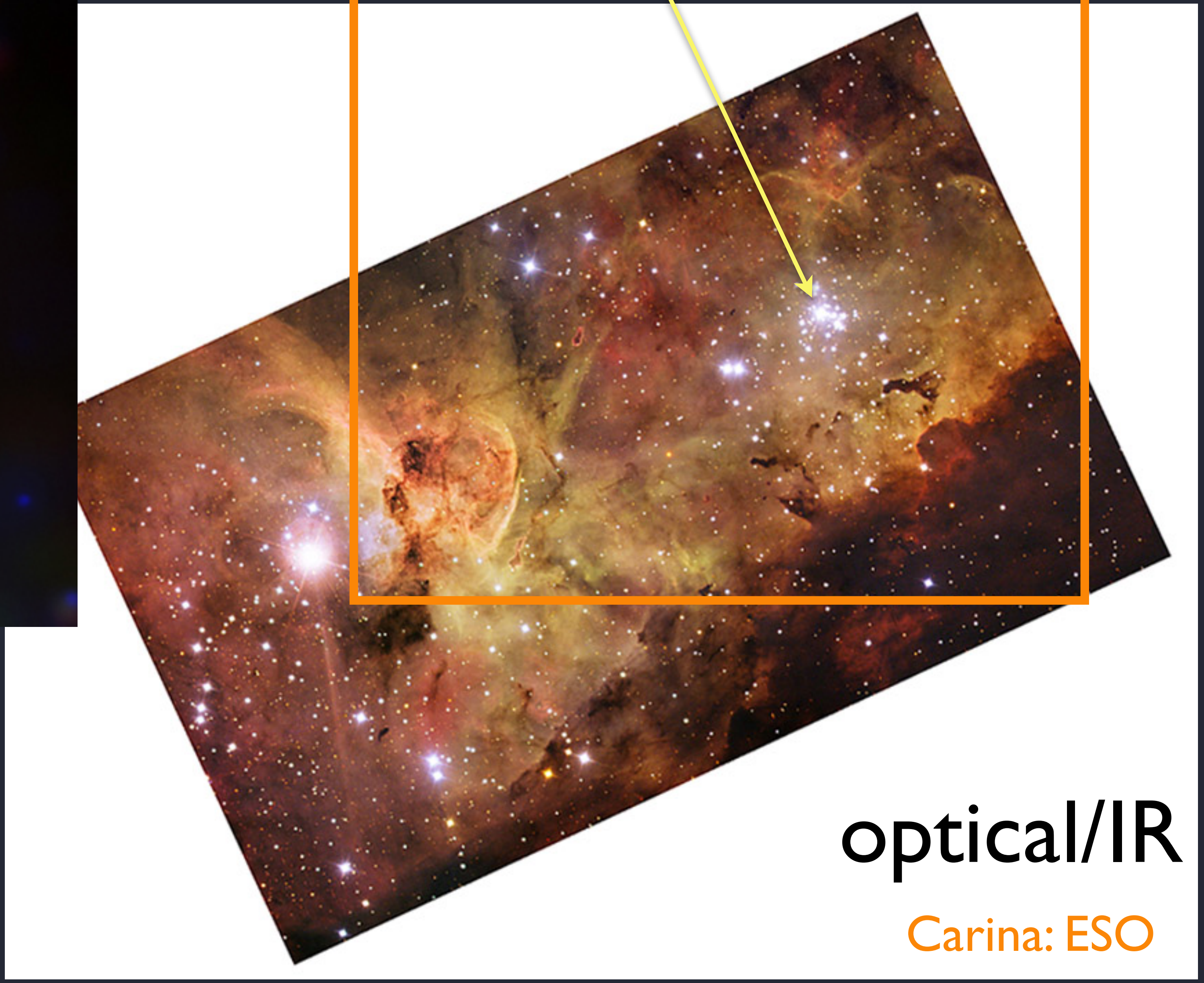

HD 93129A (O2 If) is the brightest X-ray source in this cluster

$L_x \sim 10^{33}$

red < 1 keV, green 1 - 2 keV, blue > 2 keV

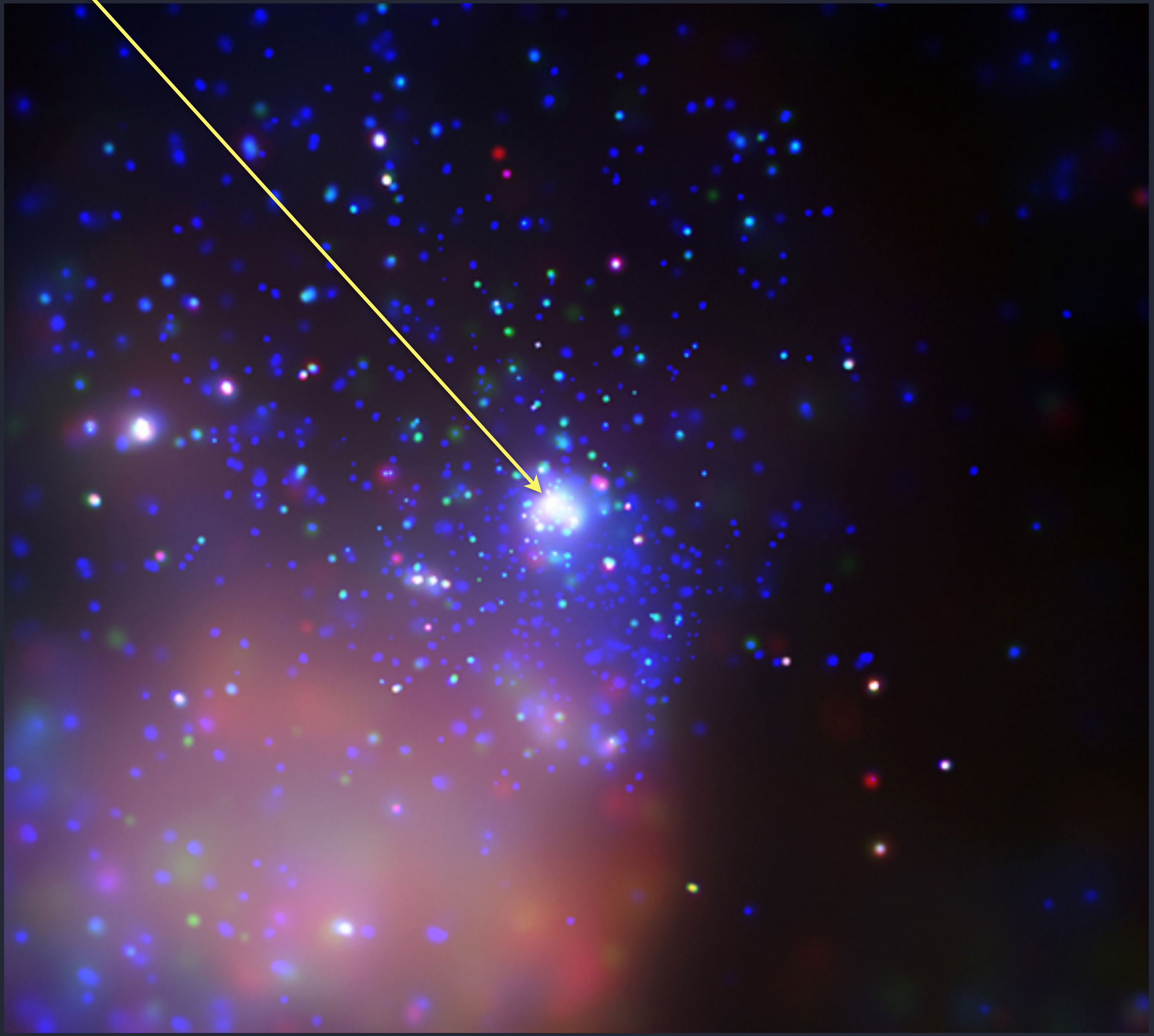

Tr 14 in Carina: *Chandra*

X-ray luminosity is correlated with bolometric luminosity

$L_x \sim 10^{-7} L_{bol}$ but with a lot of scatter

T.W. Berghöfer et al.: X-ray properties of bright OB-type stars detected in the ROSAT all-sky survey 171

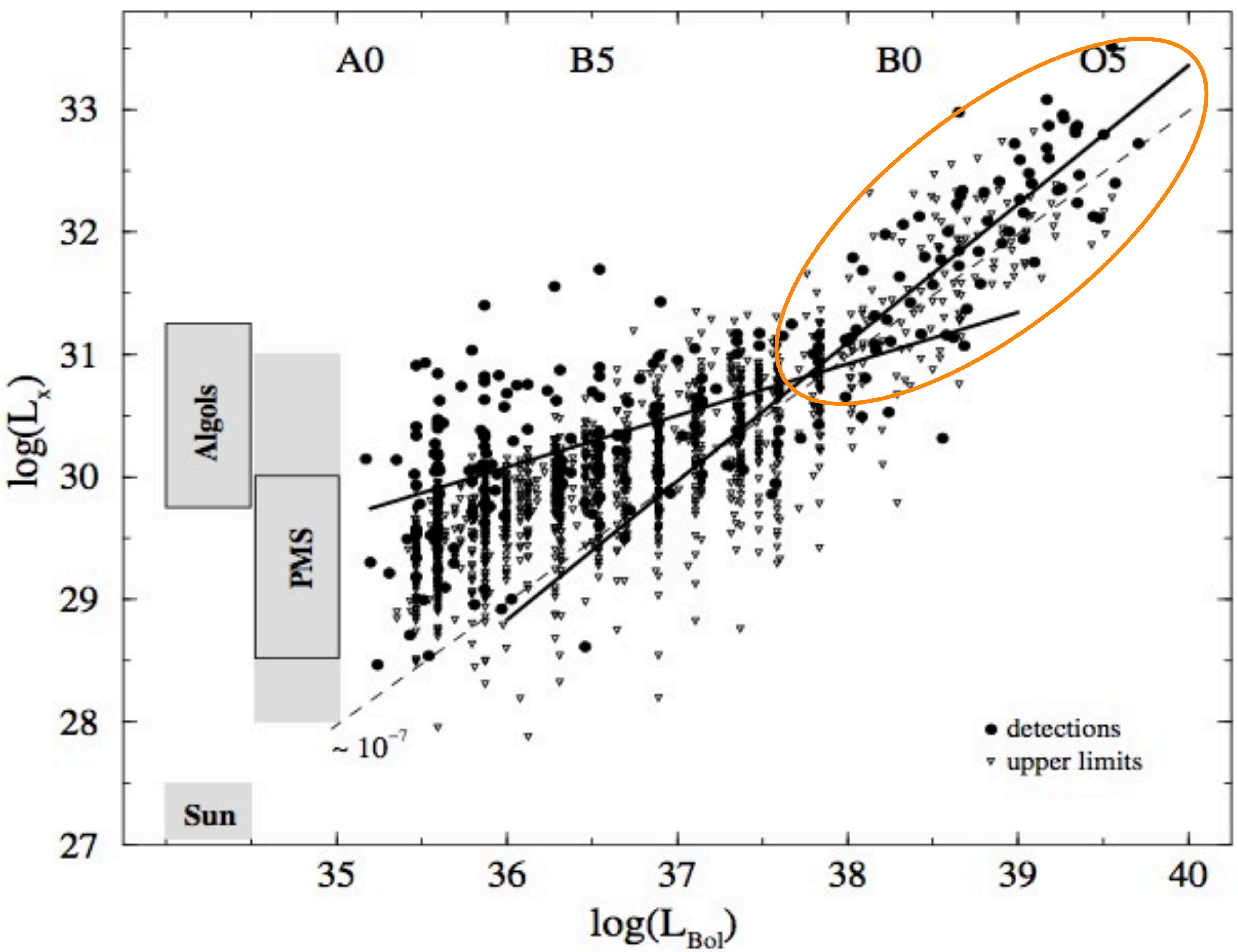

Fig. 4. X-ray luminosities L_x plotted versus bolometric luminosities L_{Bol}; solid lines represent regression lines for $L_{Bol} < 10^{38} erg\, s^{-1}$ and $L_{Bol} > 10^{38}$ erg s^{-1}, whereas the dashed line shows $L_x = 10^{-7} \times L_{Bol}$, grey bars at the left side show typical ranges for the X-ray luminosity of Algol-type systems, pre-main sequence stars (PMS), and our Sun.

Berghöfer et al. 1996

Lx ~ $10^{-7}L_{bol}$ but with a lot of scatter

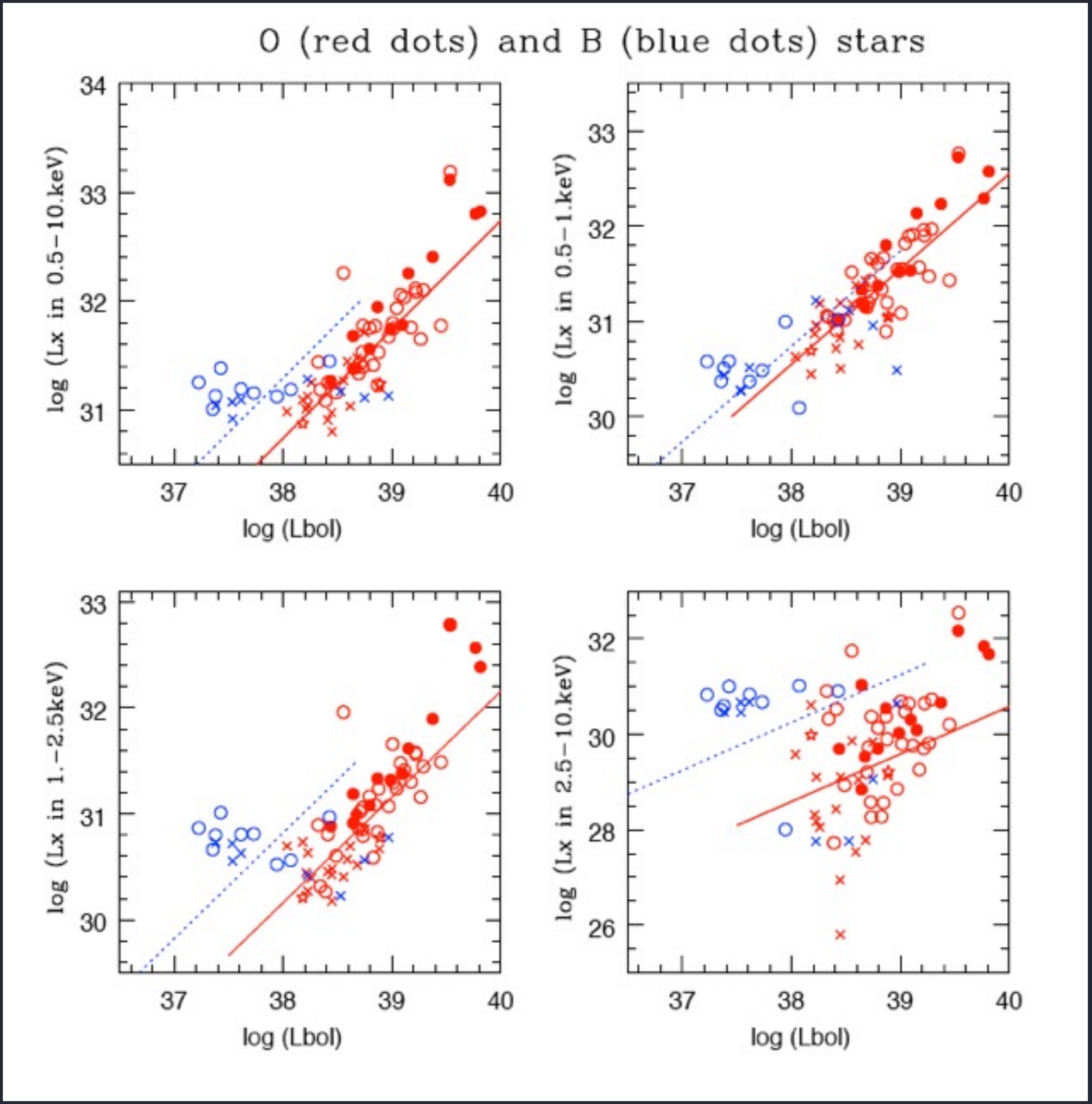

Chandra Carina Complex Project: Nazé et al. 2011

$L_X \sim 10^{-7} L_{bol}$ but with a lot of scatter

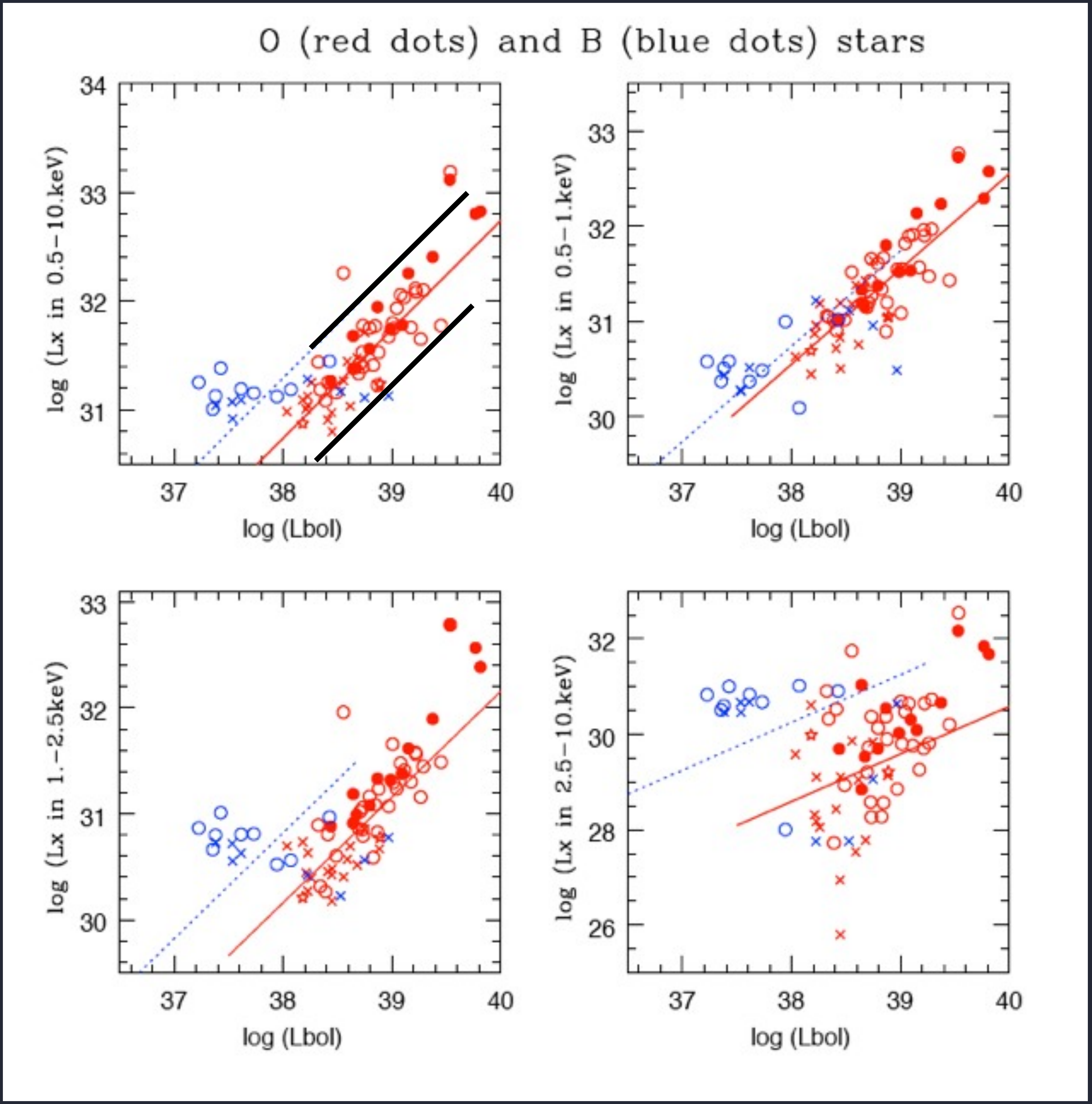

Chandra Carina Complex Project: Nazé et al. 2011

OB star winds are powerful

Hallmark of OB star winds

UV absorption in resonance lines of metal ions (e.g. C+3)

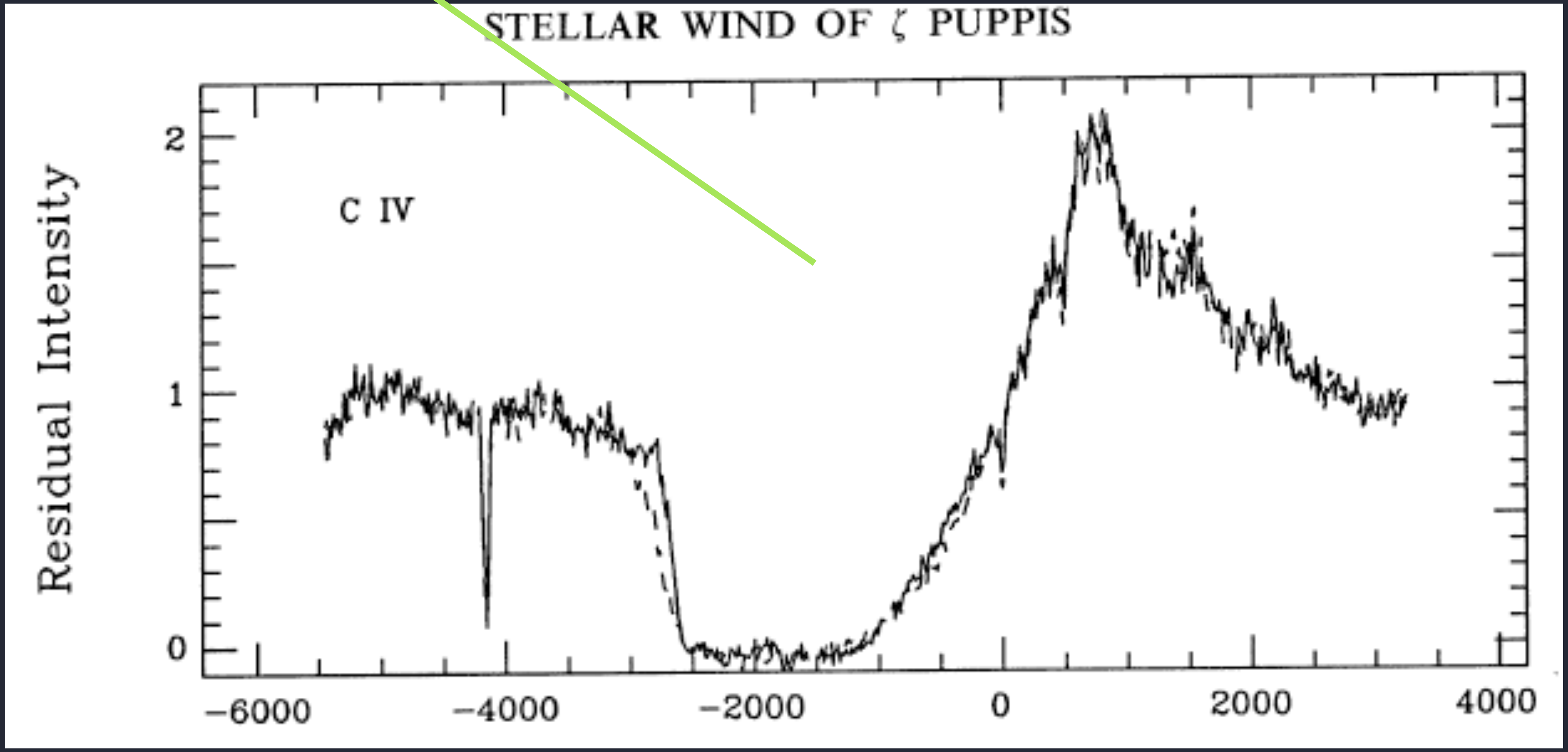

Velocity (km/s)

Prinja et al. 1992, ApJ, 390, 266

Ultraviolet spectrum showing wind feature from C^{+3}

ζ Pup (O4 supergiant): $\dot{M} \sim$ few 10^{-6} M_{sun}/yr

UV spectrum: C IV 1548, 1551 Å

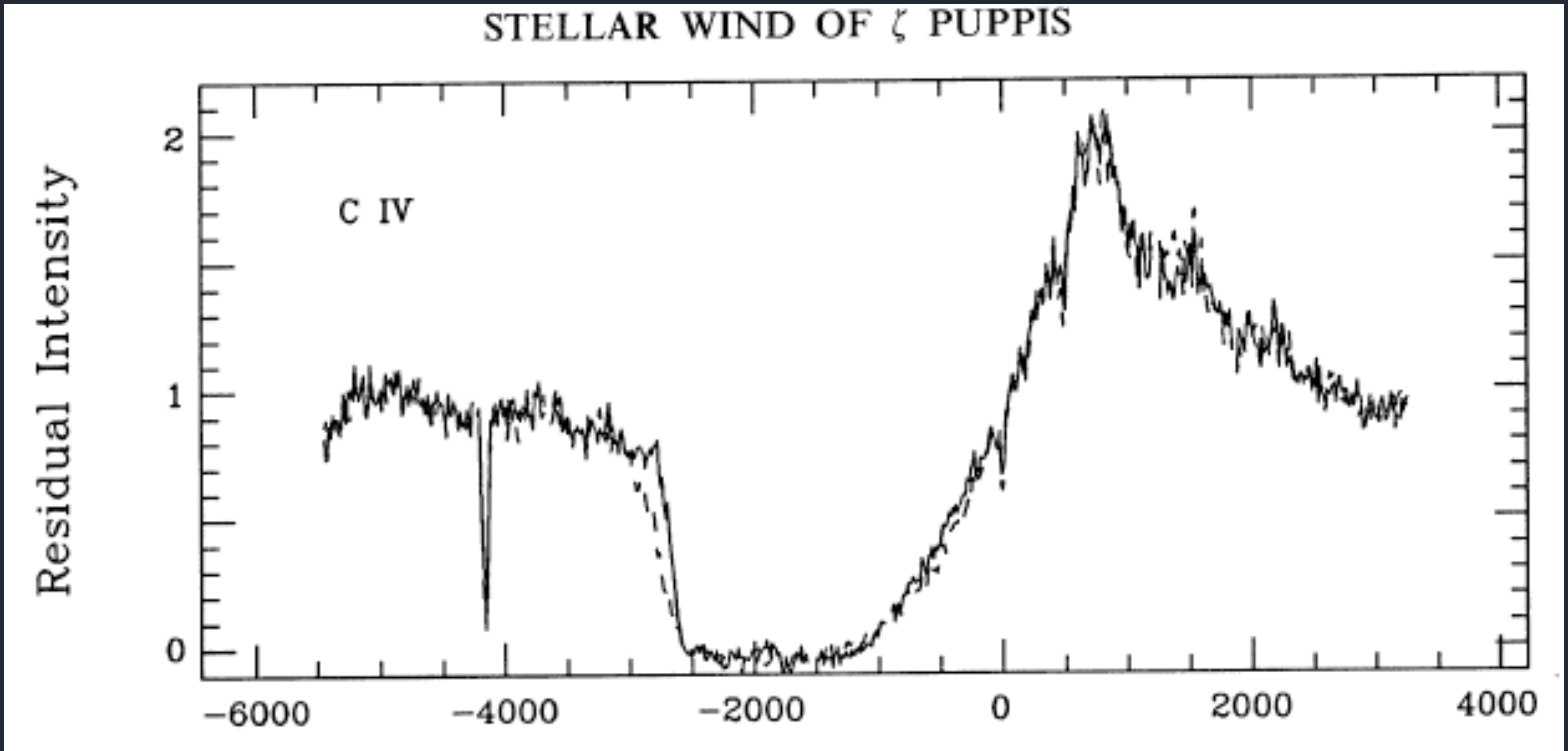

Velocity (km/s)

Prinja et al. 1992, ApJ, 390, 266

X-rays are evidence of power being dissipated in the stellar wind

kinetic power of the wind = $1/2\, \dot{M} v_\infty^2$ ($\sim 10^{-3}\, L_{bol}$)

The wind kinetic power is typically 10^4 times larger than the observed L_x

Some process - which doesn't have to be very efficient - converts a small fraction of this kinetic power to heat.

The observed X-rays are the thermal radiation from this hot stellar wind plasma.

X-rays are evidence of power being dissipated in the stellar wind

Line Deshadowing Instability (LDI), leads to shock-heating of the wind: $T \sim 10^6(\Delta v_{shock}/300\ \mathrm{km/s})^2$

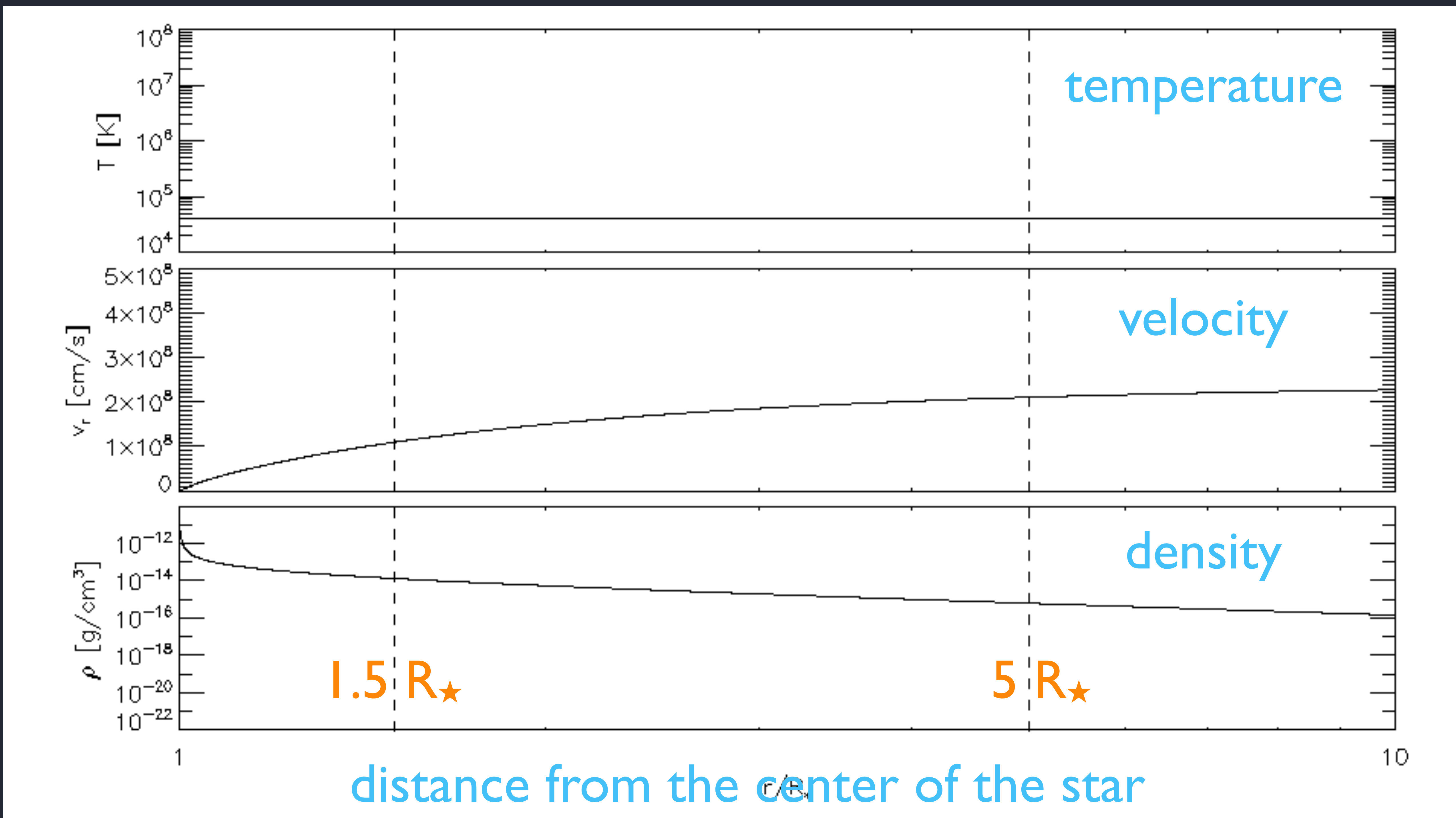

simulation by J. Sundqvist

Less than 1% of the mass of the wind is emitting X-rays

>99% of the wind is cold and X-ray *absorbing*

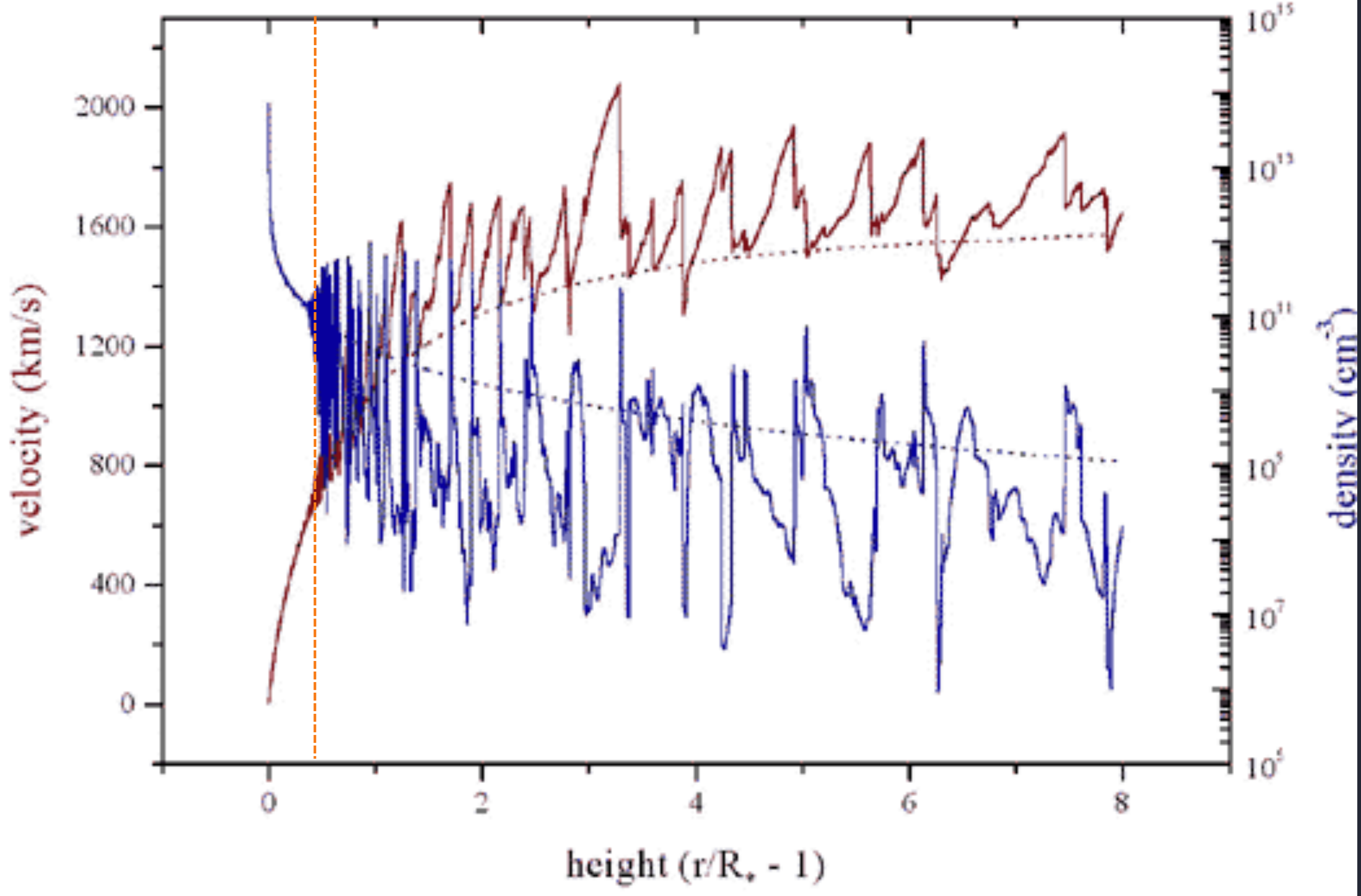

Less than 1% of the mass of the wind is emitting X-rays

>99% of the wind is cold and X-ray *absorbing*

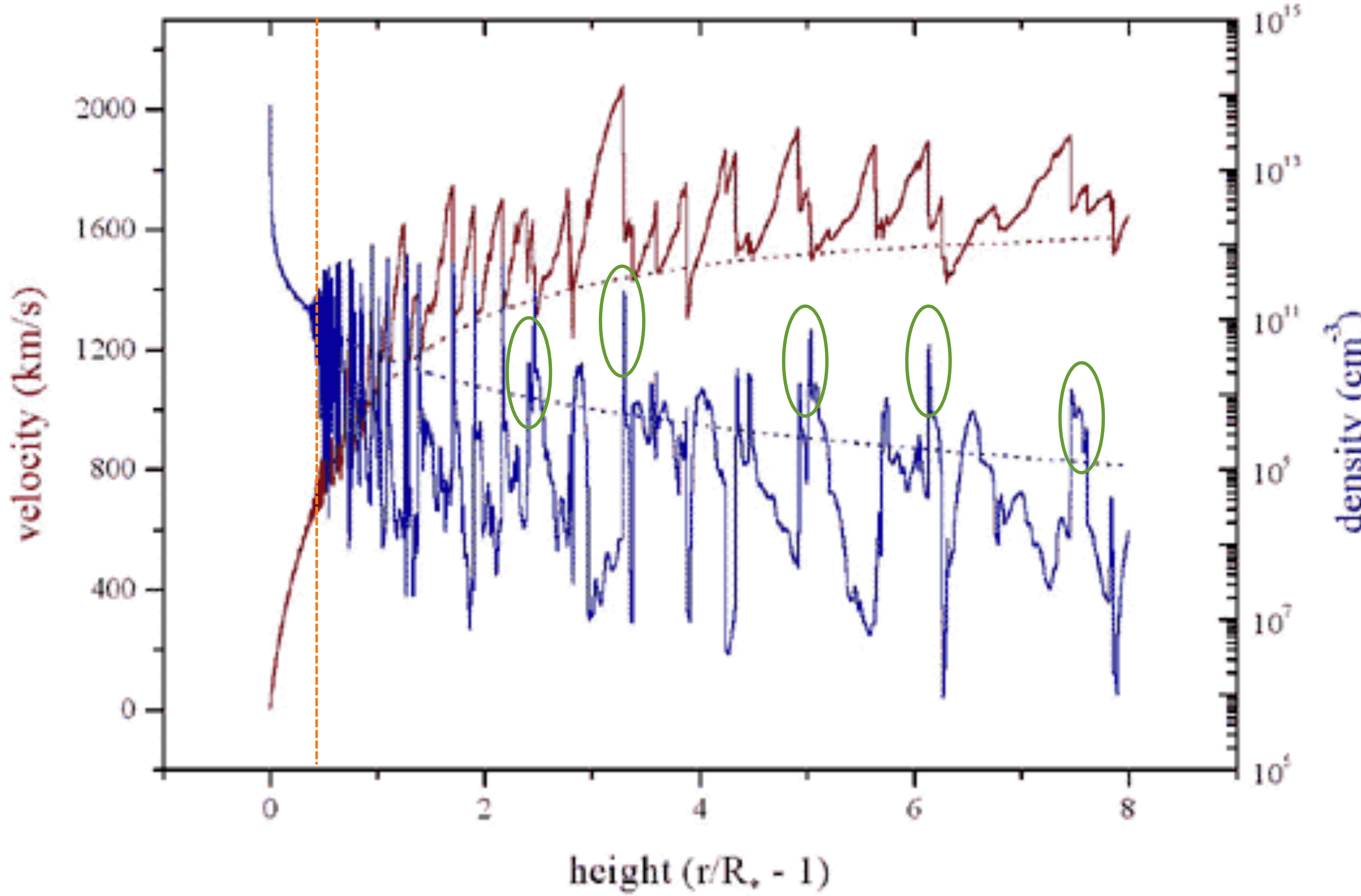

>99% of the wind is cold and X-ray *absorbing*

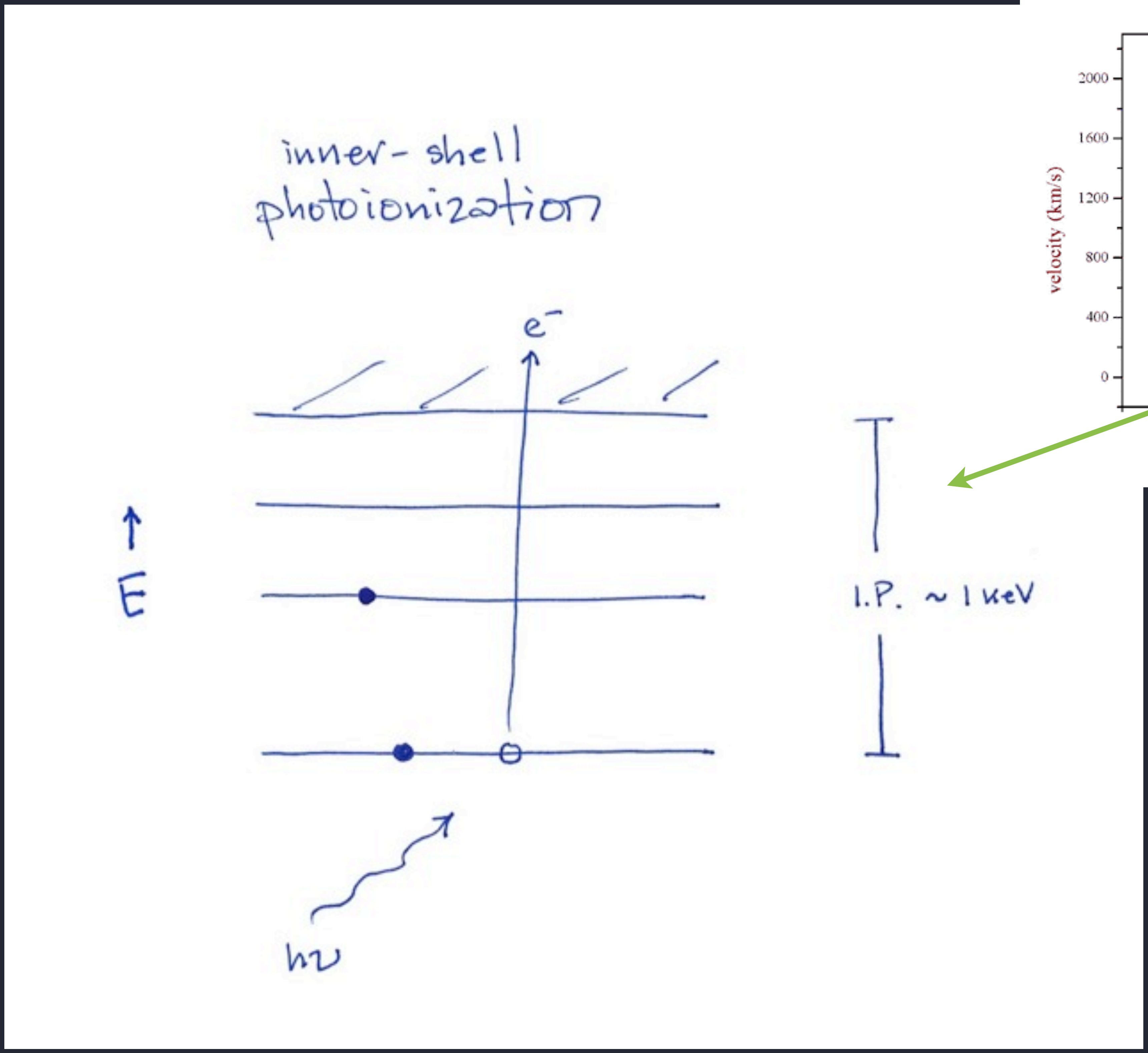

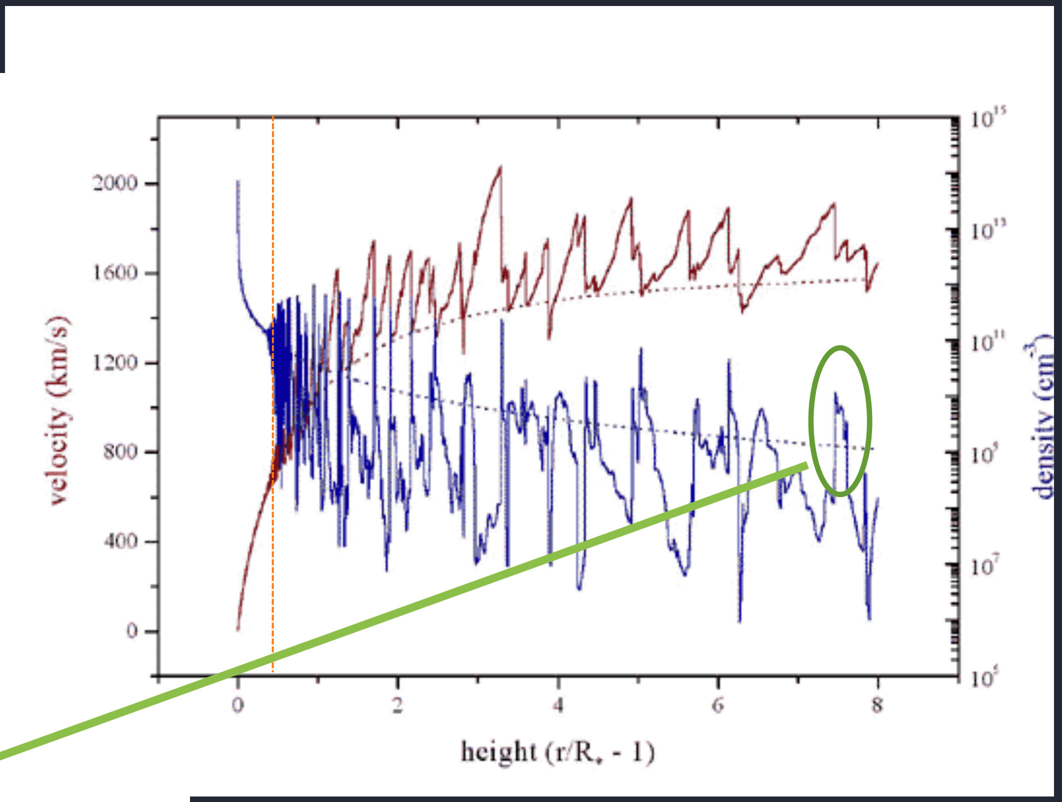

I-D simulations: spherically symmetric

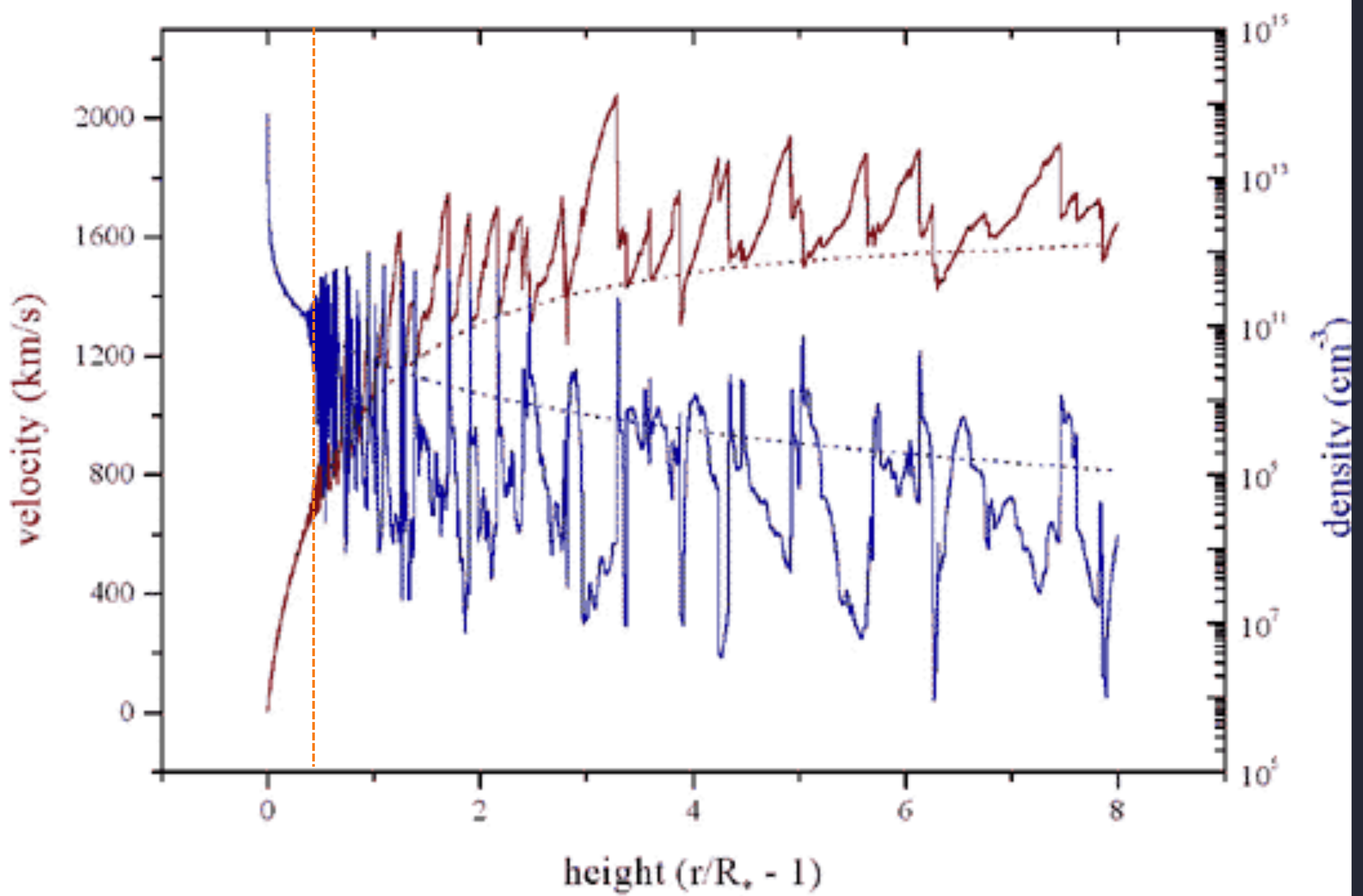

2-D radiation-hydro simulations

clumps break up to the grid scale

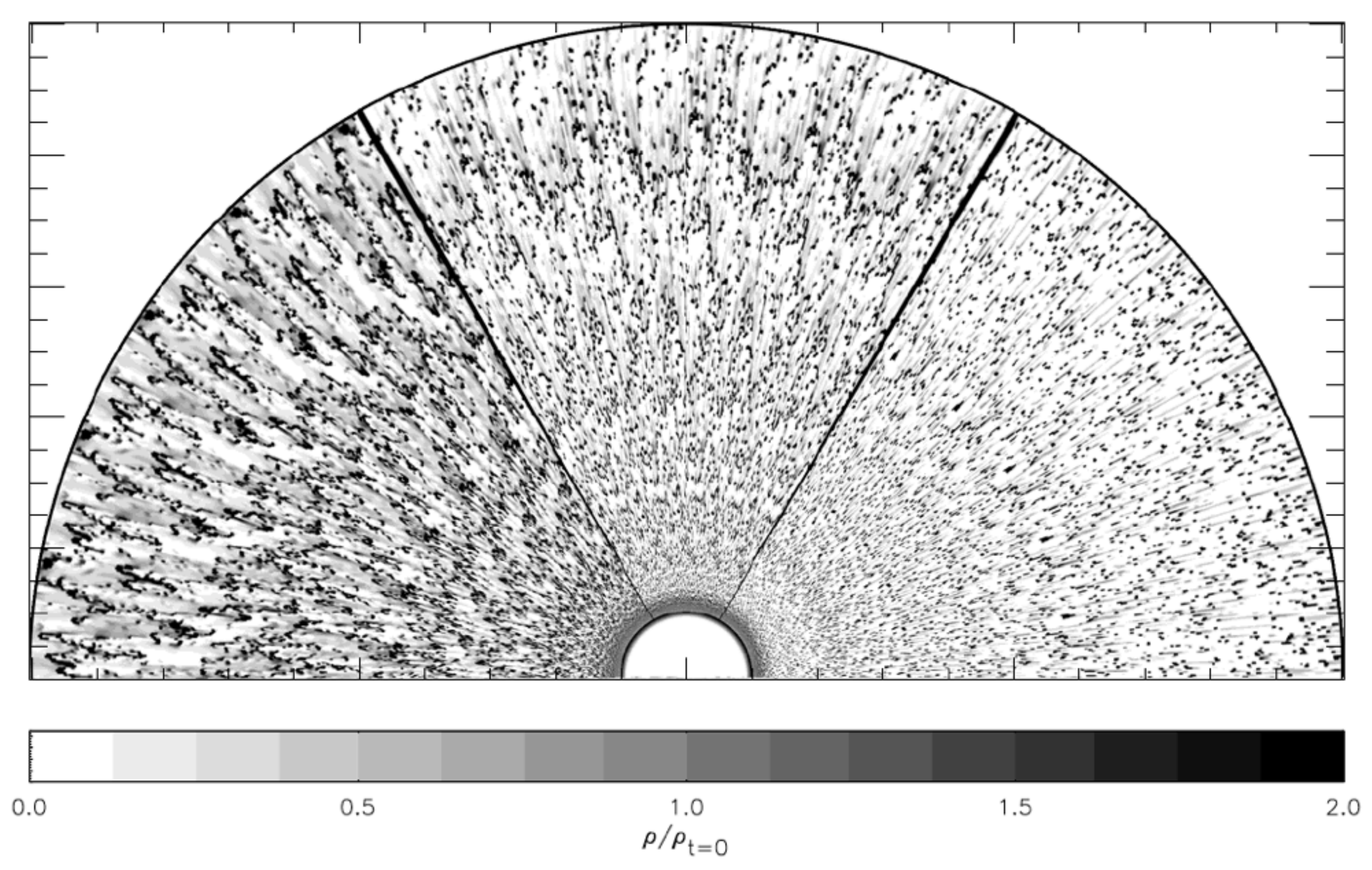

Dessart & Owocki 2003

2-D radiation-hydro simulations

Keep in mind: the bulk of the wind mass is in these dense, cold (~ T_{eff}) clumps. They are the site of most of the UV wind absorption observed from metals and also of the hydrogen recombination that leads to the observed H-alpha emission.

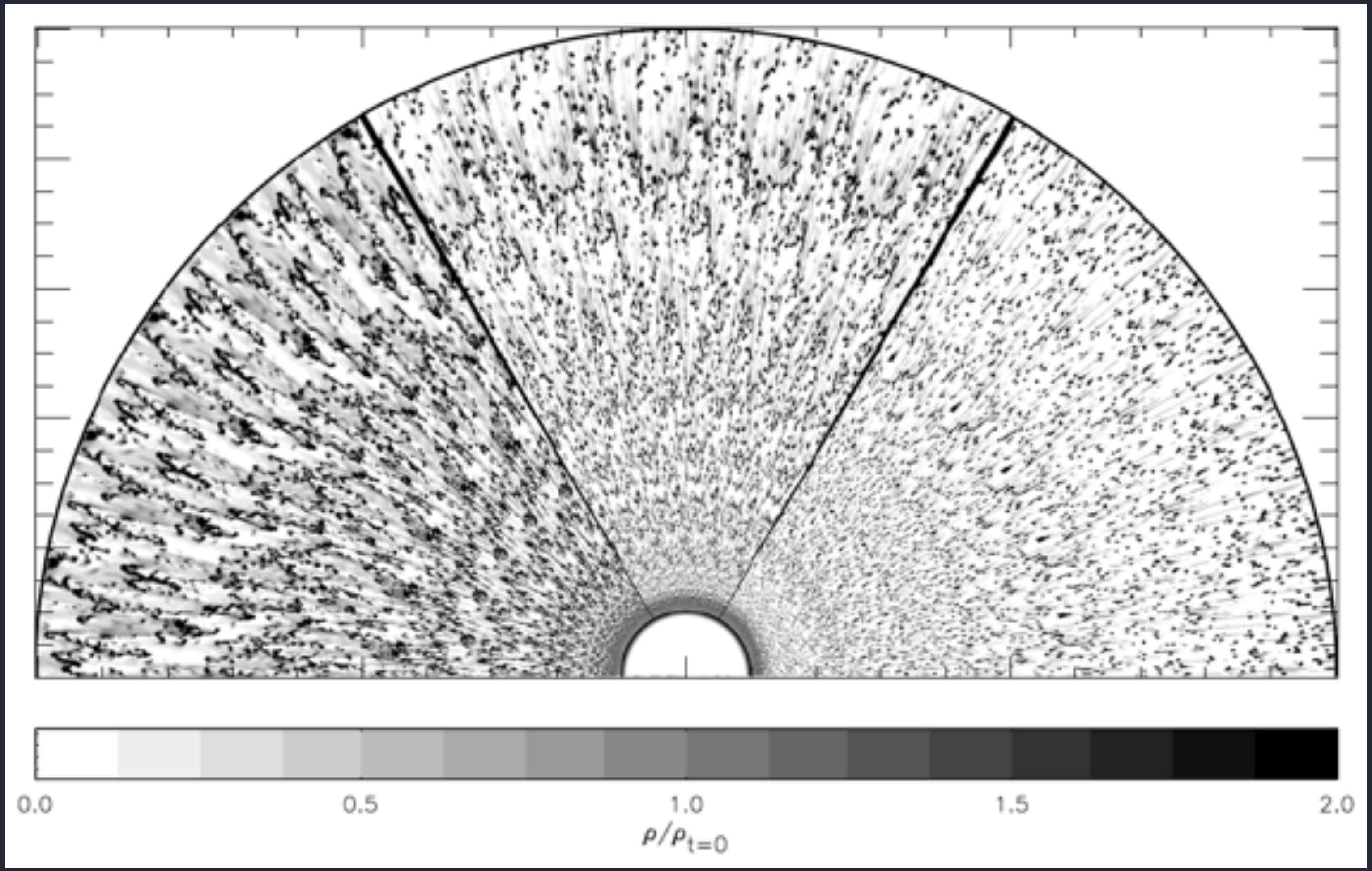

Dessart & Owocki 2003

Thermal properties of the plasma

Heating from shocks *combined with* cooling - which may be primarily adiabatic *or* radiative

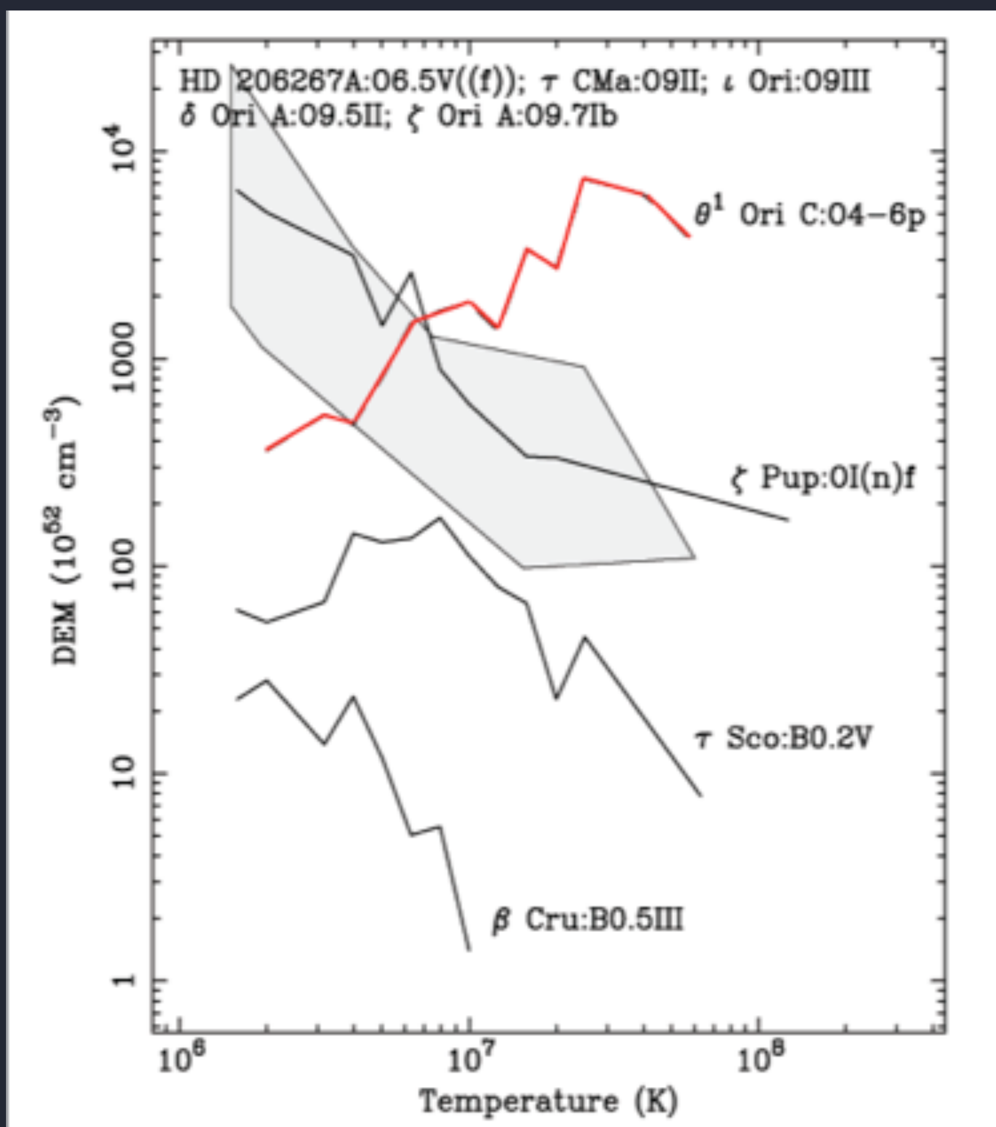

Wojdowski & Schulz 2005

X-ray plasma temperature in O stars is quite low (few million K)

...compared to low-mass stars, for example, or some *magnetic* massive stars

Thermal properties of the plasma

Heating from shocks *combined with* cooling - which may be primarily adiabatic *or* radiative

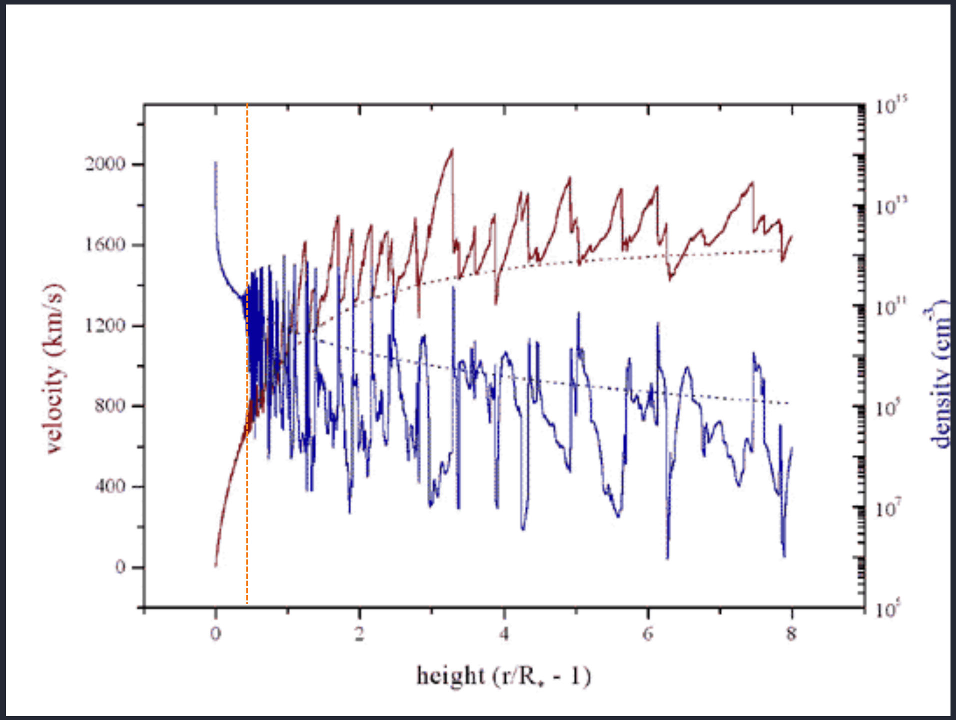

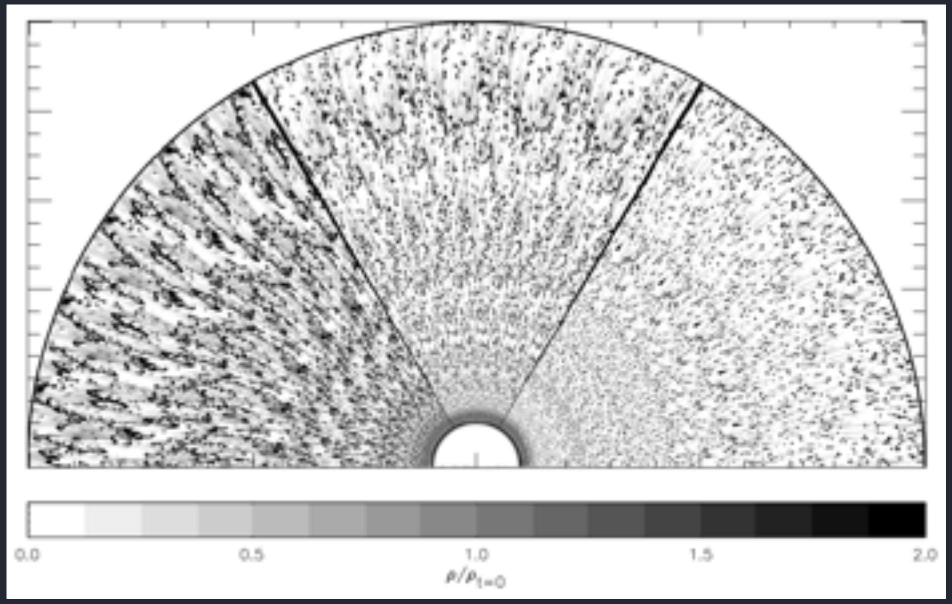

numerical LDI simulations are not yet mature enough to make strong predictions about X-ray temperatures

X-ray emission process

thermal emission from collisional plasma

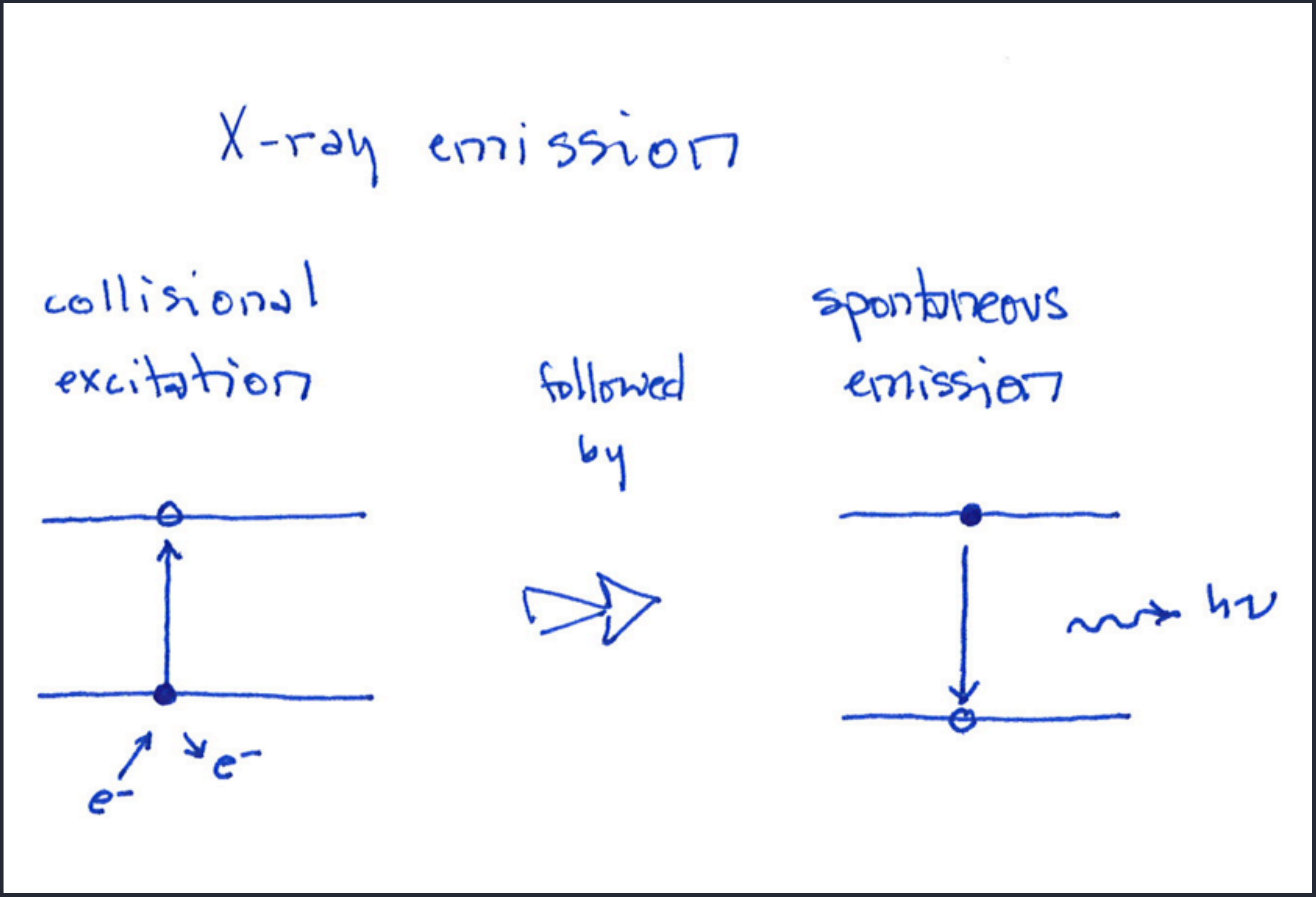

X-ray line emission spectroscopy

Provides important information via Doppler-broadened profiles

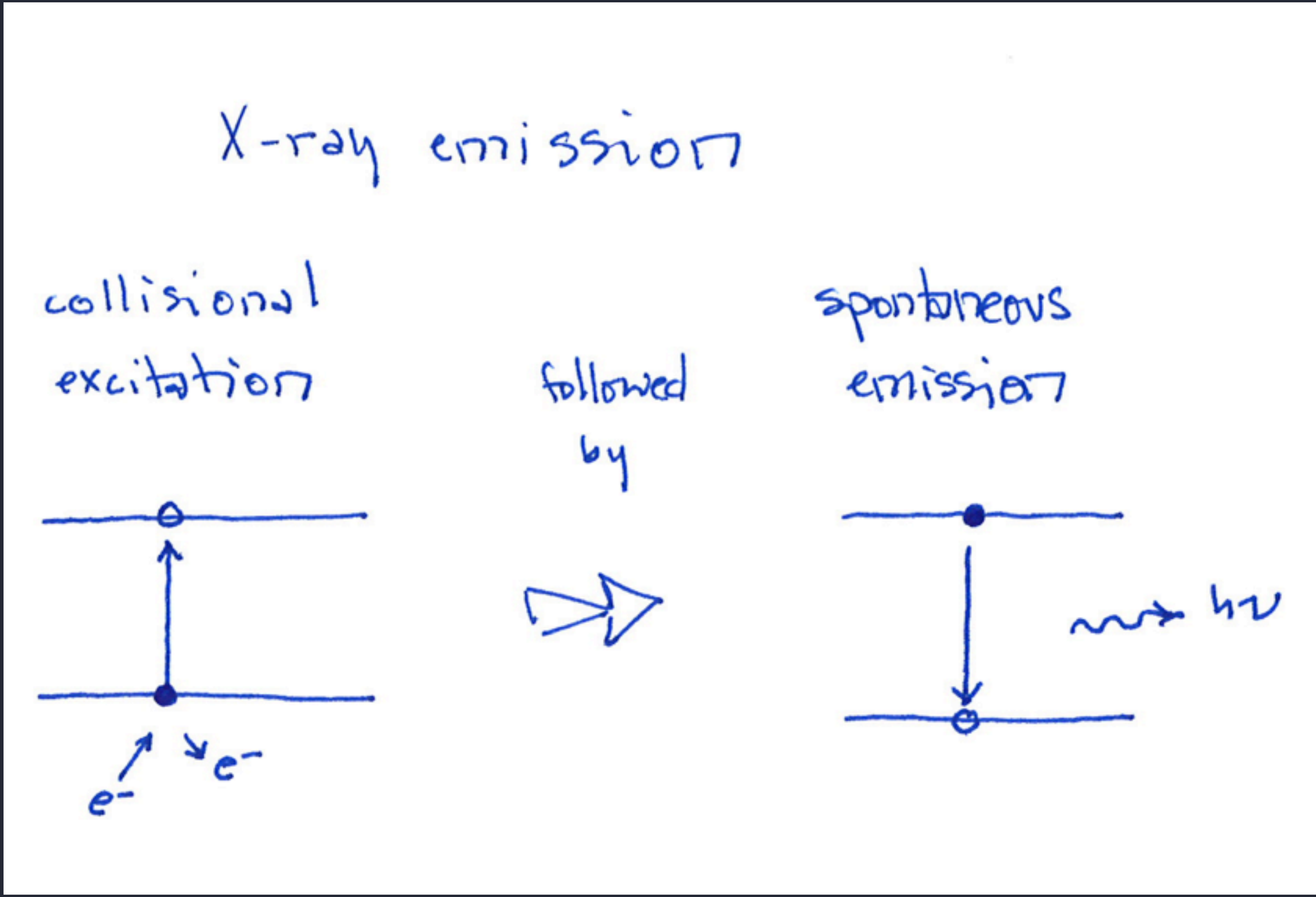

Chandra grating spectroscopy (R < 1000)

ζ Pup (O4 If)

cool stars vs. hot stars

starfish, *in situ*, at the Monterey, California Aquarium (photo: D. Cohen)

Chandra grating (HETGS/MEG) spectra

ζ Pup (O4 If)

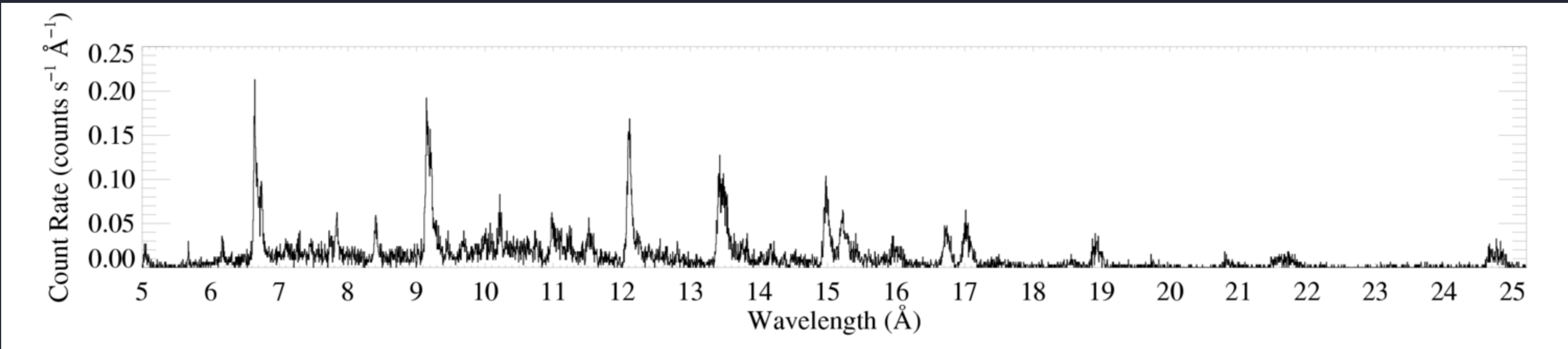

5Å 15Å 25Å

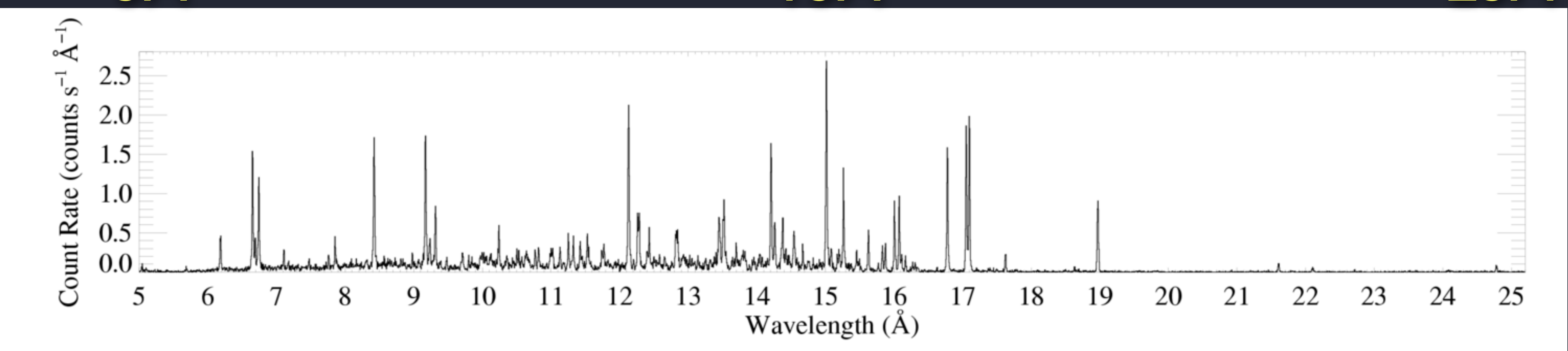

Capella (G5 III)

emission lines + bremsstrahlung + recombination

ζ Pup (O4 If)

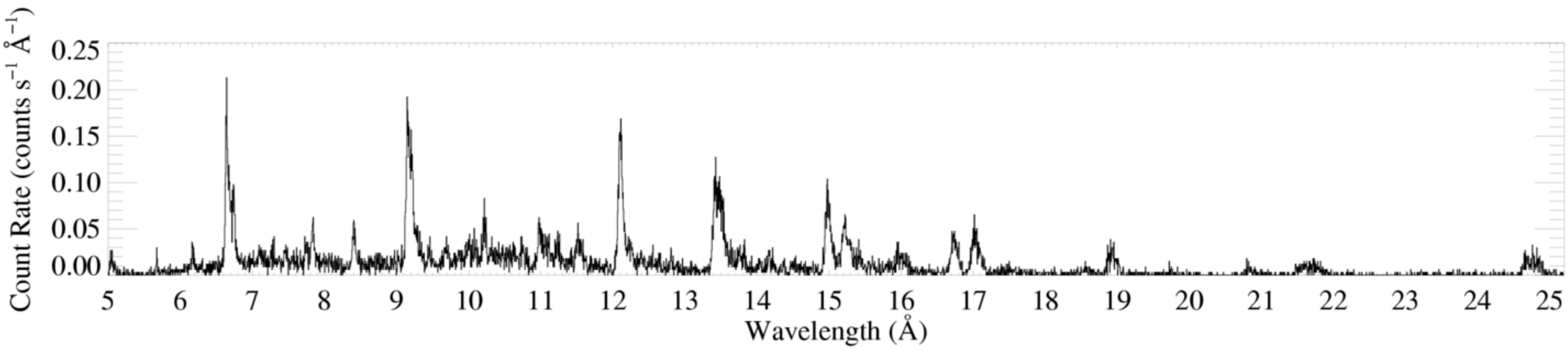

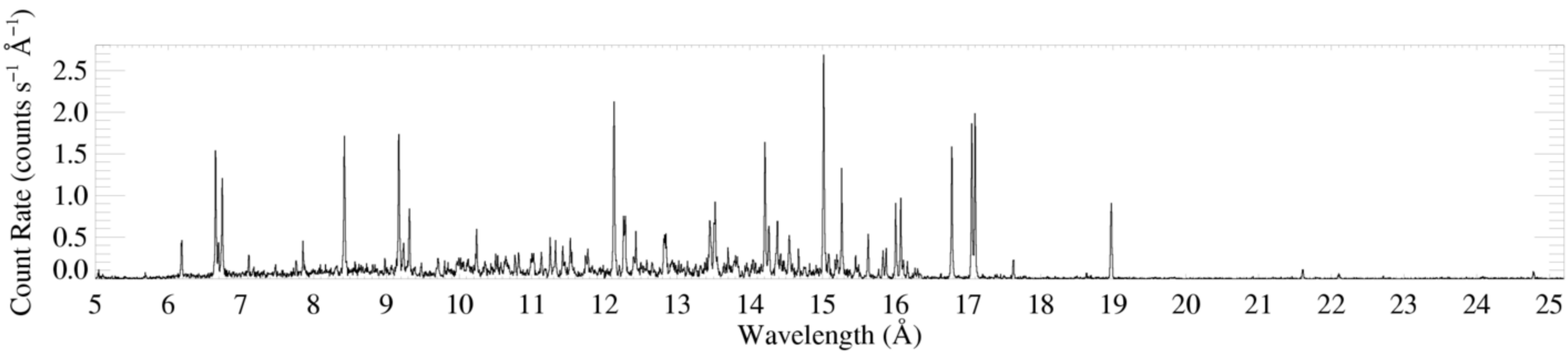

Capella (G5 III)

Chandra grating (HETGS/MEG) spectra

ζ Pup (O4 If)

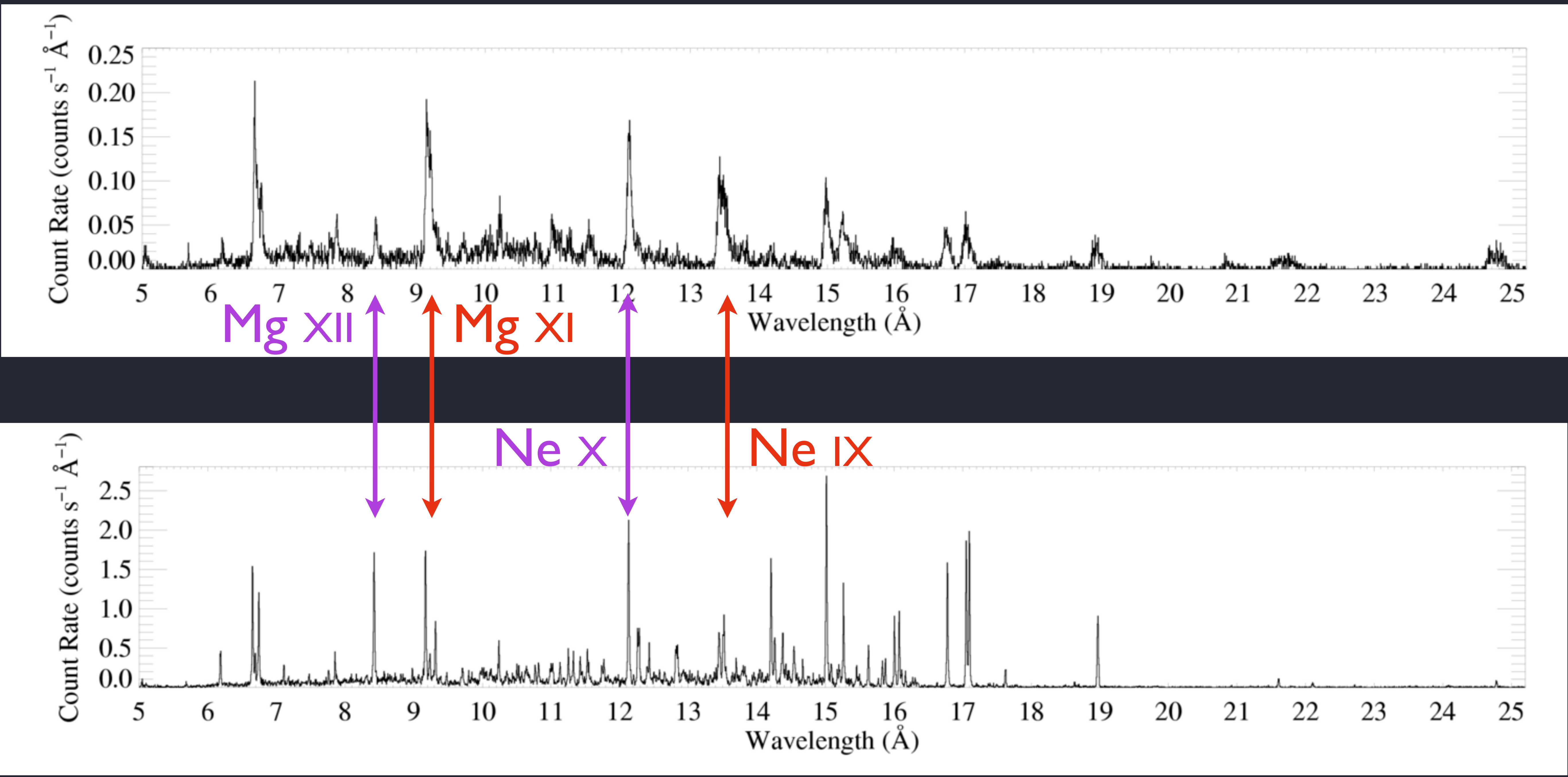

Capella (G5 III)

typical temperatures $T \sim$ few 10^6 K

(late-type stellar coronae tend to be hotter)

ζ Pup (O4 If)

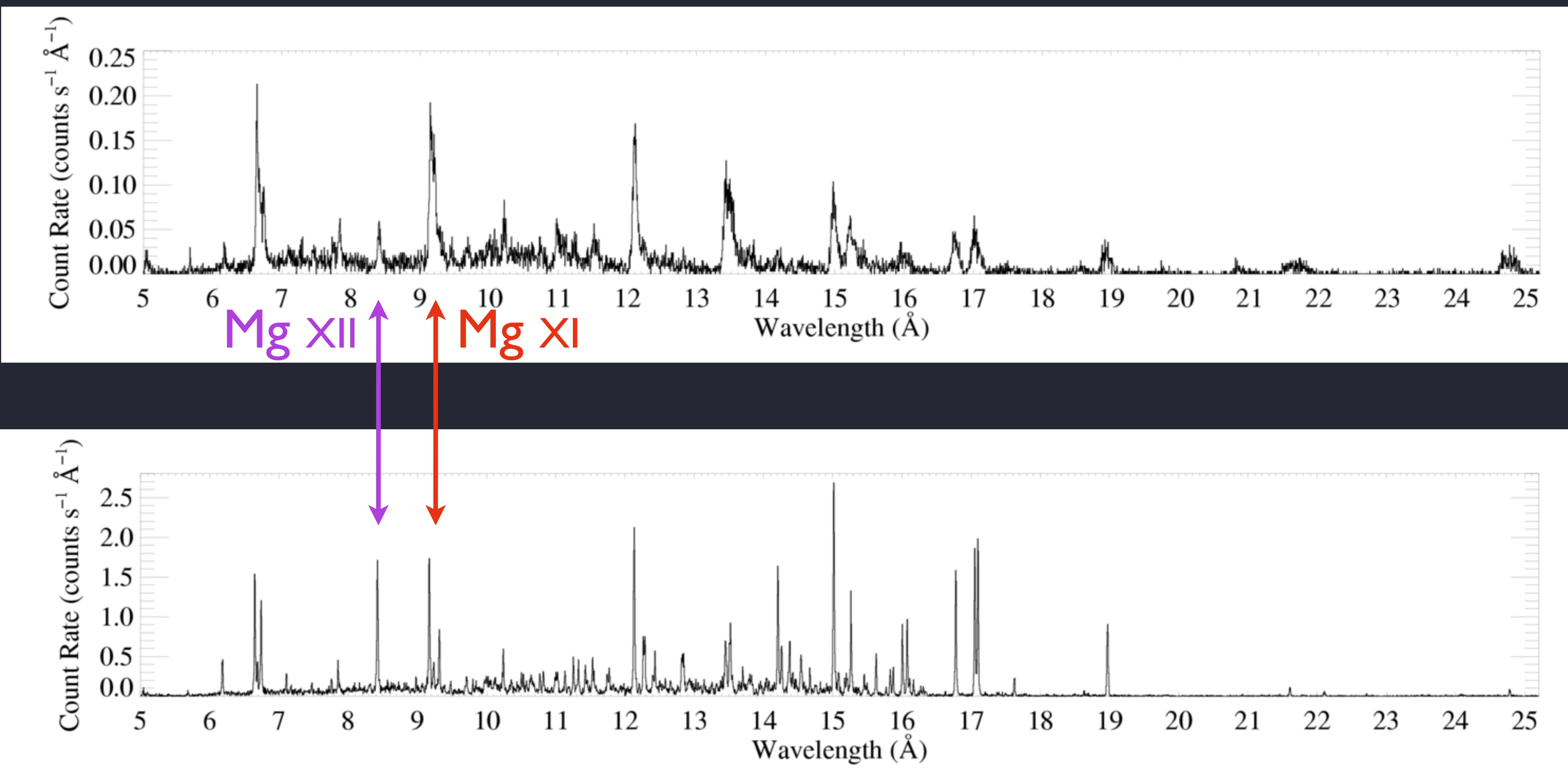

Capella (G5 III)

Zoom in

ζ Pup (O4 If)

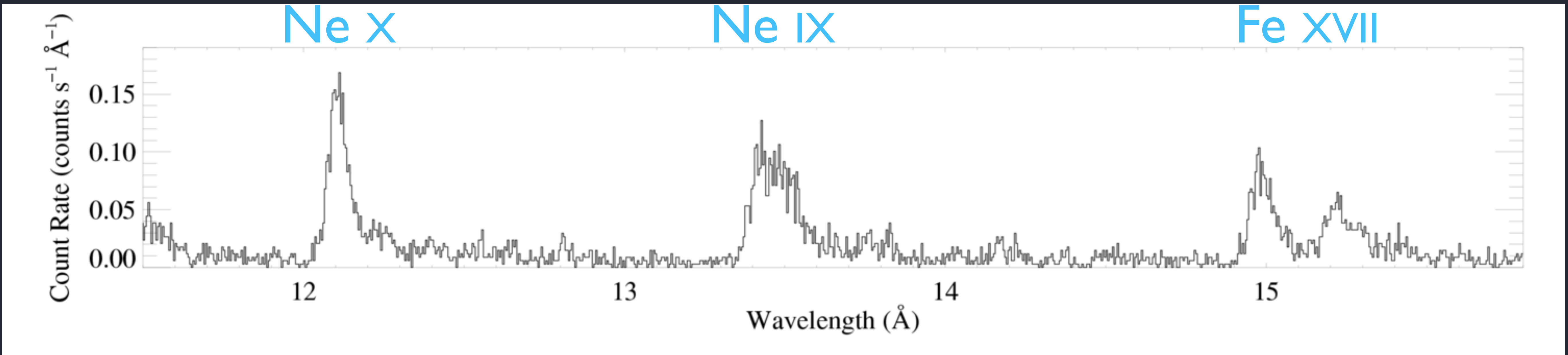

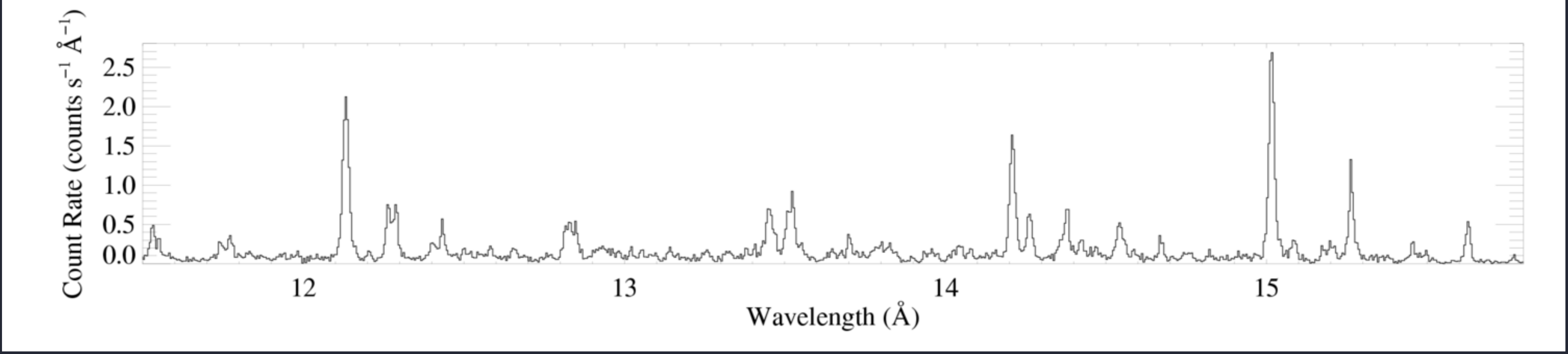

Capella (G5 III)

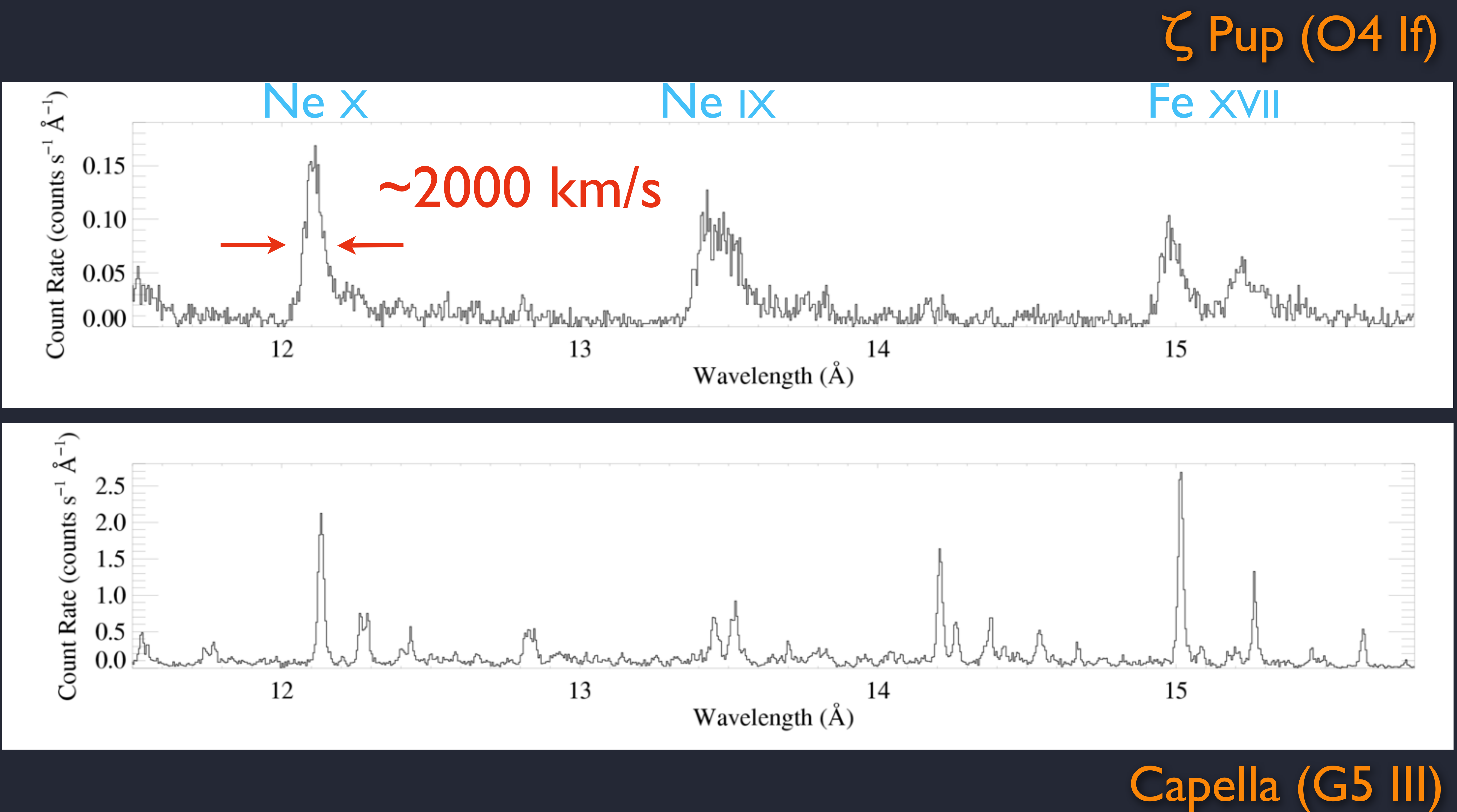
ζ Pup (O4 If)
Ne X
Ne IX
Fe XVII
~2000 km/s
Count Rate (counts s⁻¹ Å⁻¹)
0.15
0.10
0.05
0.00
12
13
14
15
Wavelength (Å)
Count Rate (counts s⁻¹ Å⁻¹)
2.5
2.0
1.5
1.0
0.5
0.0
12
13
14
15
Wavelength (Å)
Capella (G5 III)

ζ Pup (O4 If)

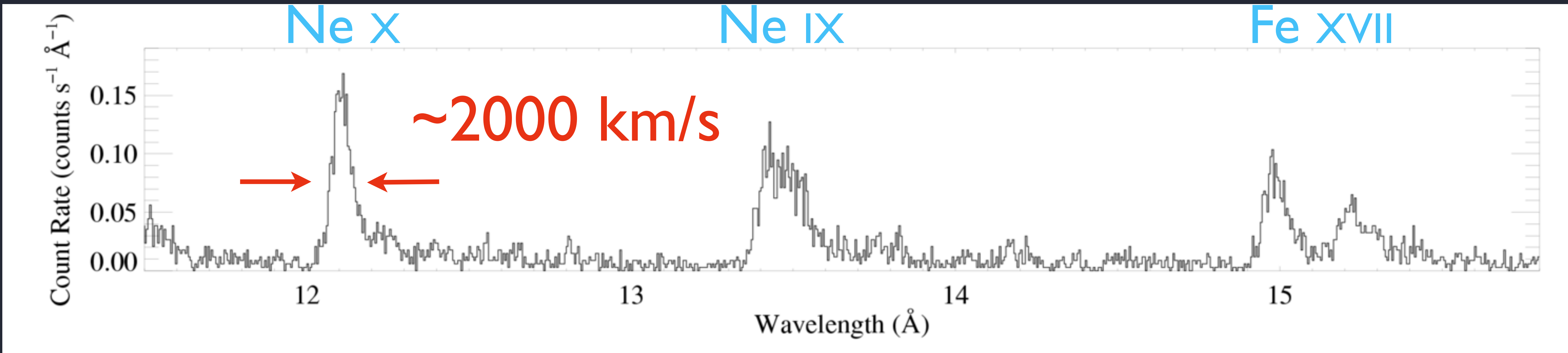

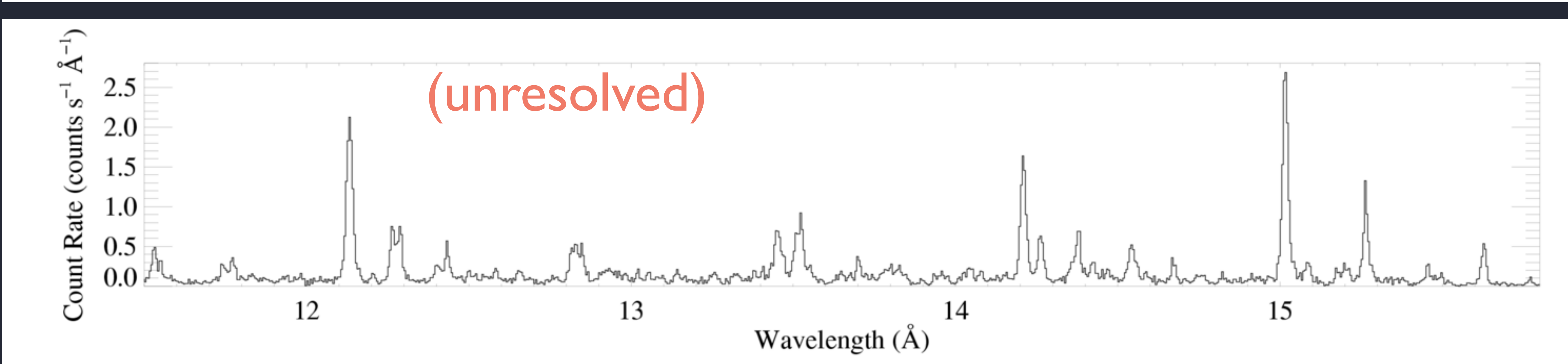

Capella (G5 III)

cool stars: narrow lines = magnetically confined coronal plasma

hot stars: broad lines = outflowing, shock-heated wind plasma

lines are *asymmetric*

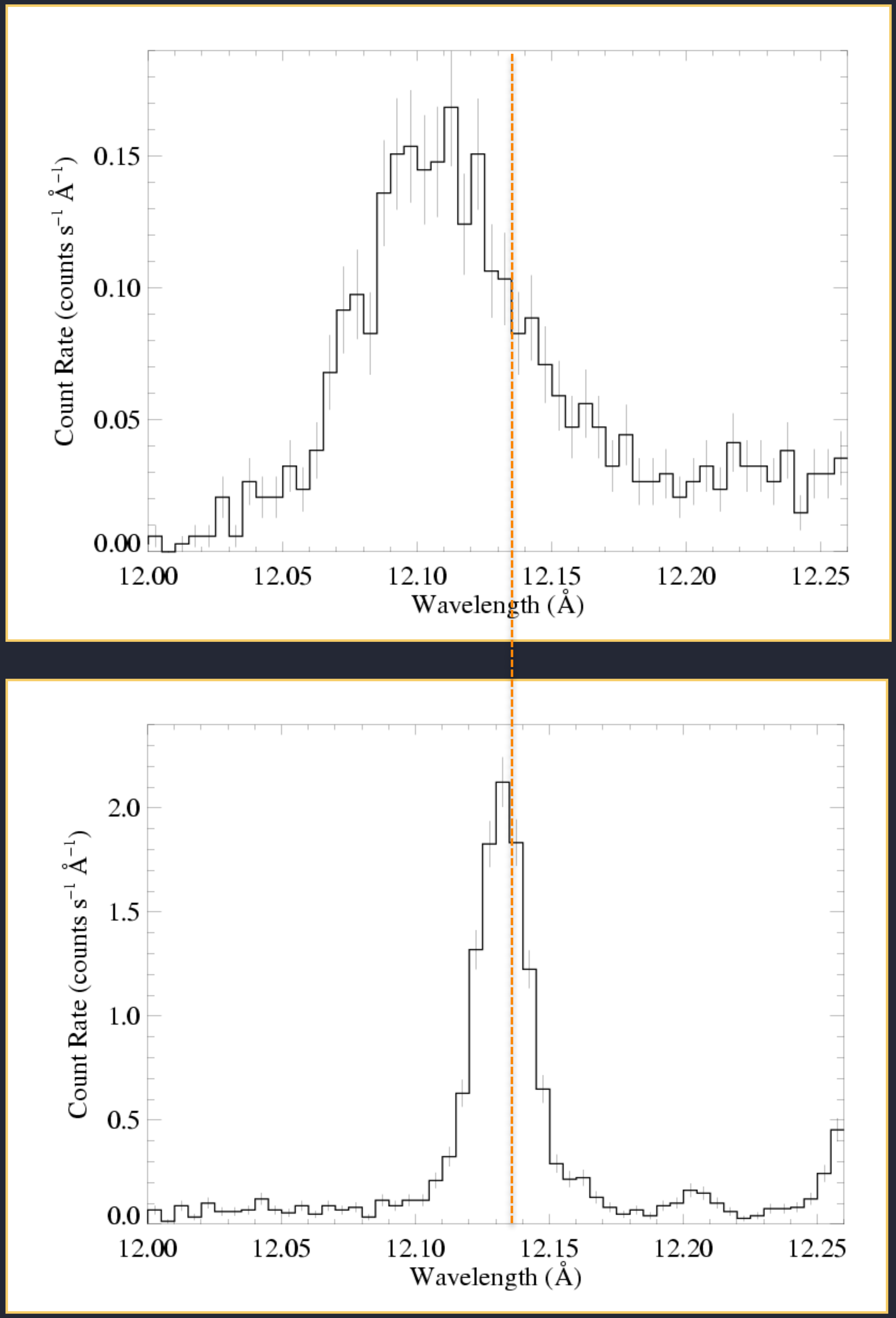

The key is X-ray absorption

>99% of the wind is cold and X-ray *absorbing*

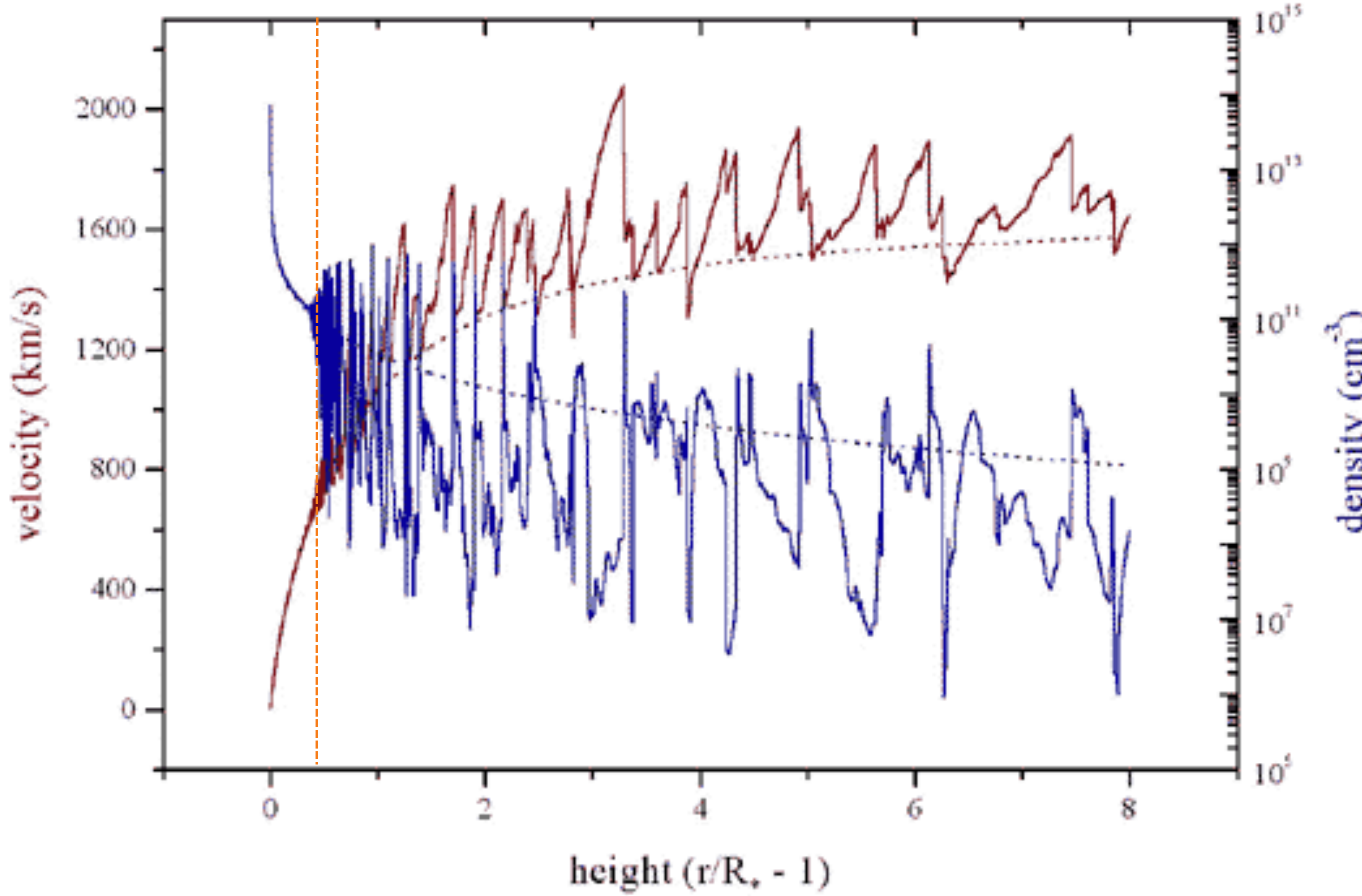

Absorption in the cold wind component

due to inner-shell photoionization

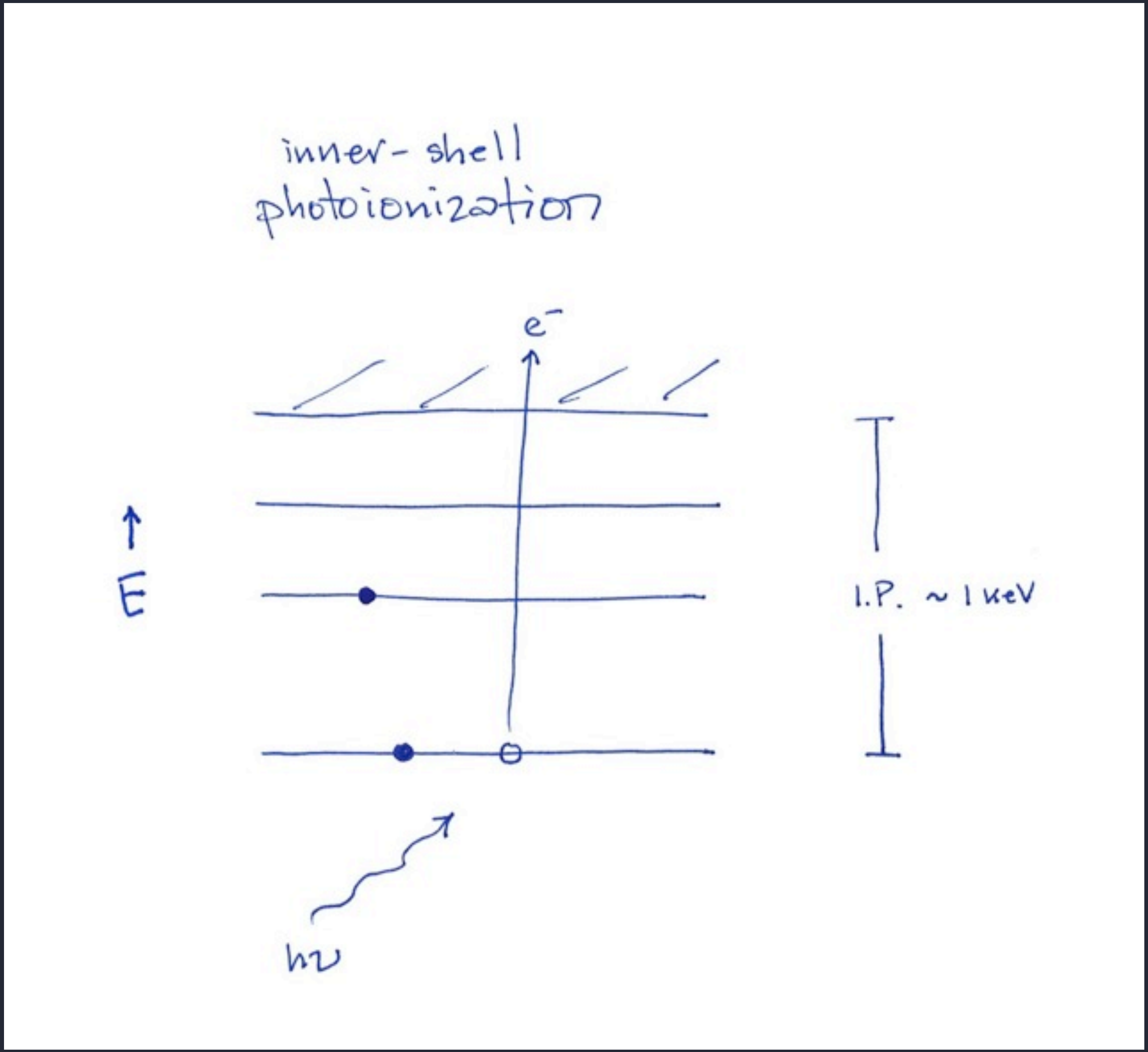

Absorption in the cold wind component

due to inner-shell photoionization

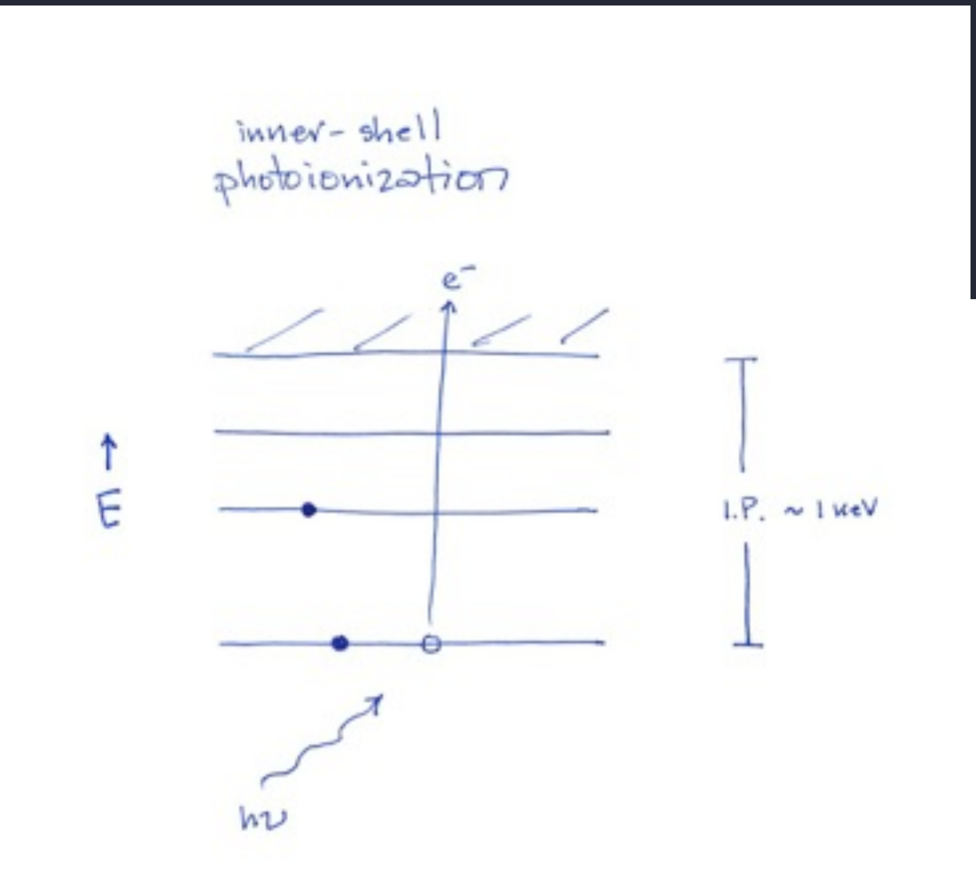

Absorption in the cold wind component

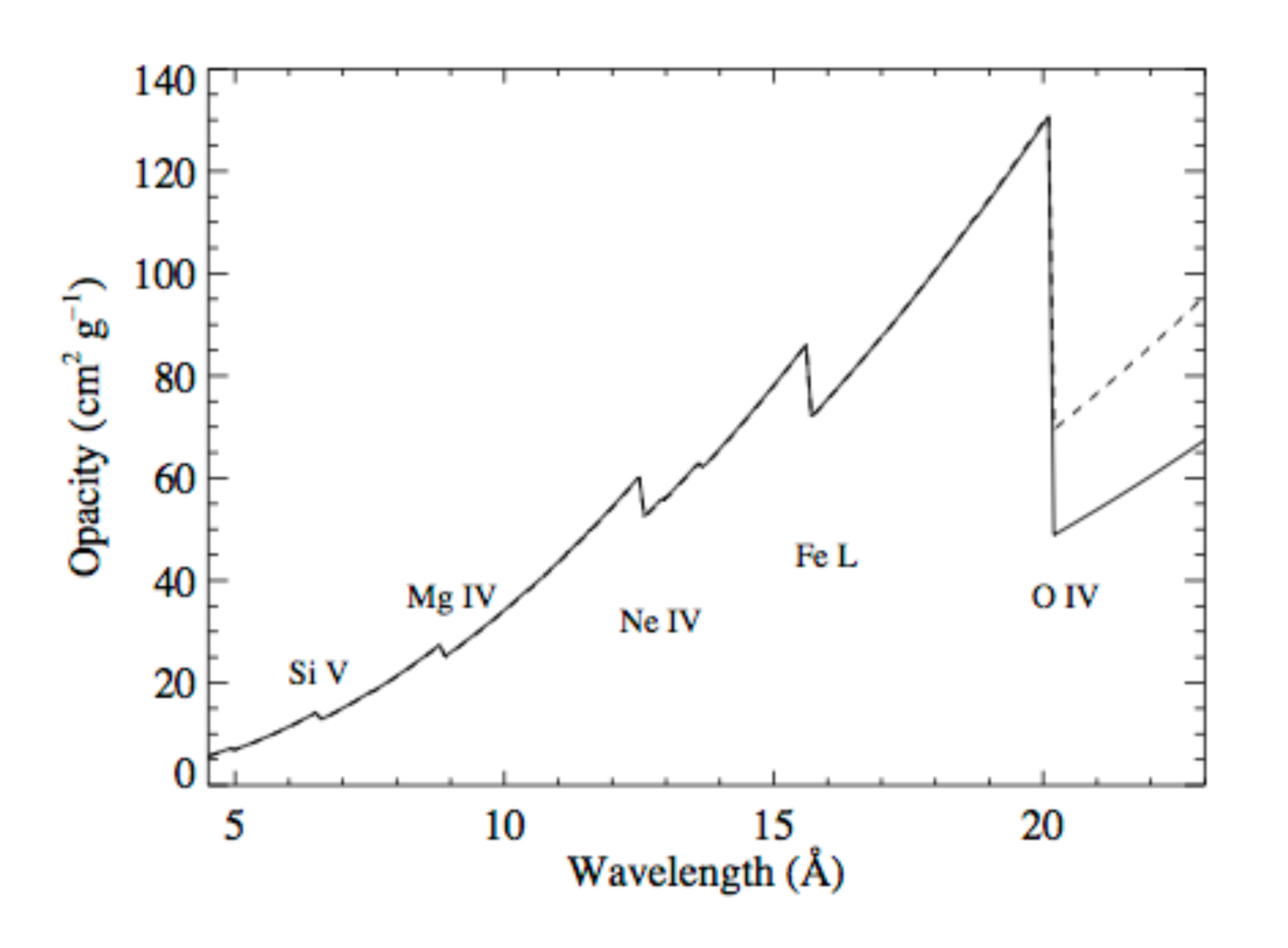

$v = v_\infty(1-r/R_\star)^\beta$

beta velocity law assumed

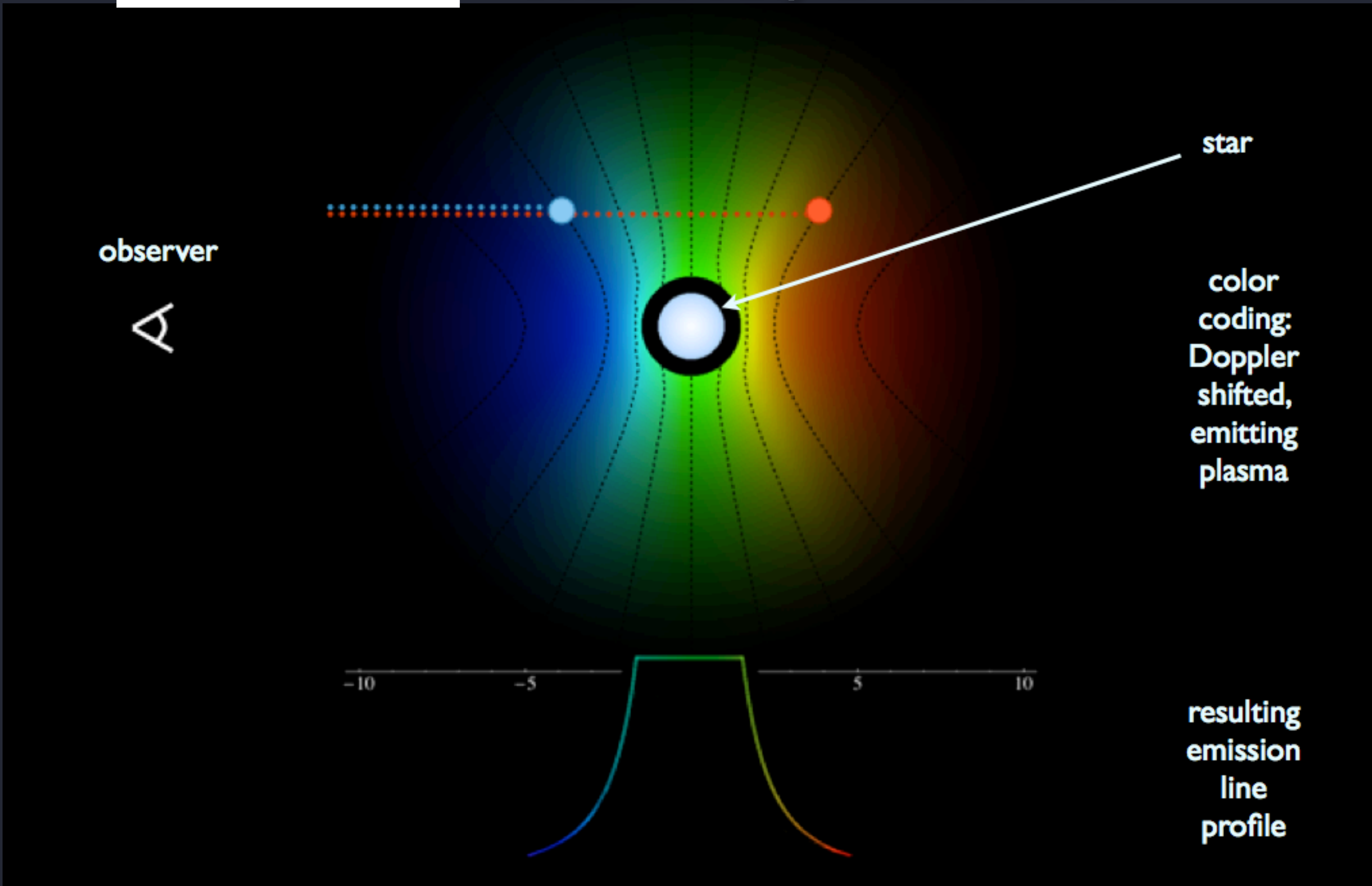

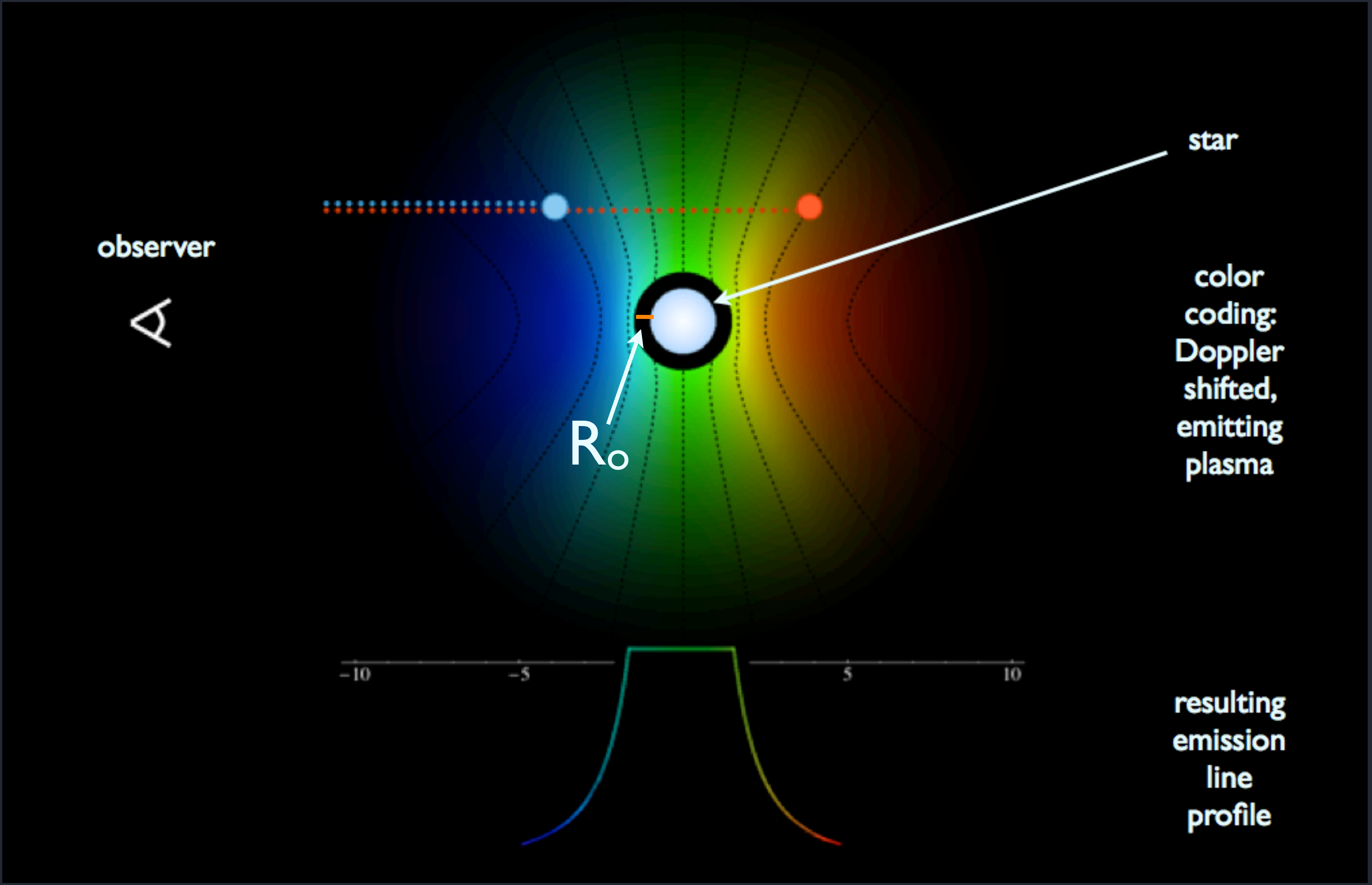

star
observer
color coding: Doppler shifted, emitting plasma
R₀
−10
−5
5
10
resulting emission line profile

Line Asymmetry

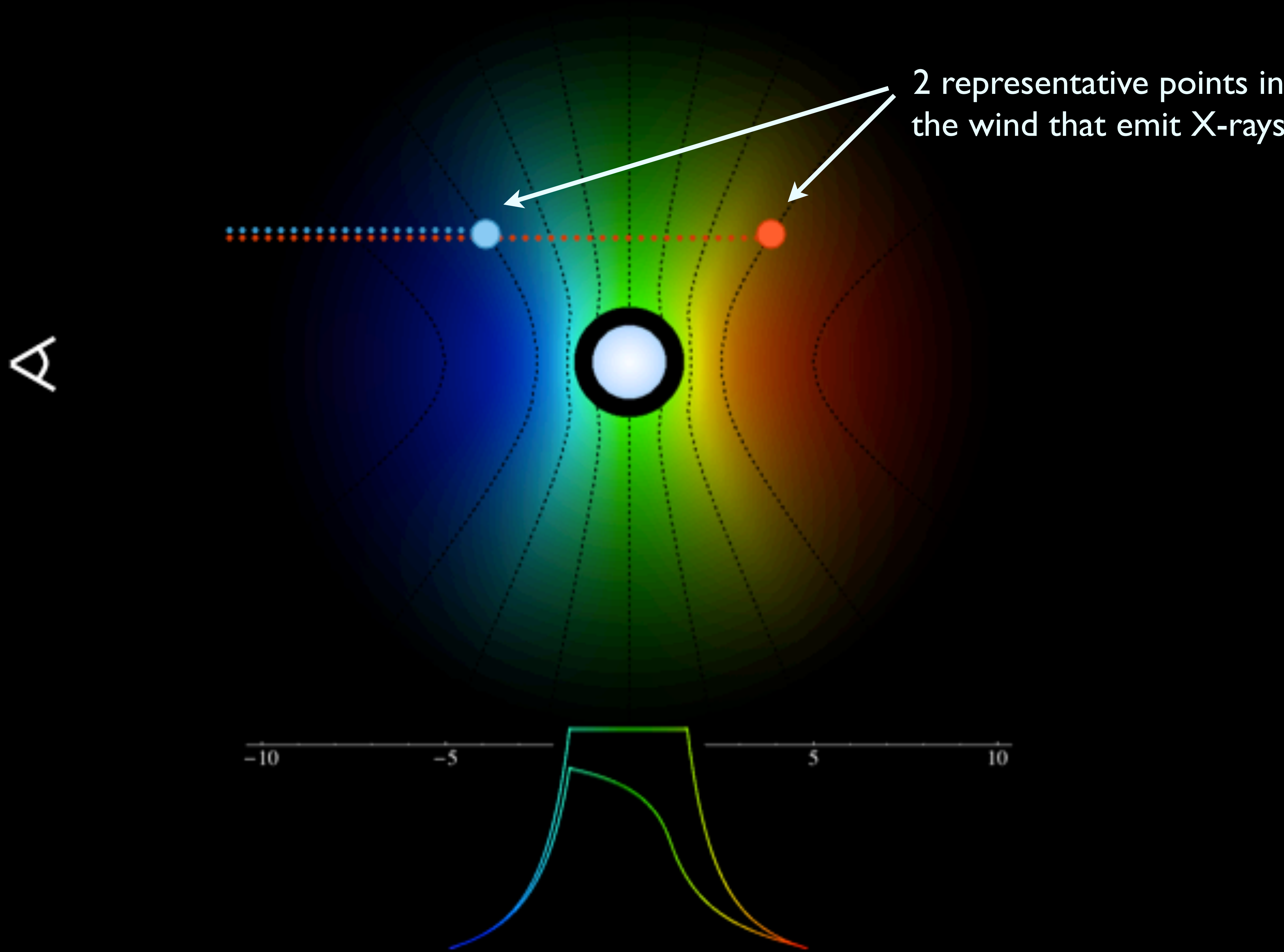

Line Asymmetry

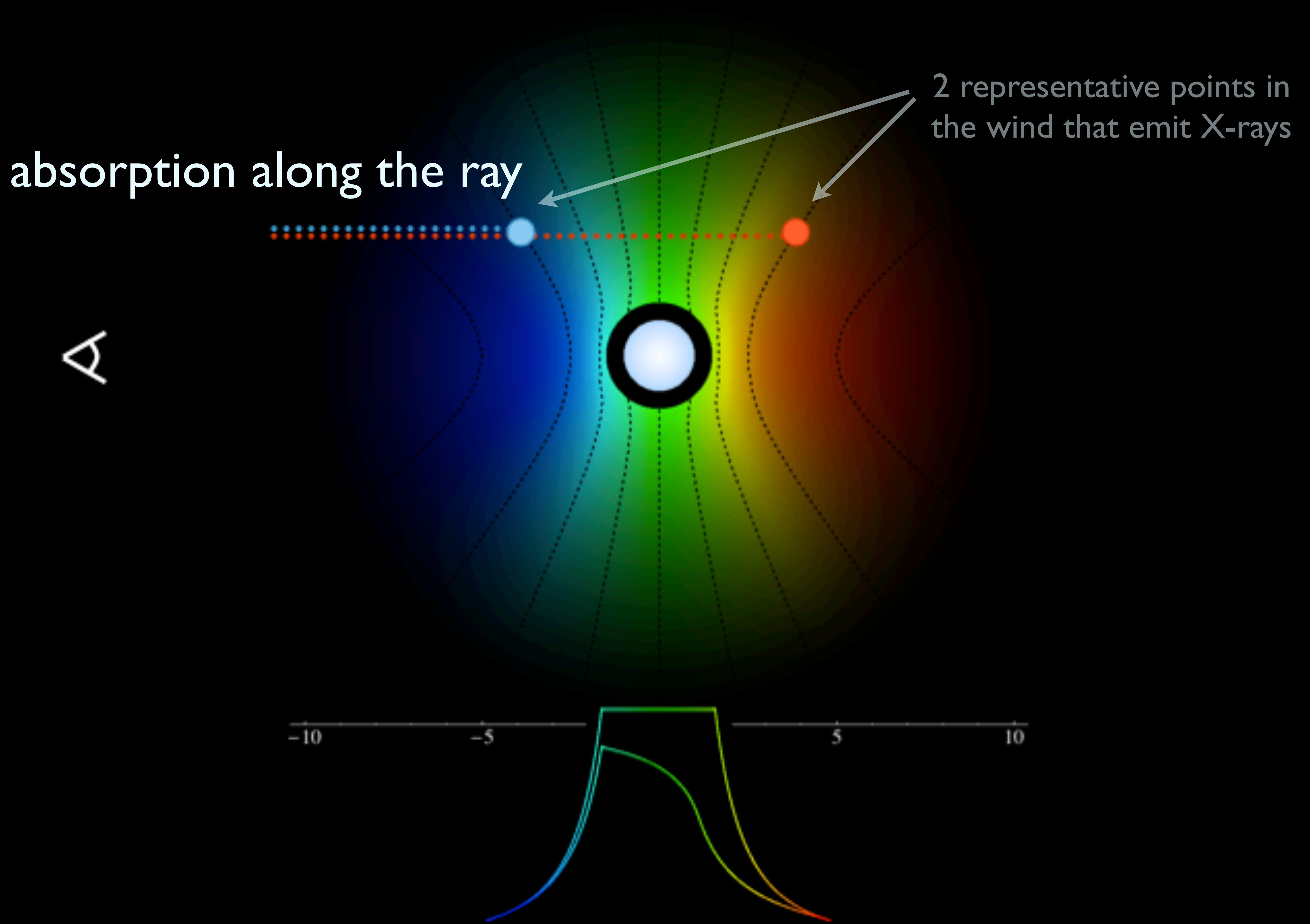

Line Asymmetry

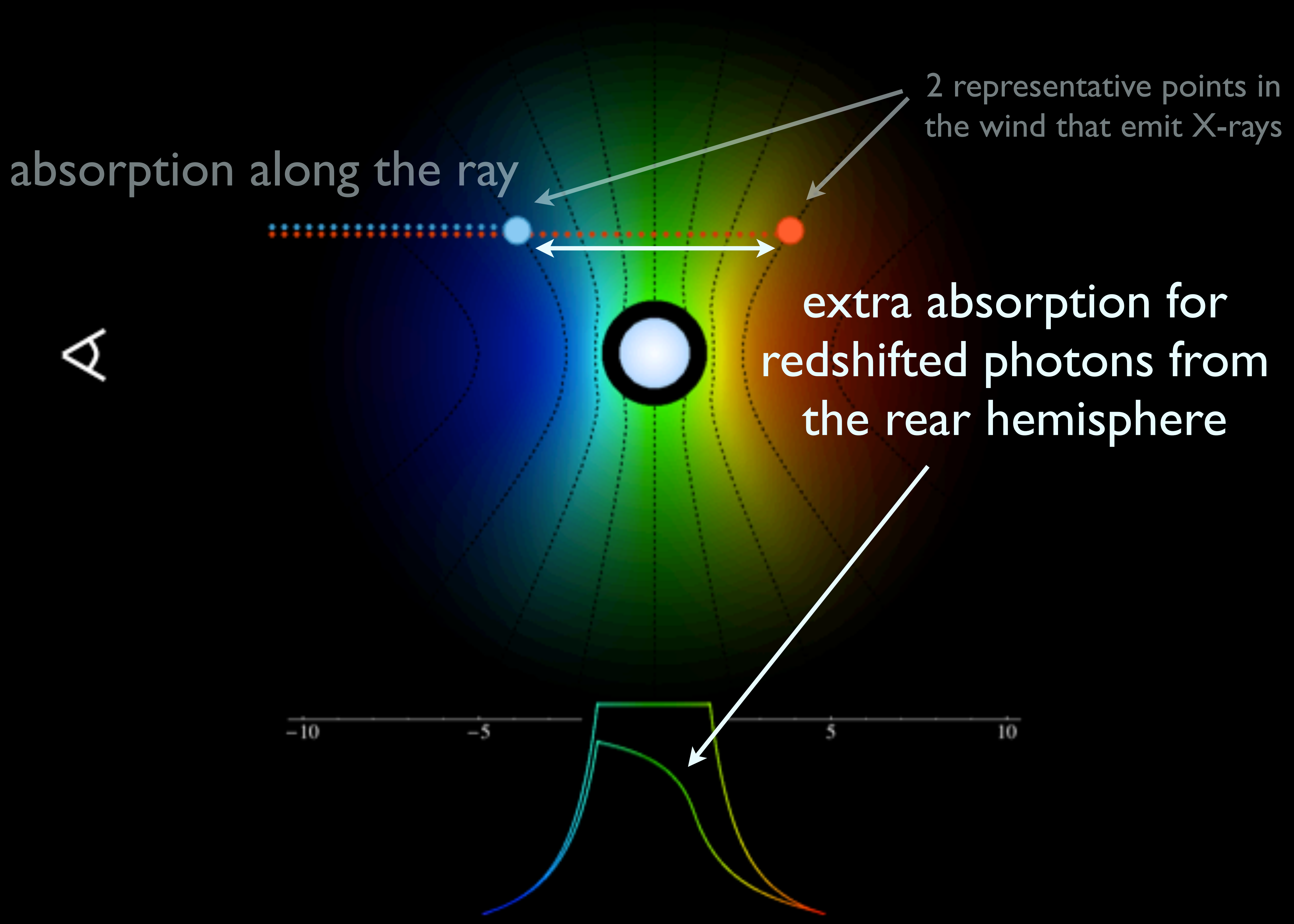

Wind Profile Model

for mass-loss rates ~10^{-6} : expect wind to be modestly optically thick

$$\tau_* = \frac{\kappa \dot{M}}{4\pi R_* v_\infty}$$

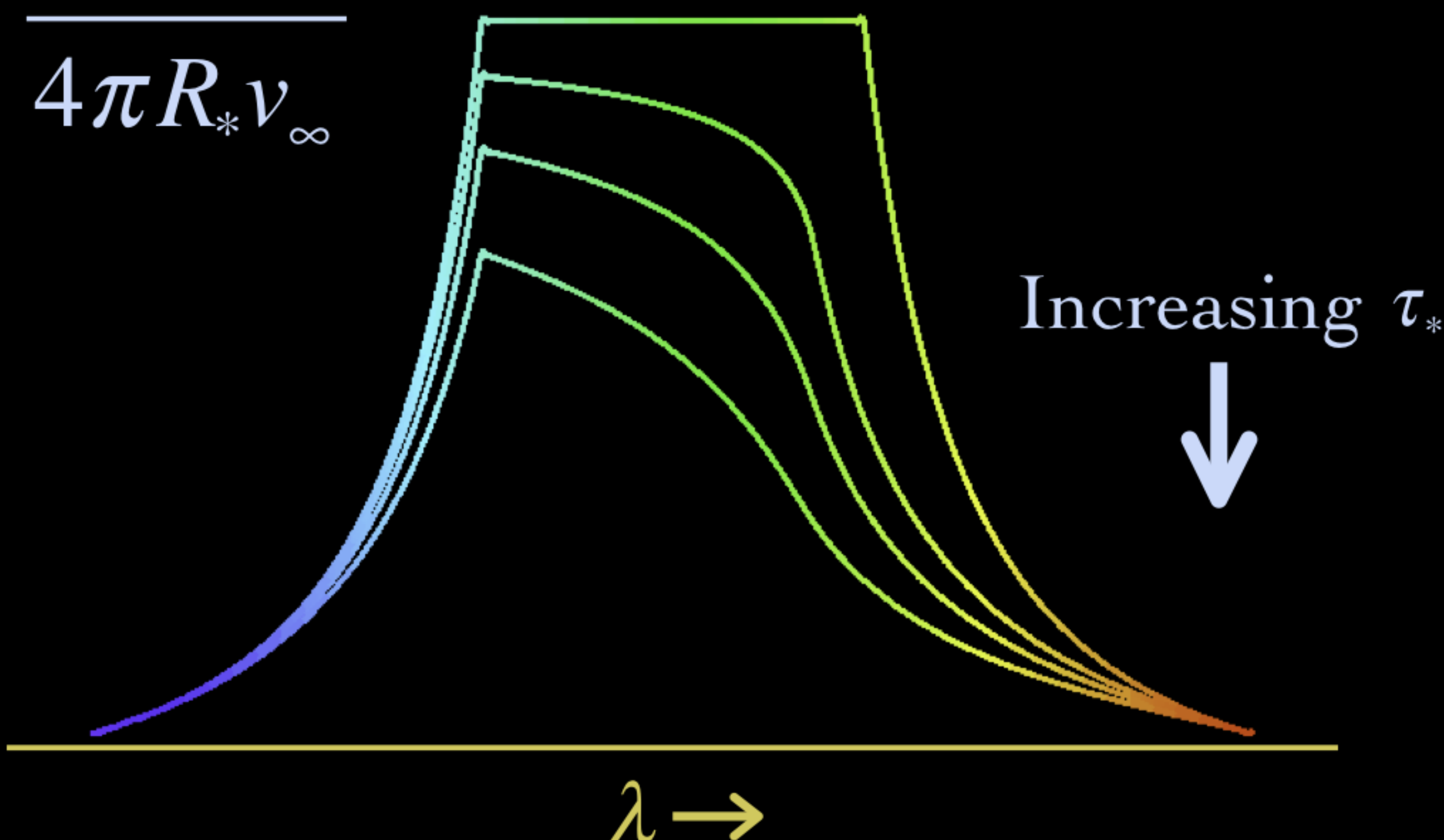

Line profile shapes

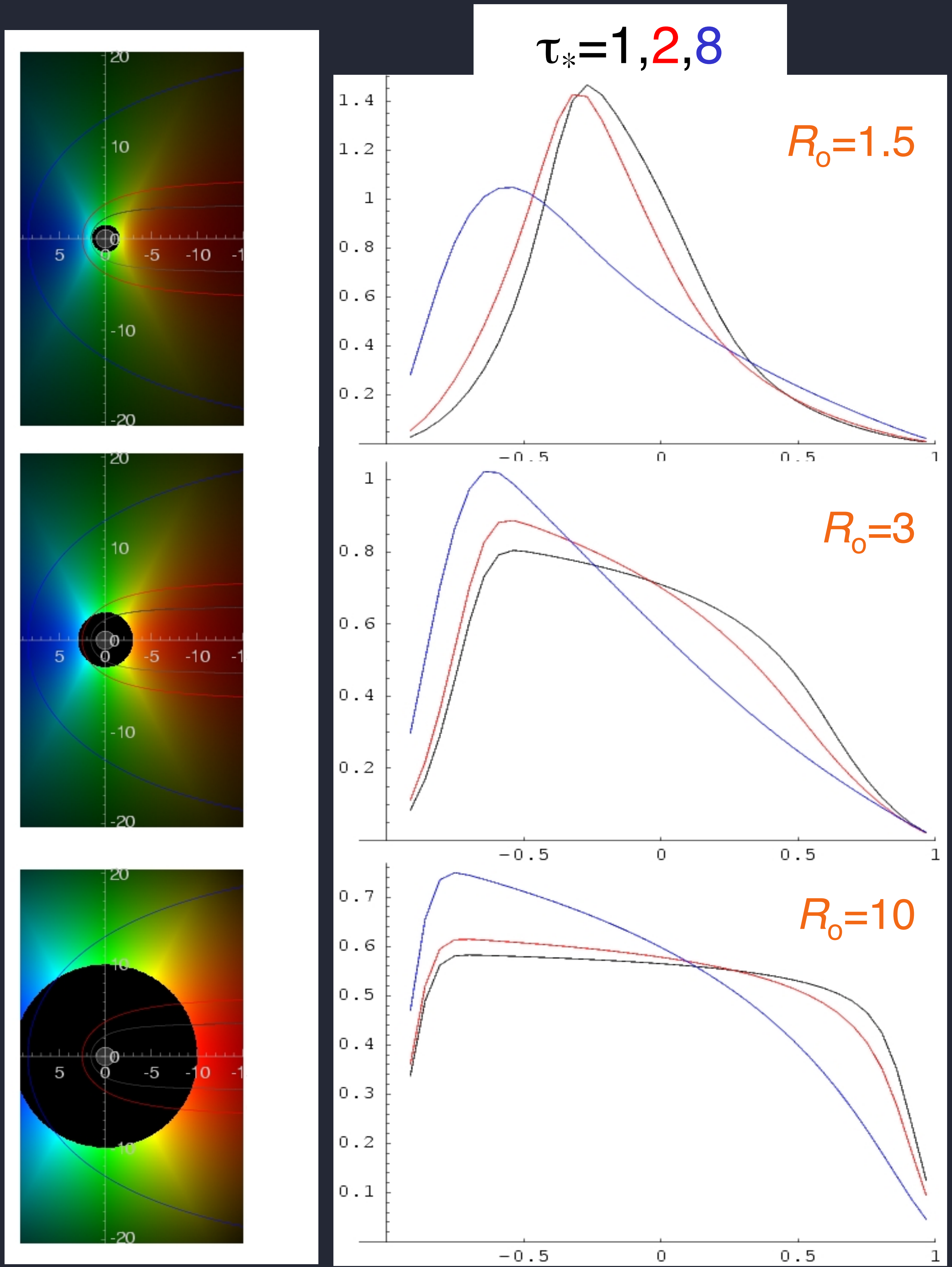

key parameters: R_o & $\tau_\star$

$$v = v_\infty(1 - r/R_\star)^\beta$$

$j \sim \rho^2$ for $r/R_* > R_o$,

$= 0$ otherwise

$$\tau = \tau_* \int_z^\infty \frac{R_* dz'}{r'^2 (1 - R_*/r')^\beta}$$

$$\tau_* \equiv \frac{\kappa \dot{M}}{4\pi R_* v_\infty}$$

Owocki & Cohen 2001

Fit the model to data

ζ Pup: *Chandra*

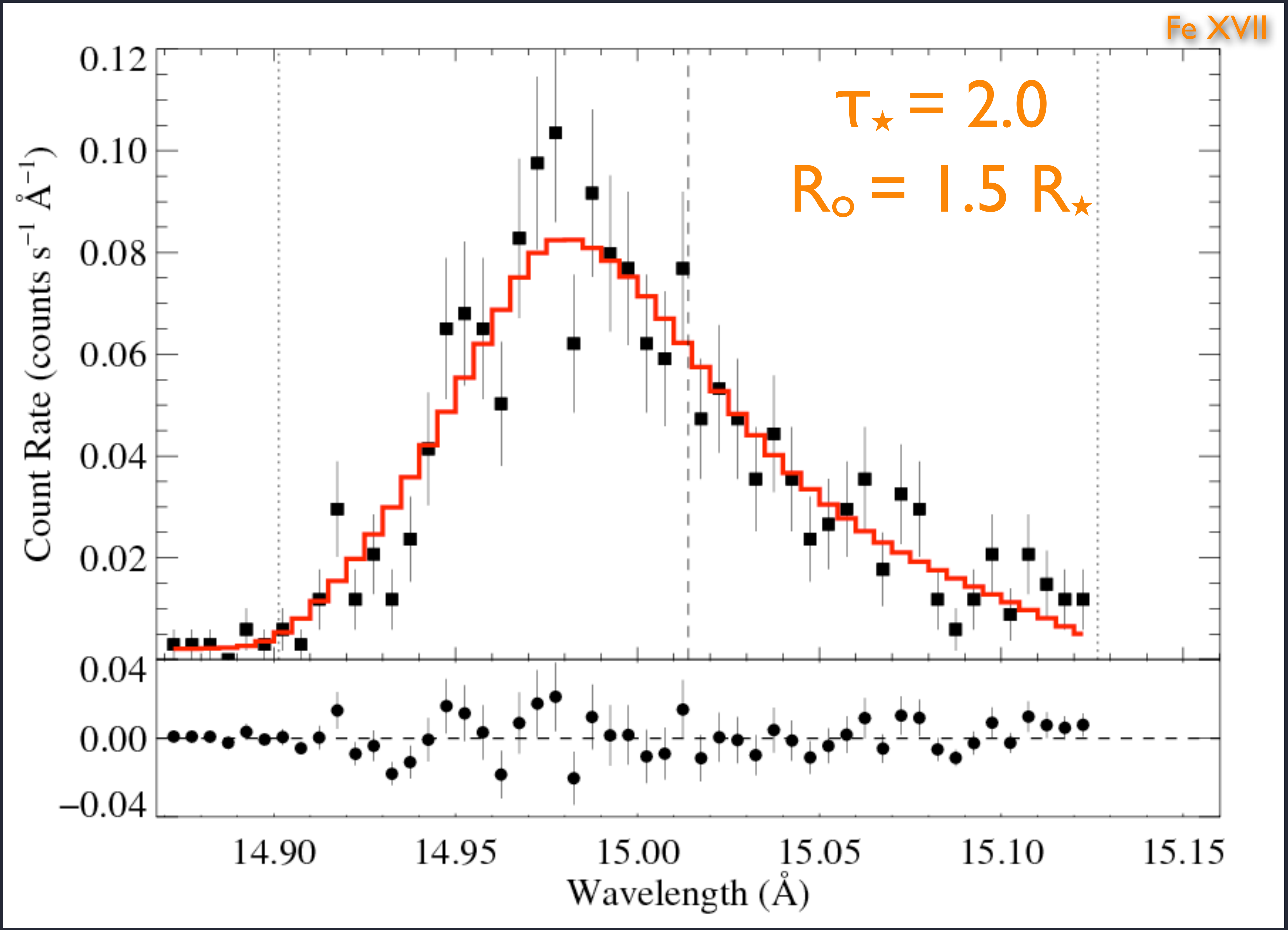

Distribution of R_o values for ζ Pup

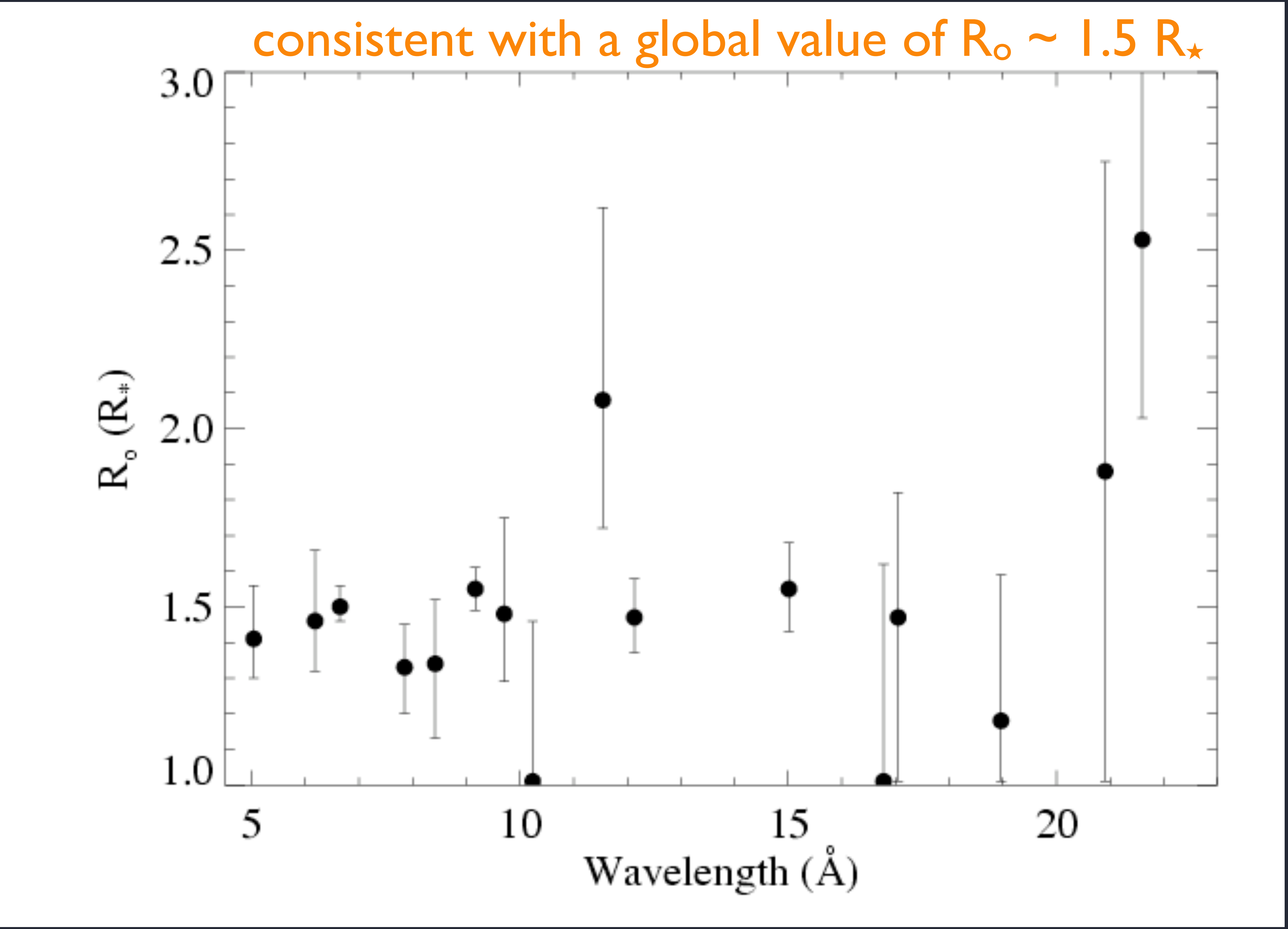

Quantifying the wind optical depth

opacity of the cold wind component (due to photoionization of C, N, O, Ne, Fe)

wind mass-loss rate

$$\dot{M} = 4\pi r^2 v\rho$$

$$\tau_* \equiv \frac{\kappa \dot{M}}{4\pi R_* v_\infty}$$

stellar radius

wind terminal velocity

soft X-ray wind opacity

note: absorption arises in the dominant, cool wind component

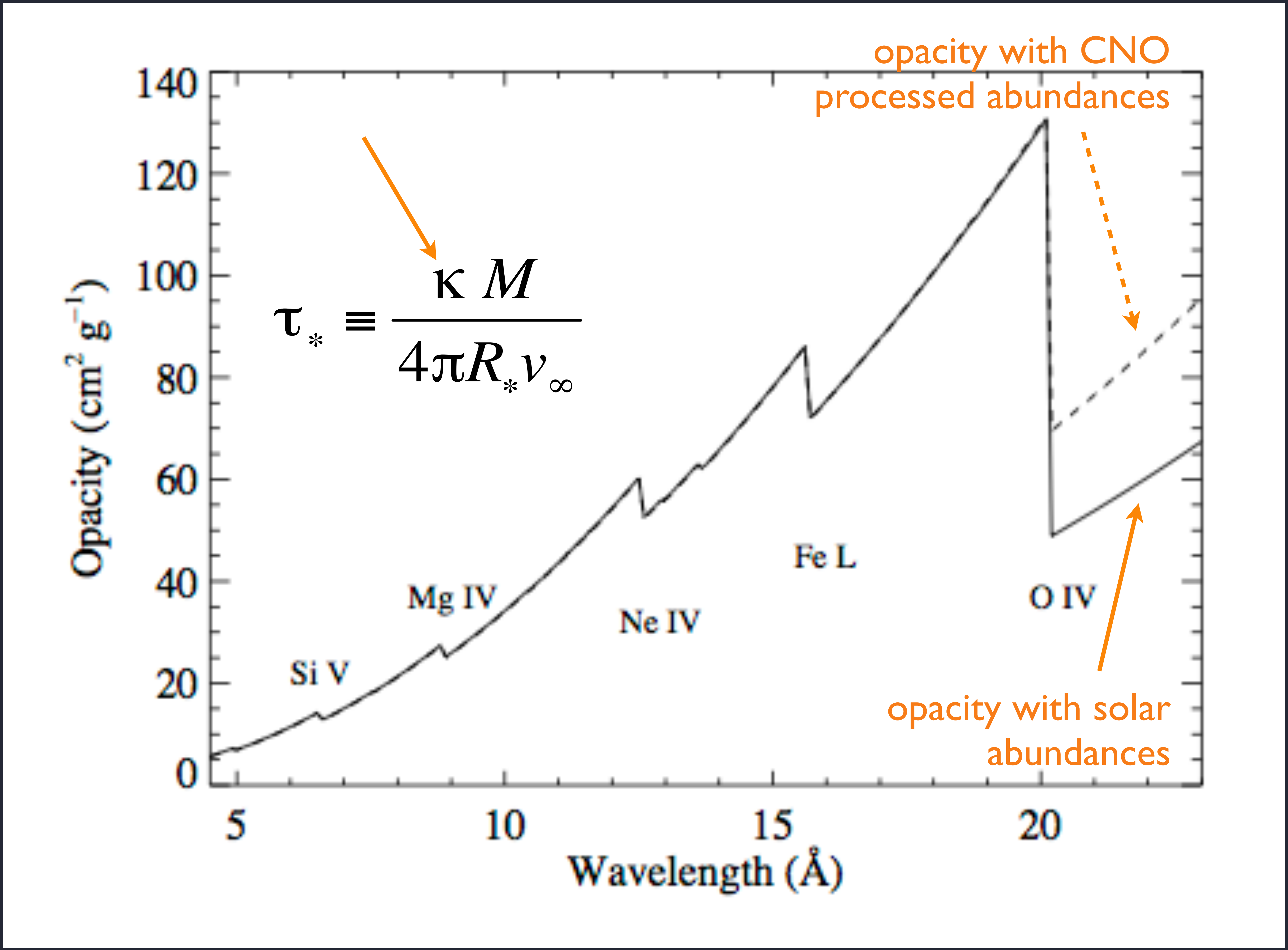

ζ Pup *Chandra*: three emission lines

Mg Lyα: 8.42 Å　　Ne Lyα: 12.13 Å　　O Lyα: 18.97 Å

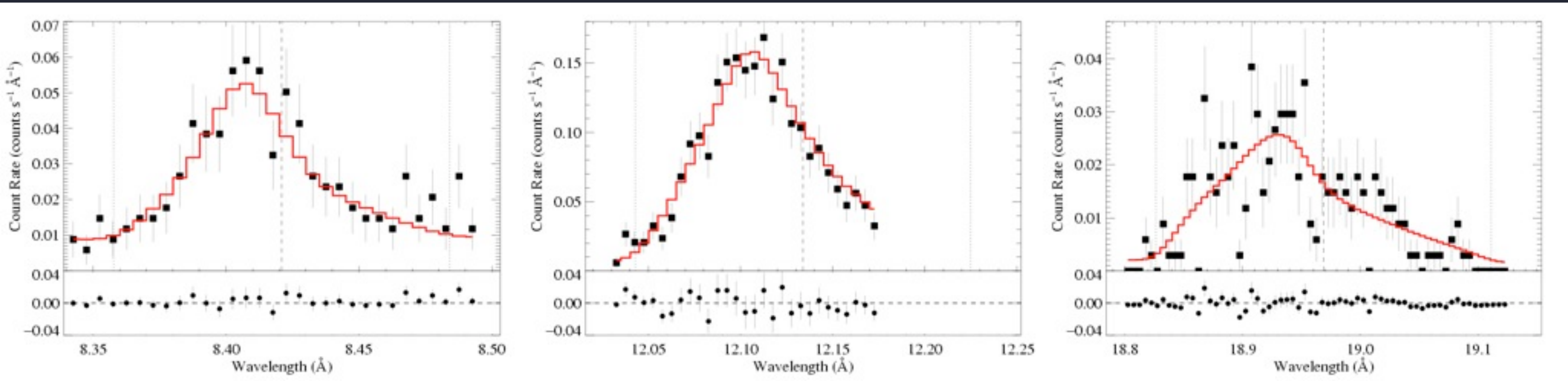

$\tau_* \sim 1$　　$\tau_* \sim 2$　　$\tau_* \sim 3$

Recall:

$$\tau_* \equiv \frac{\kappa \dot{M}}{4\pi R_* v_\infty}$$

Results from the 3 line fits shown previously

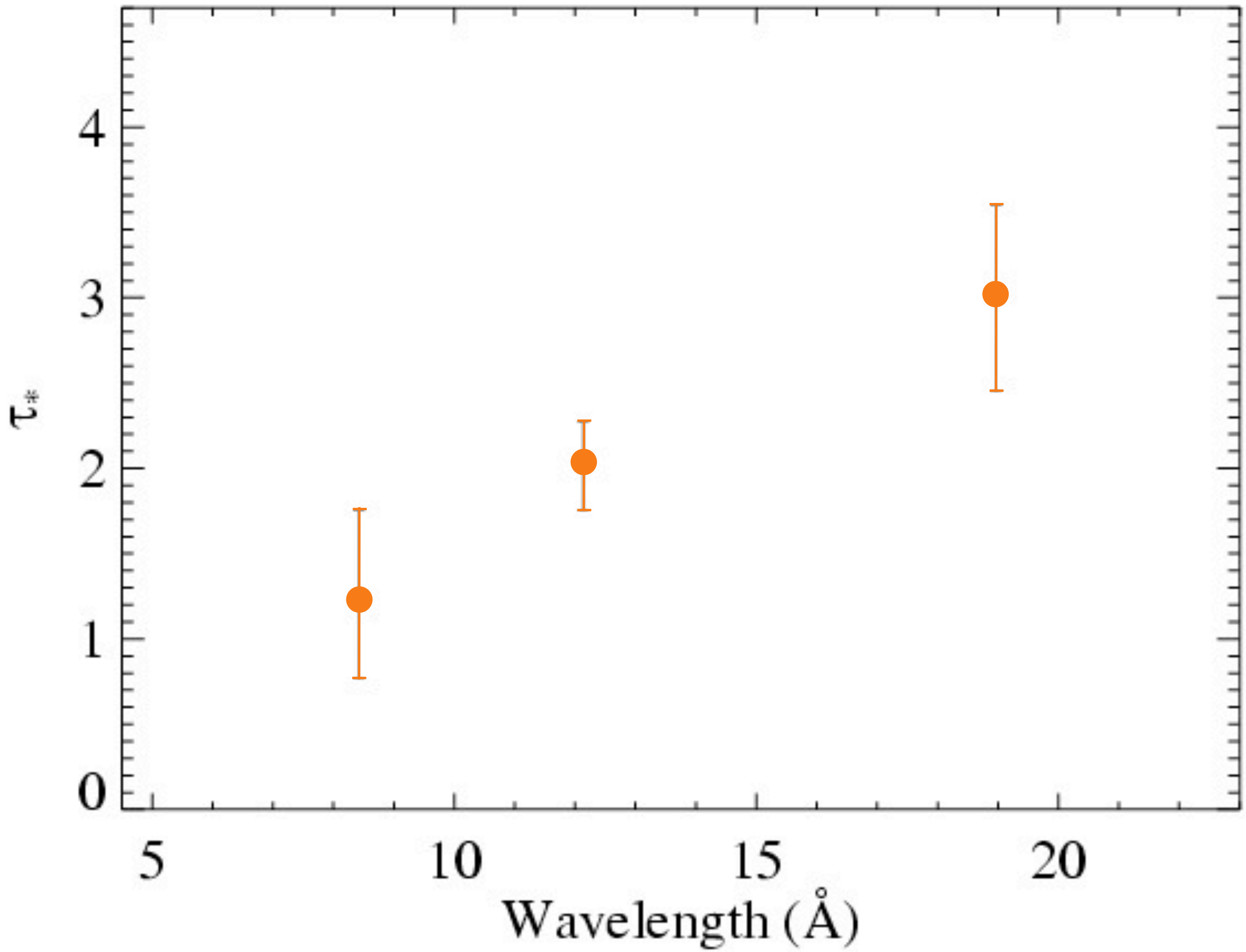

Fits to 16 lines in the *Chandra* spectrum of ζ Pup

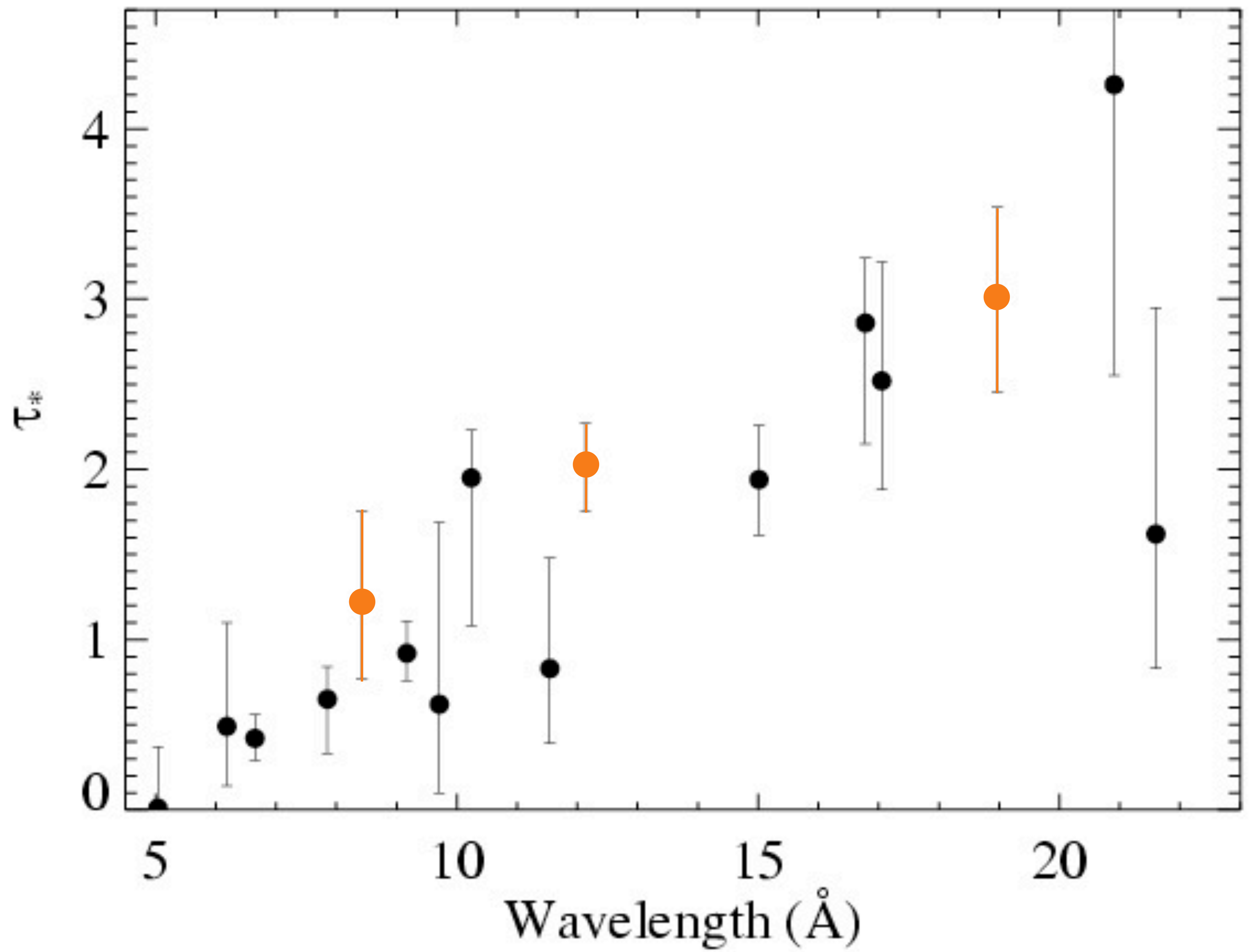

Fits to 16 lines in the *Chandra* spectrum of ζ Pup

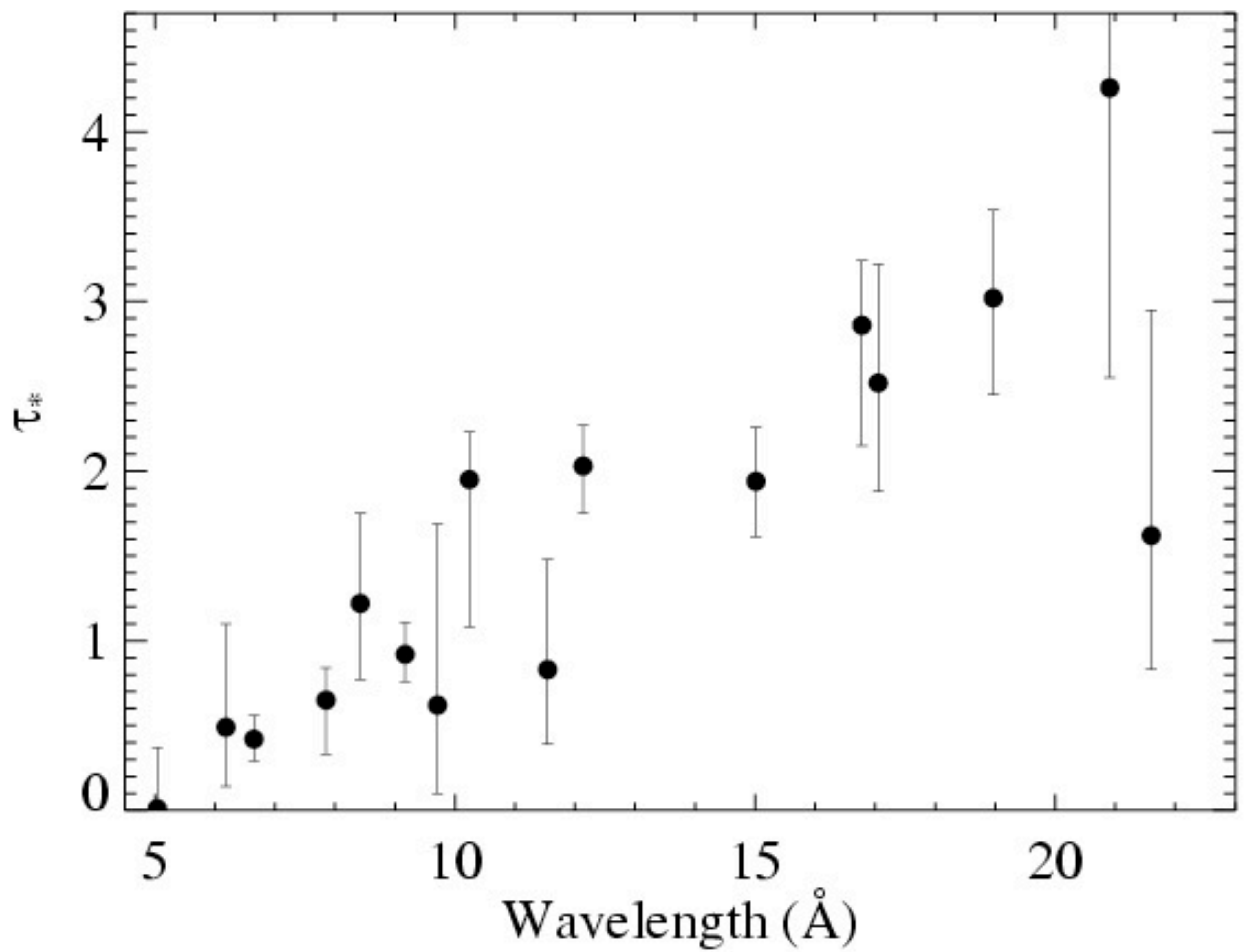

Fits to 16 lines in the *Chandra* spectrum of ζ Pup

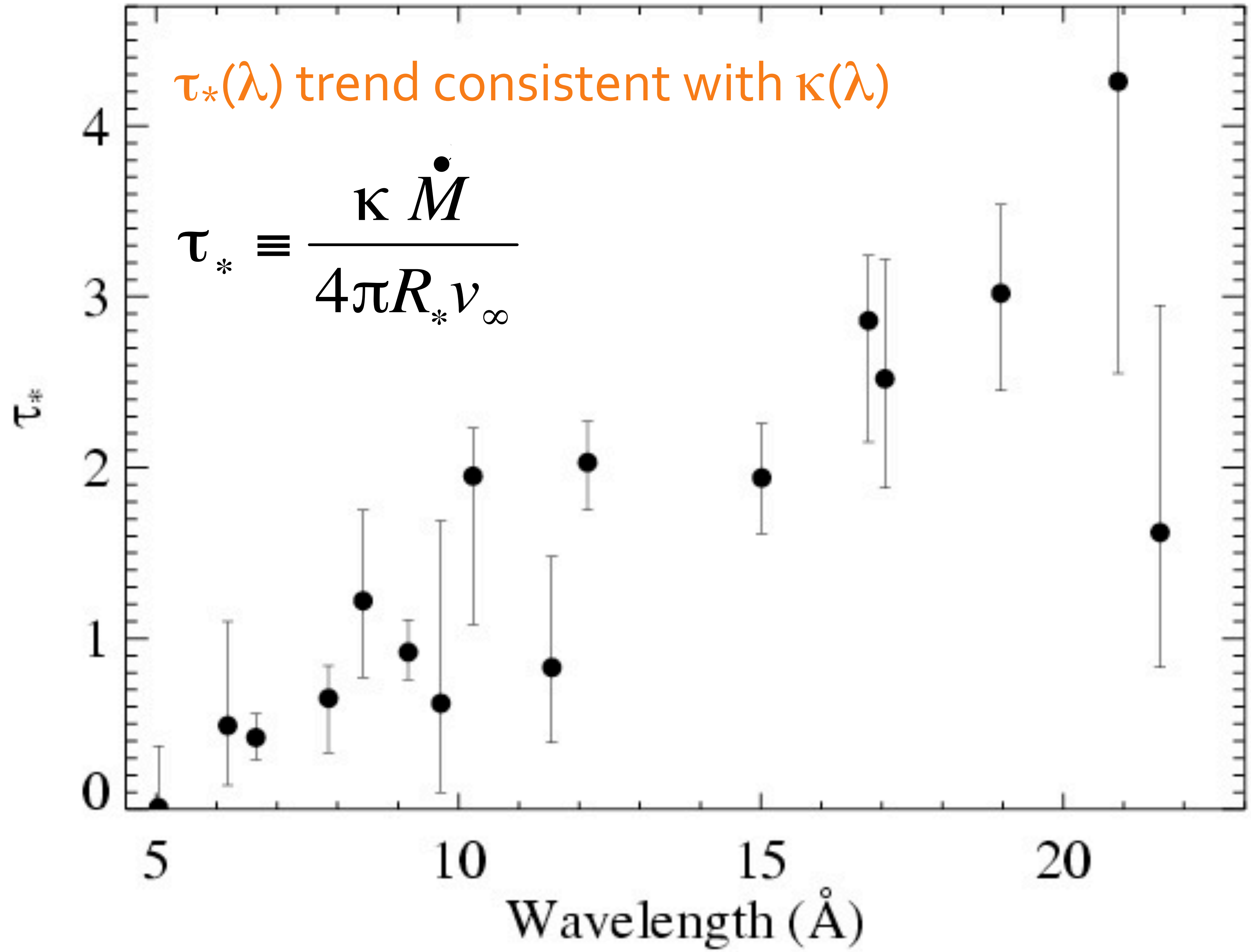

$$\tau_* \equiv \frac{\kappa \dot{M}}{4\pi R_* v_\infty}$$

$\dot{M}$ becomes the free parameter of the **fit** to the $\tau_*(\lambda)$ trend

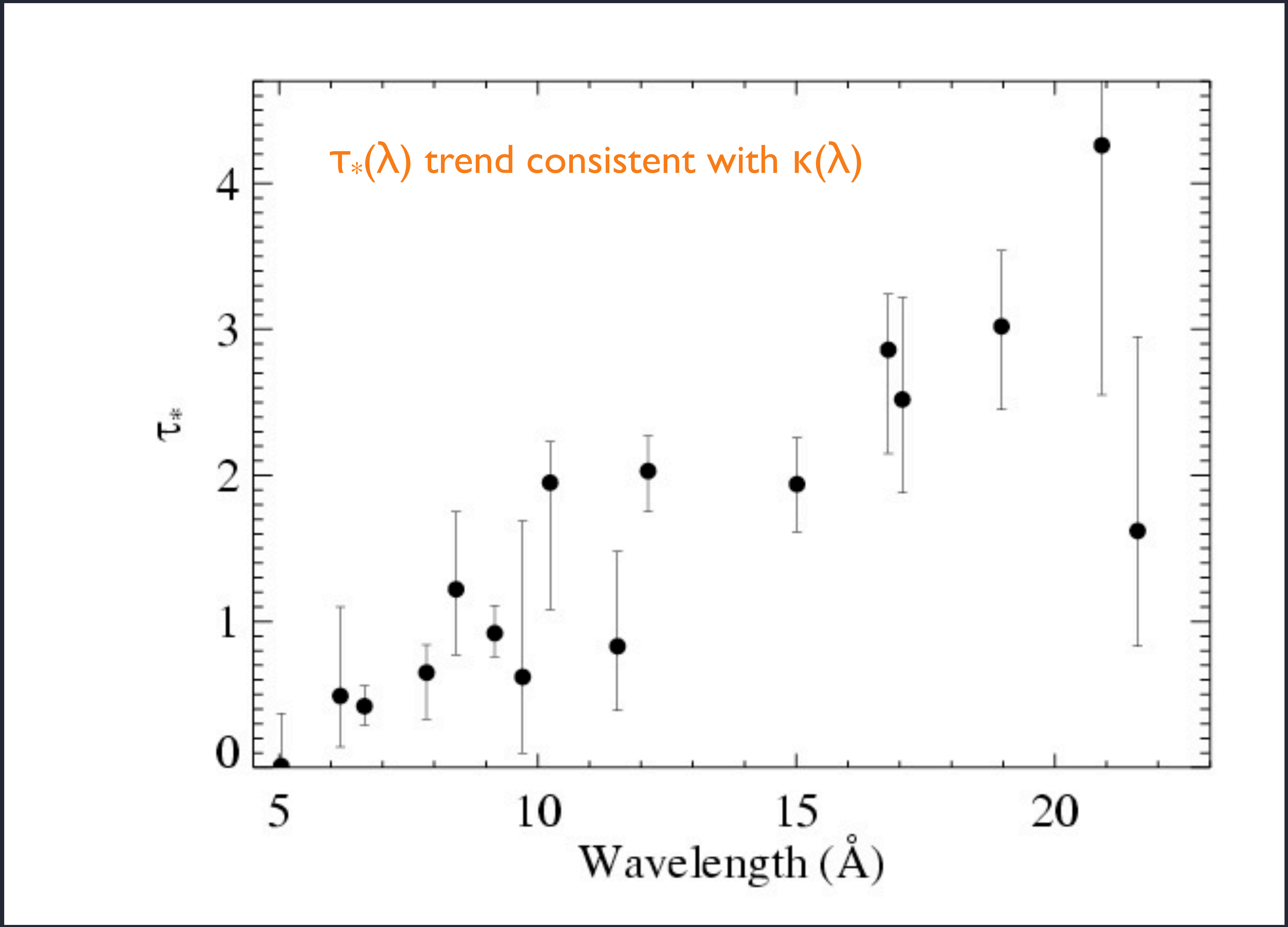

$$\tau_* \equiv \frac{\kappa \dot{M}}{4\pi R_* v_\infty}$$

$\dot{M}$ becomes the free parameter of the **fit** to the $\tau_*(\lambda)$ trend

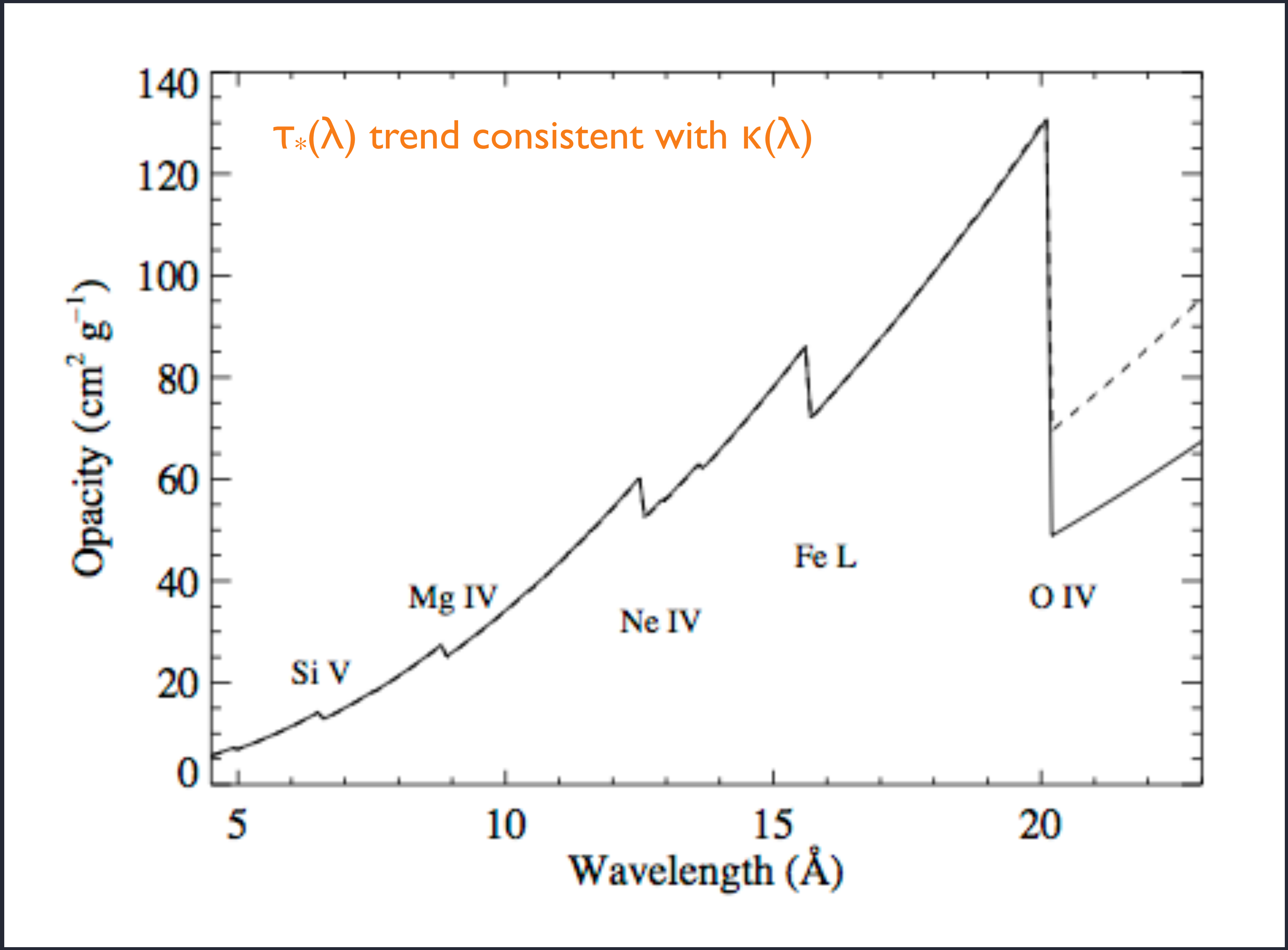

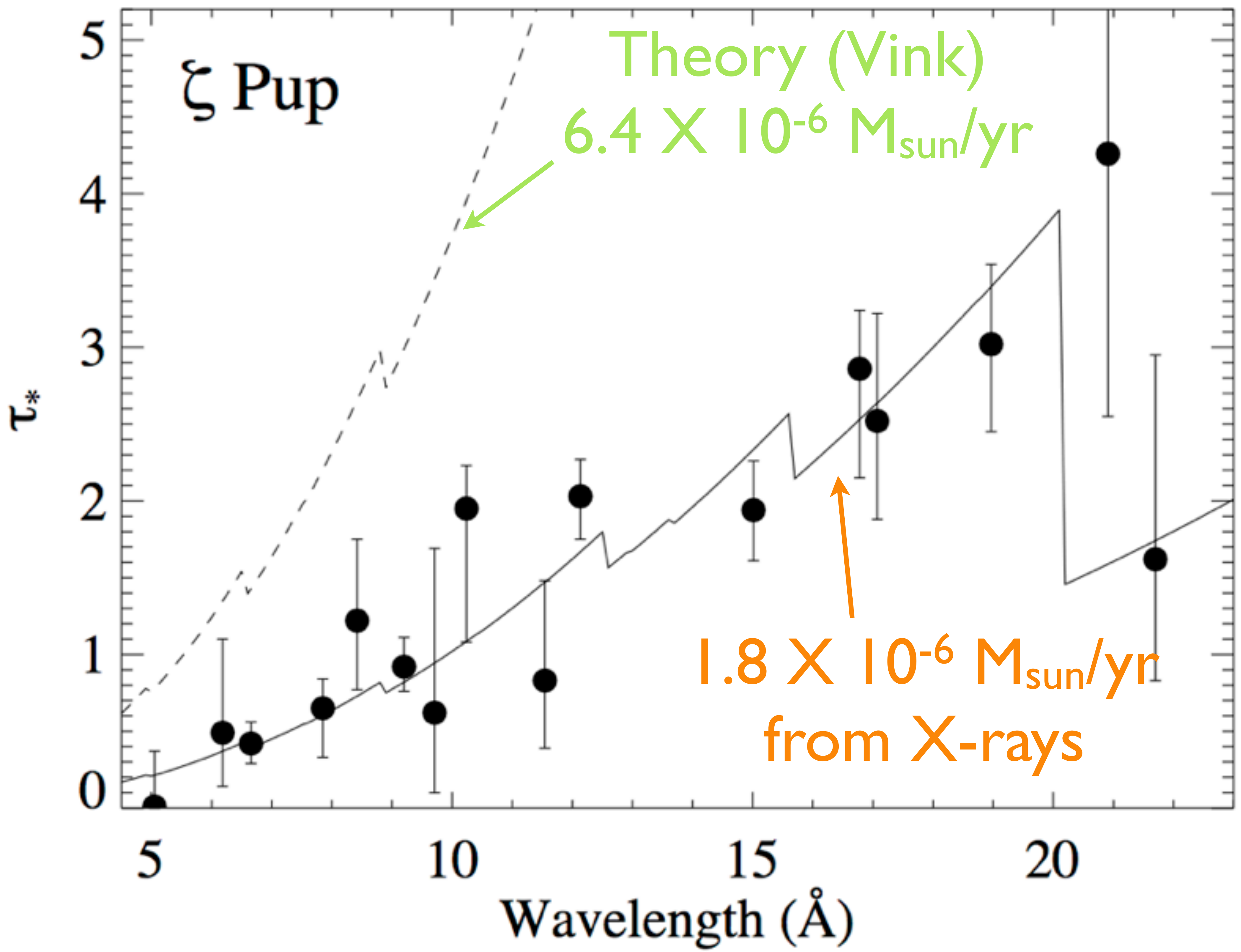

ζ Pup
Theory (Vink)
6.4 X 10-6 Msun/yr
1.8 X 10-6 Msun/yr
from X-rays
τ*
Wavelength (Å)
0
1
2
3
4
5
5
10
15
20

1.8 - 3.5 X 10^{-6} also from Hervé12,Bouret12, Najarro11, Oskinova07

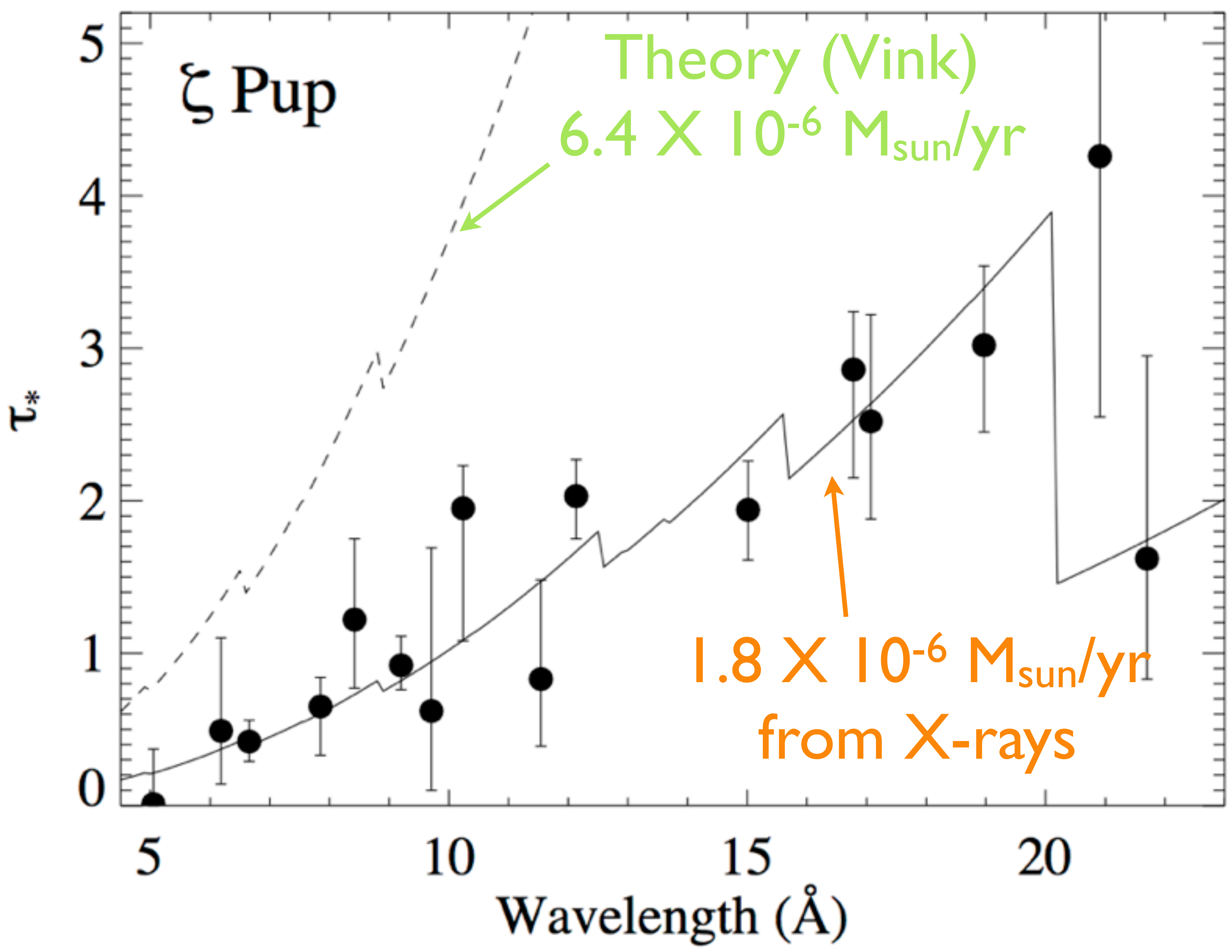

2-D radiation-hydro simulations

clumping

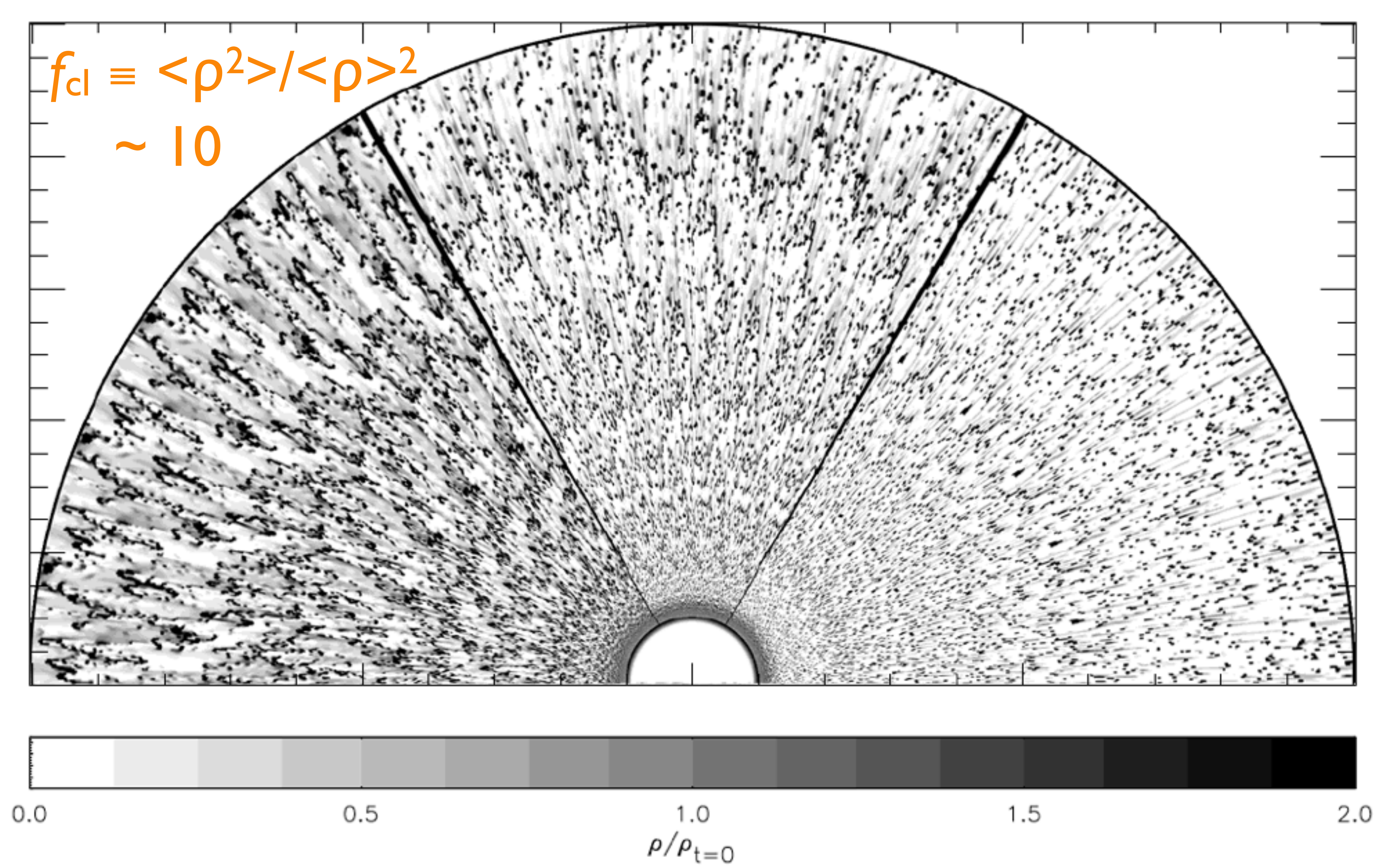

Dessart & Owocki 2003

2-D radiation-hydro simulations

clumping

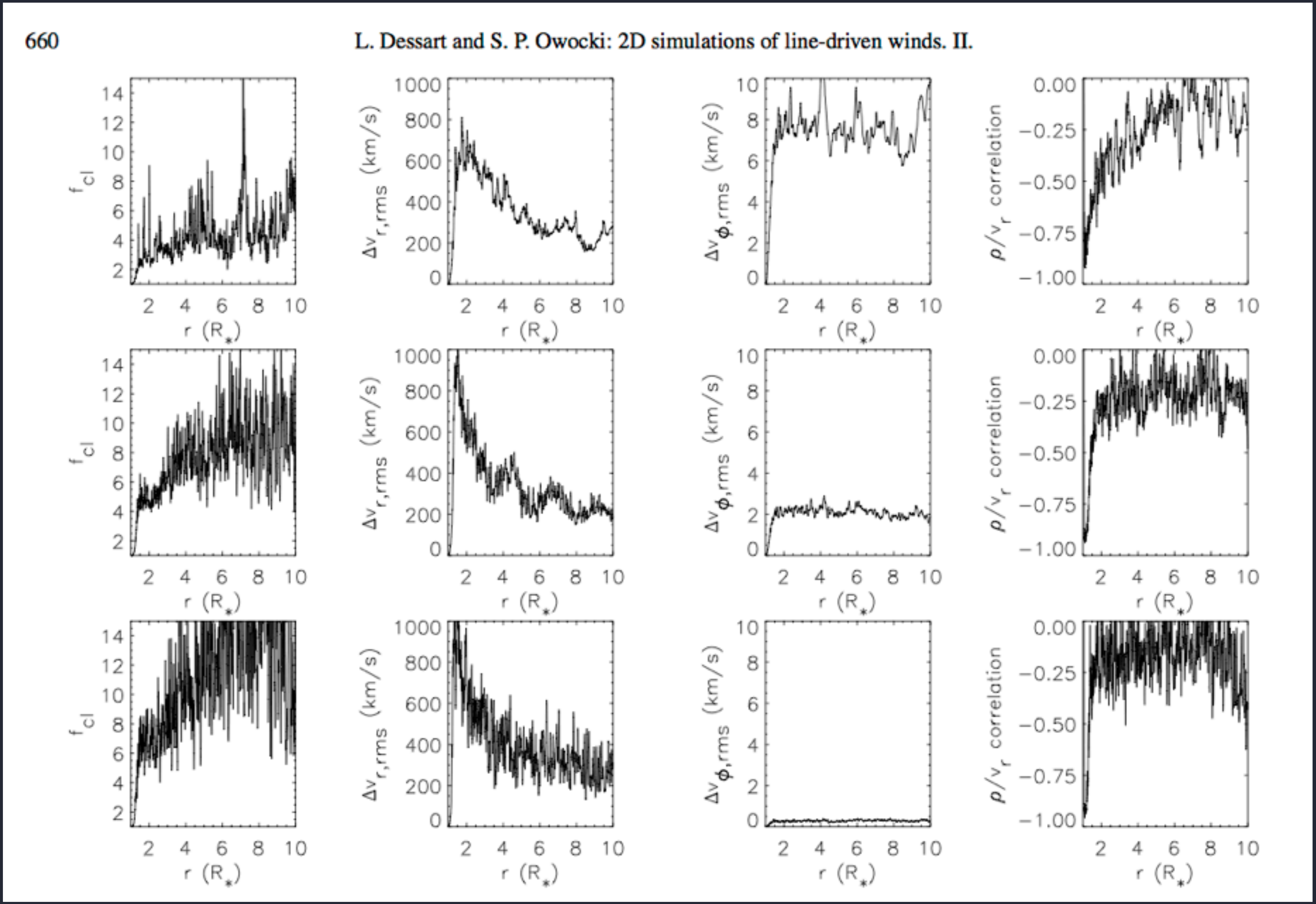

clumping factor ~10 to ~20 (Najarro et al. 2011)

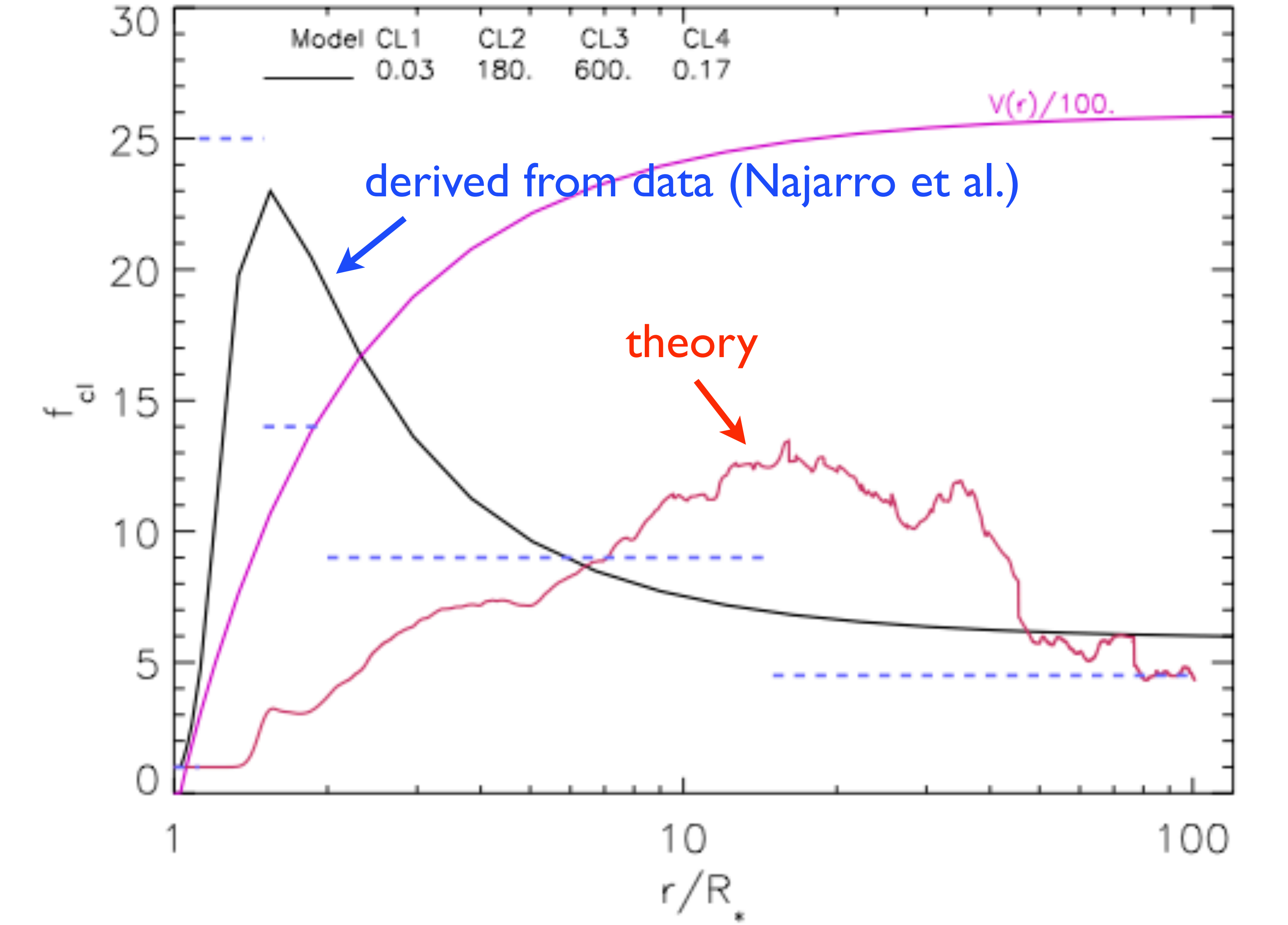

Fig. 18. Radial stratification of the clumping factor, $f_{\rm cl}$, for ζ Pup. Black solid: clumping law derived from our model fits. Red solid: Theoretical predictions by Runacres & Owocki (2002) from hydrodynamical models, with self-excited line driven instability. Dashed: Average clumping factors derived by Puls et al. (2006) assuming an outer wind matching the theoretical predictions. Magenta solid: run of the velocity field in units of 100 km s^{-1}. See also Sect. 4.

X-ray line profile based mass-loss rate: implications for clumping

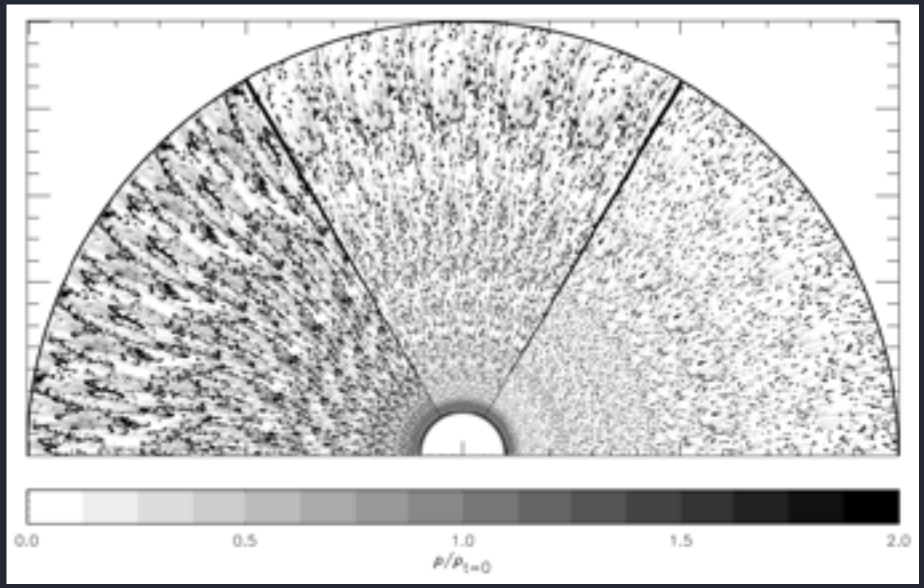

basic definition: $f_{cl} \equiv \langle\rho^2\rangle/\langle\rho\rangle^2$

clumping factor

ignoring clumping will cause you to *overestimate* the mass-loss rate

X-ray line profile based mass-loss rate: implications for clumping

basic definition: $f_{cl} \equiv \langle\rho^2\rangle/\langle\rho\rangle^2$

clumping factor

from (column) density diagnostic like $\tau_\star$ from X-ray profiles

from density-squared diagnostics like Hα, IR & radio free-free

X-ray line profile based mass-loss rate: implications for clumping

clumping factor $f_{cl} \equiv \langle \dot{M}^2 \rangle_{H\alpha} / \langle \dot{M} \rangle^2_{X\text{-ray}}$

$f_{cl} \sim 20$ for ζ Pup

but see Puls et al. 2006: radial variation of clumping factor

clumping factor ~10 to ~20 (Najarro et al. 2011)

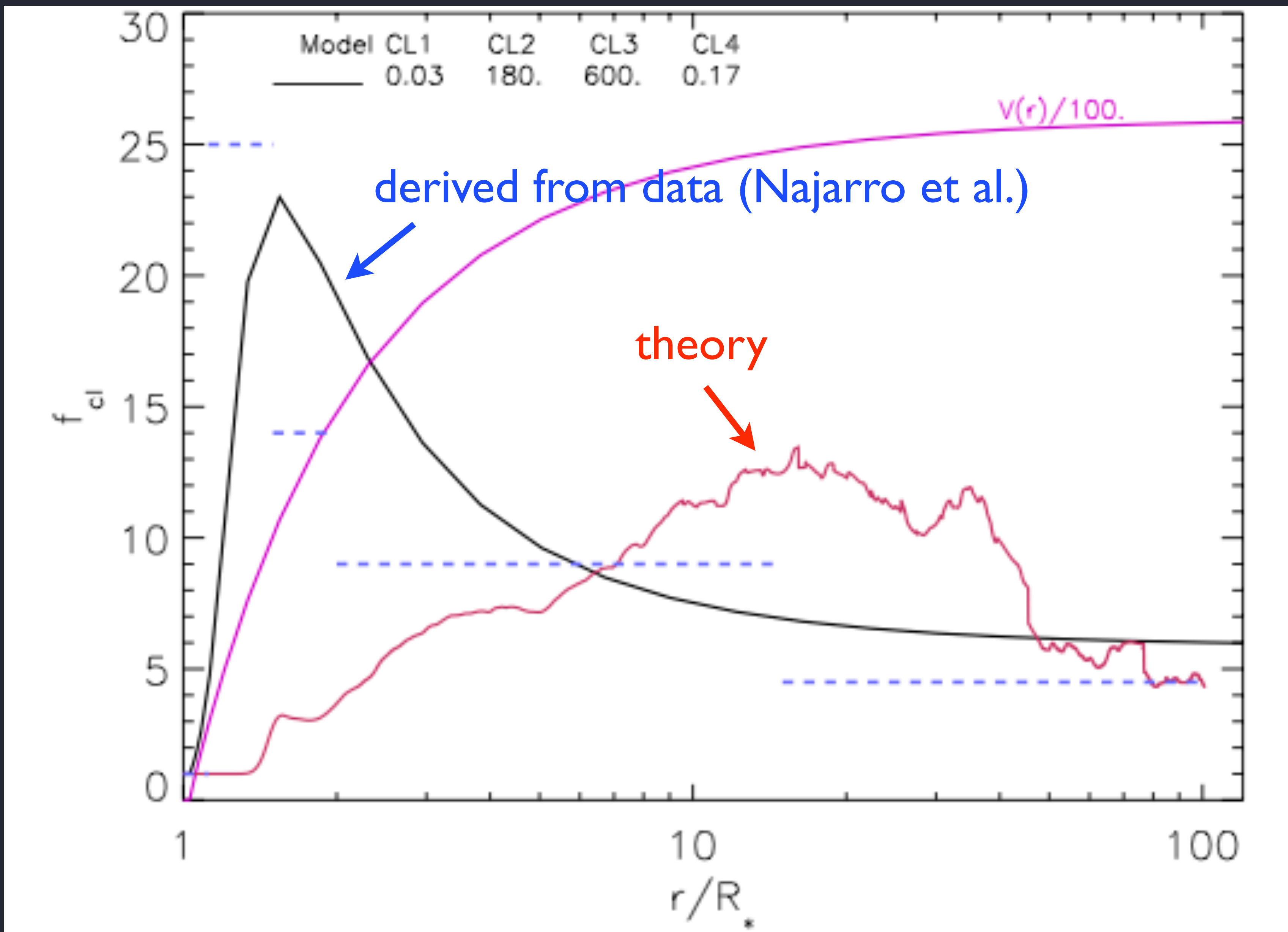

Fig. 18. Radial stratification of the clumping factor, $f_{\rm cl}$, for ζ Pup. Black solid: clumping law derived from our model fits. Red solid: Theoretical predictions by Runacres & Owocki (2002) from hydrodynamical models, with self-excited line driven instability. Dashed: Average clumping factors derived by Puls et al. (2006) assuming an outer wind matching the theoretical predictions. Magenta solid: run of the velocity field in units of 100 km s^{-1}. See also Sect. 4.

Latest numerical simulations of the LDI

include limb darkening and photospheric sound-wave perturbations

and generate more structure near the wind base

1842 *J. O. Sundqvist and S. P. Owocki*

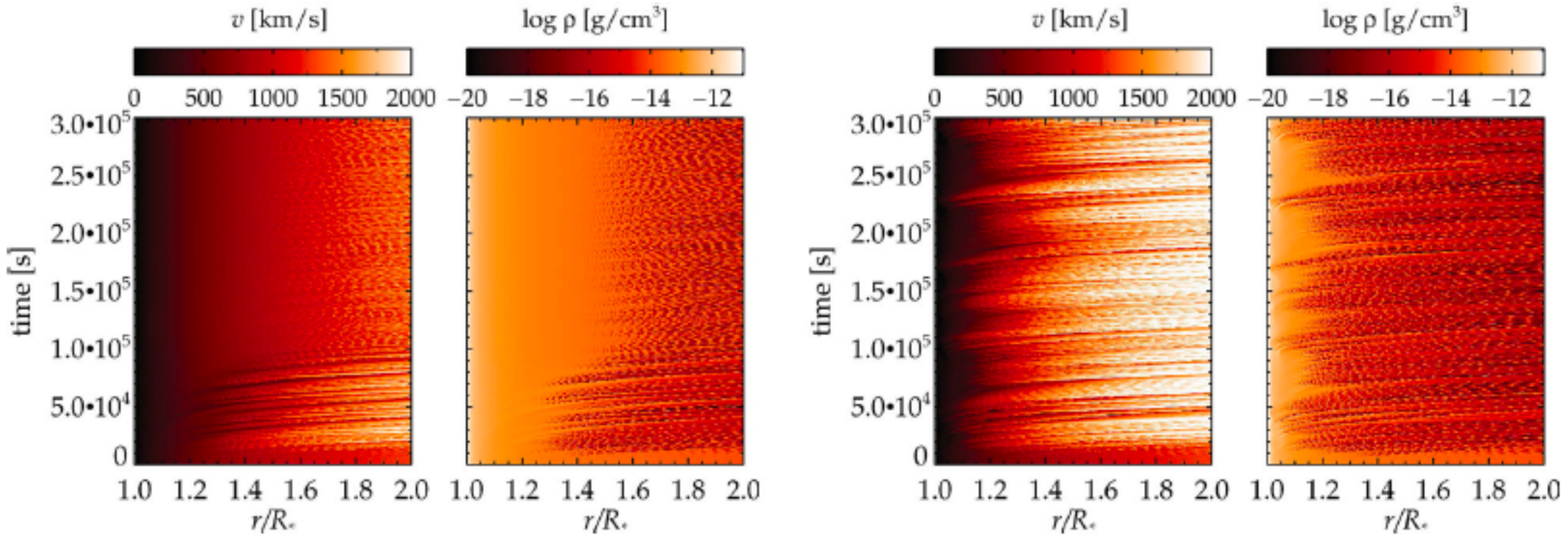

Figure 4. Inner wind time evolutions of a simulation without limb darkening and photospheric perturbations (left) and one including both effects (right).

HD 93129A

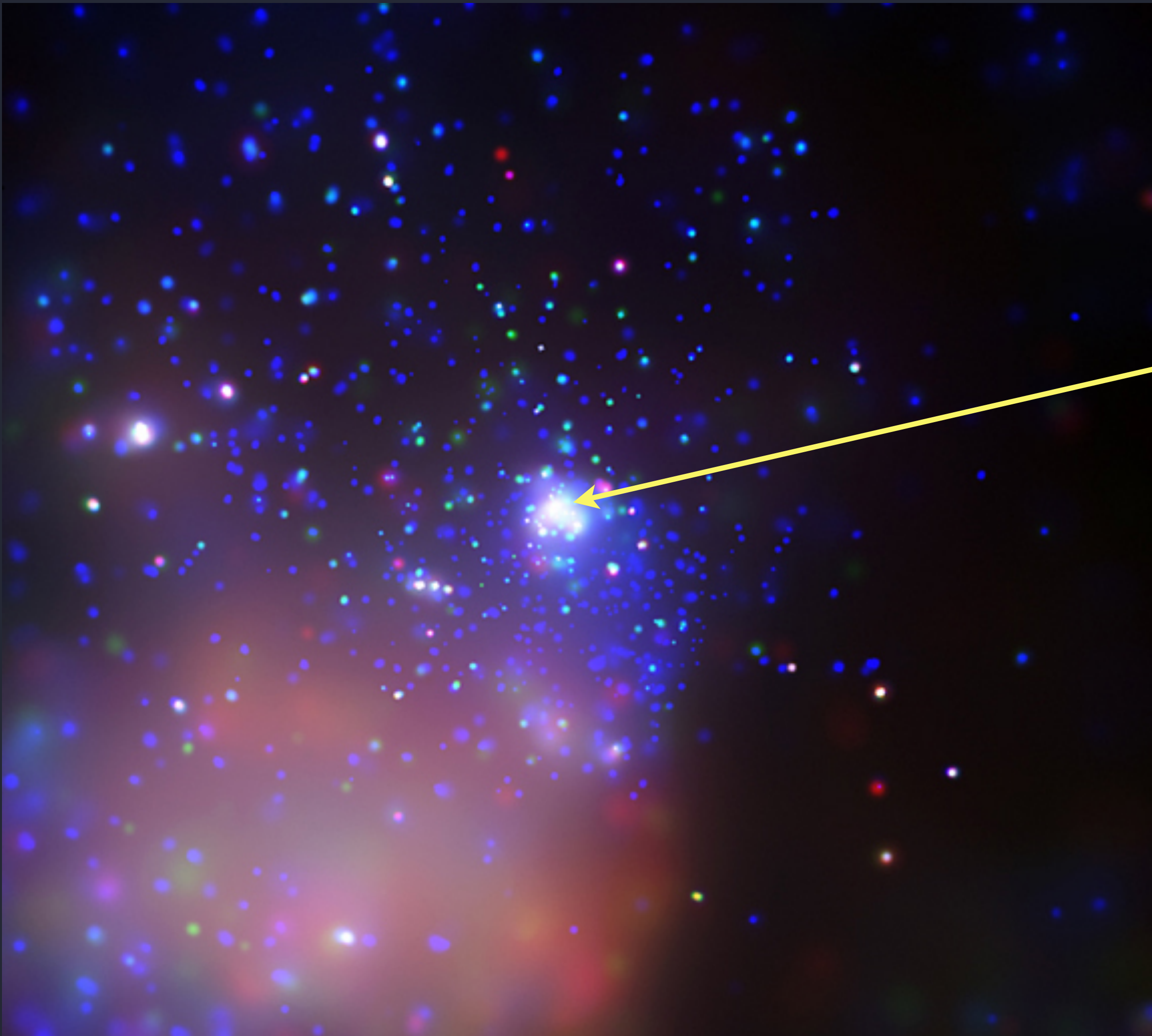

Tr 14: *Chandra*

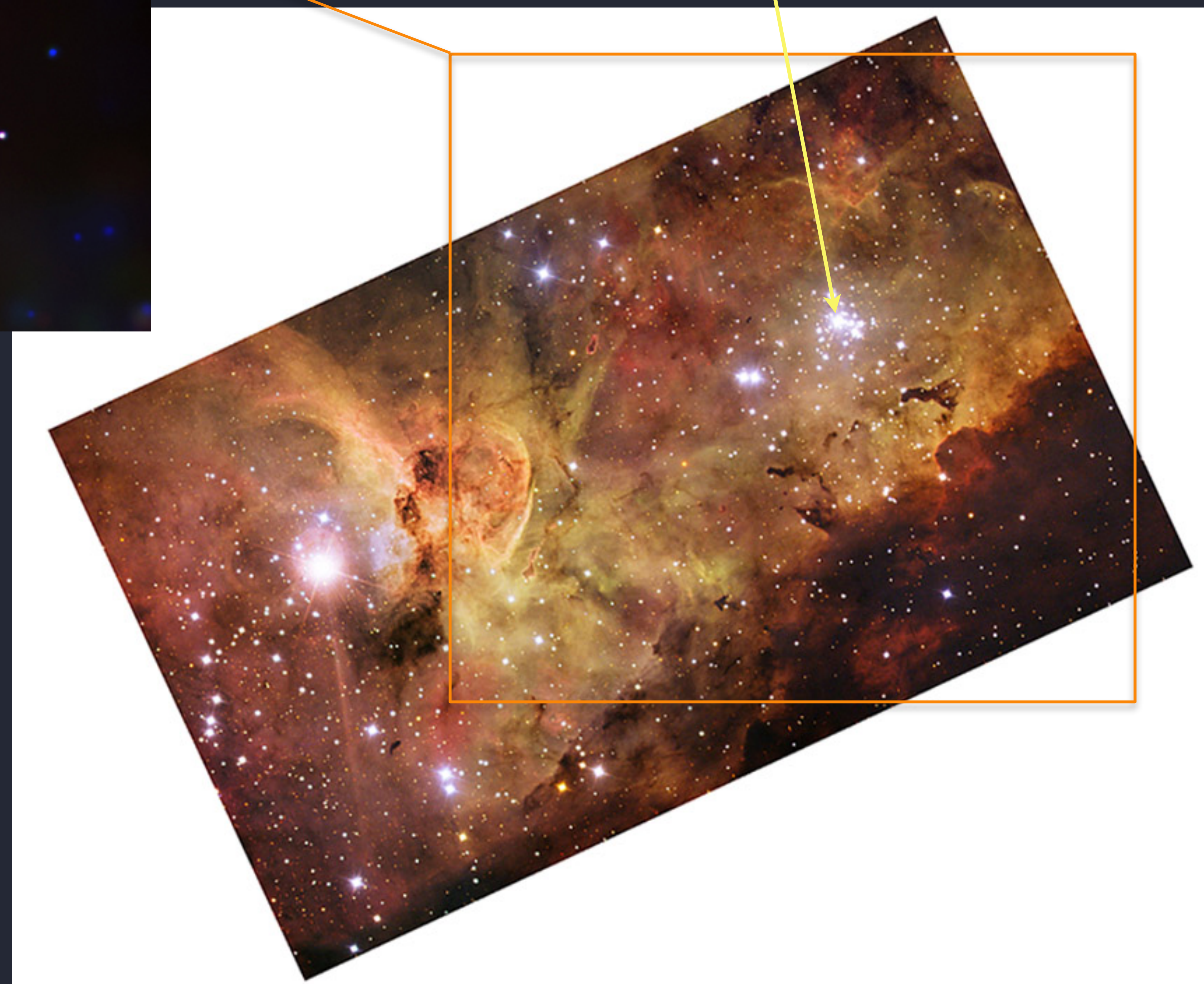

Carina: ESO

Chandra grating spectra of HD 93129A

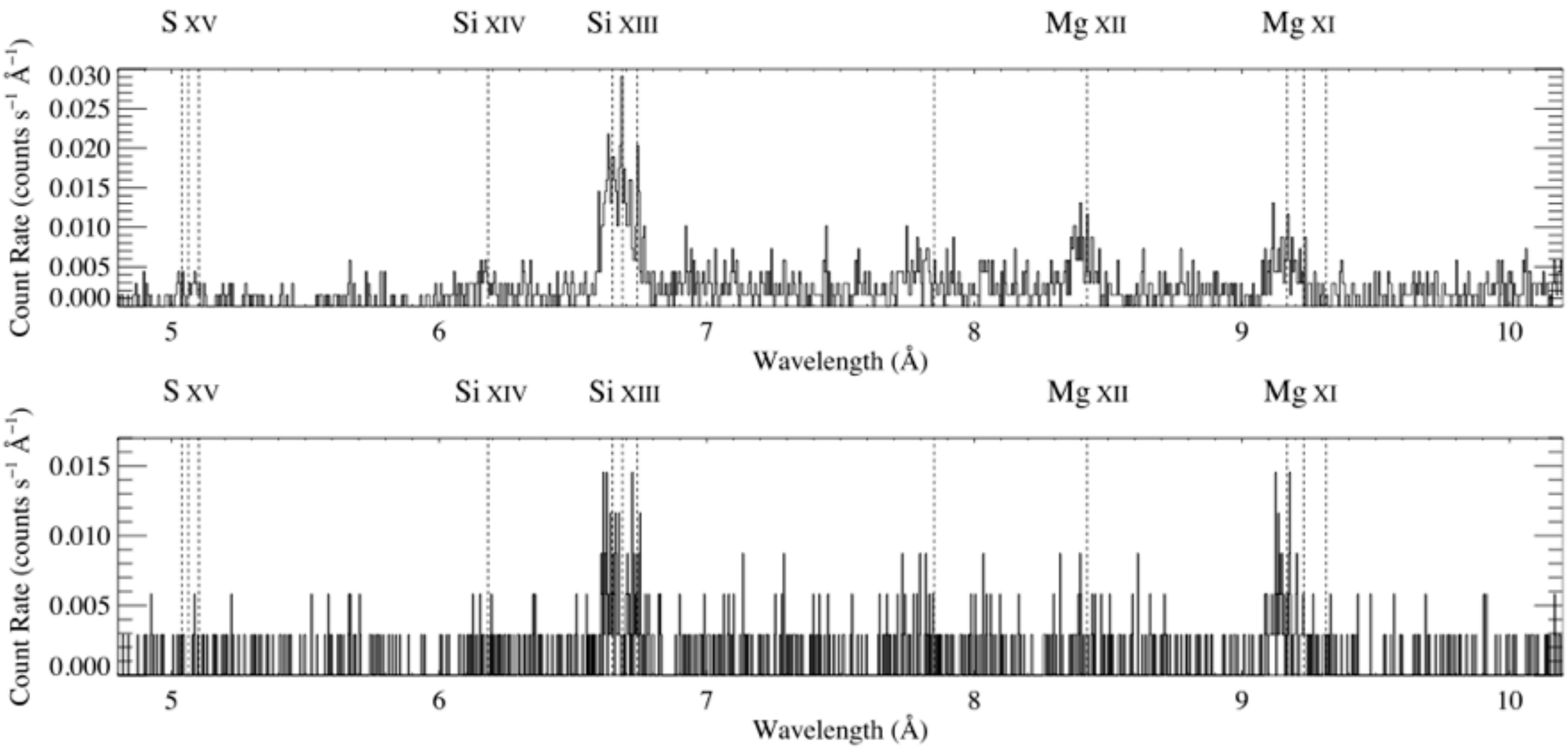

Figure 3. The extracted MEG (top) and HEG (bottom) spectra from the seven coadded pointings. Note the different y-axis scales on the two figures. The wavelengths of lines expected to be present in normal O star *Chandra* spectra are indicated by the vertical dotted lines.

Strong stellar wind: traditional diagnostics

UV

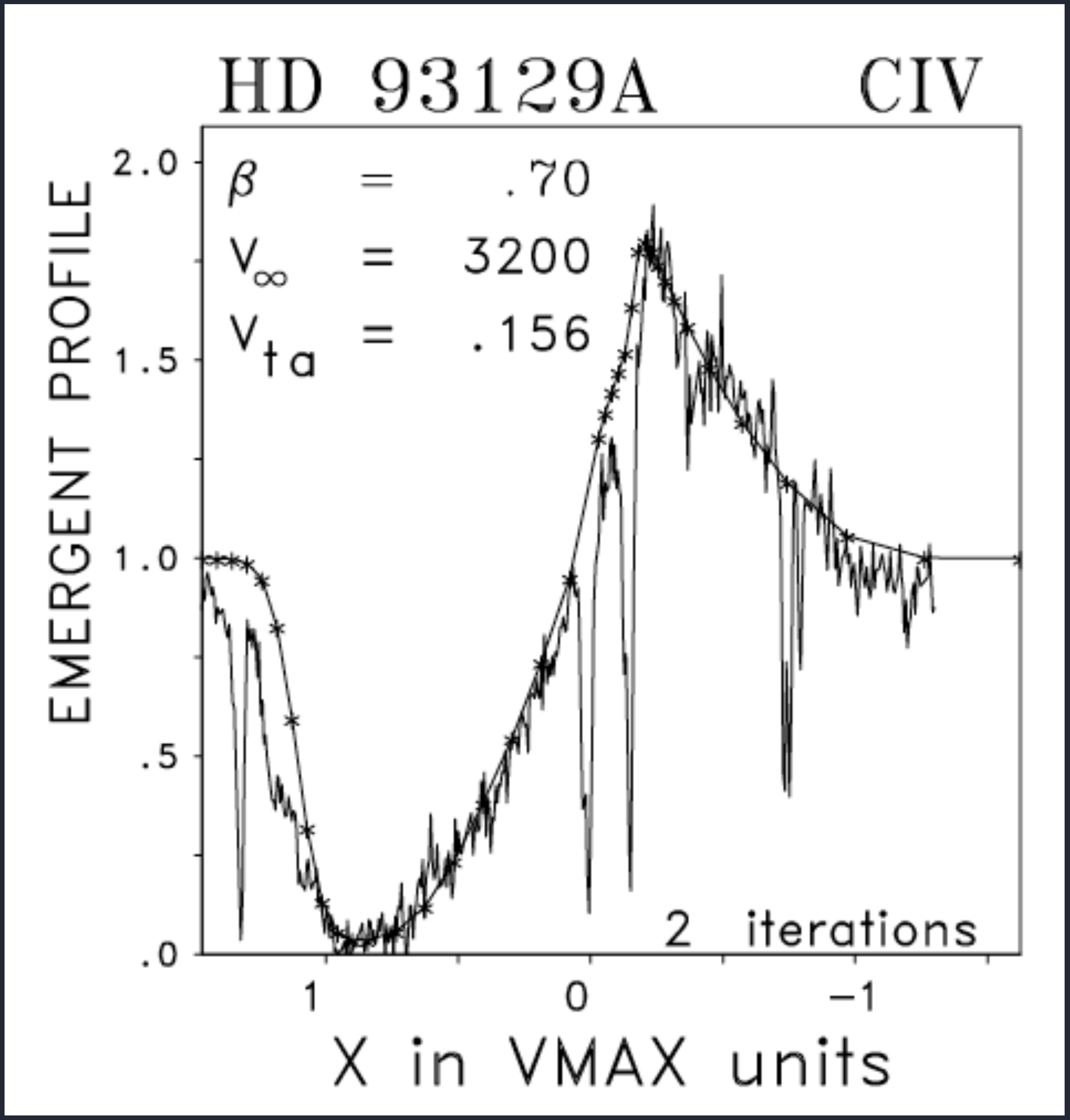

Taresch et al. (1997)

$\dot{M} = 2 \times 10^{-5}\ M_{sun}/yr$

$v_\infty = 3200$ km/s

Hα

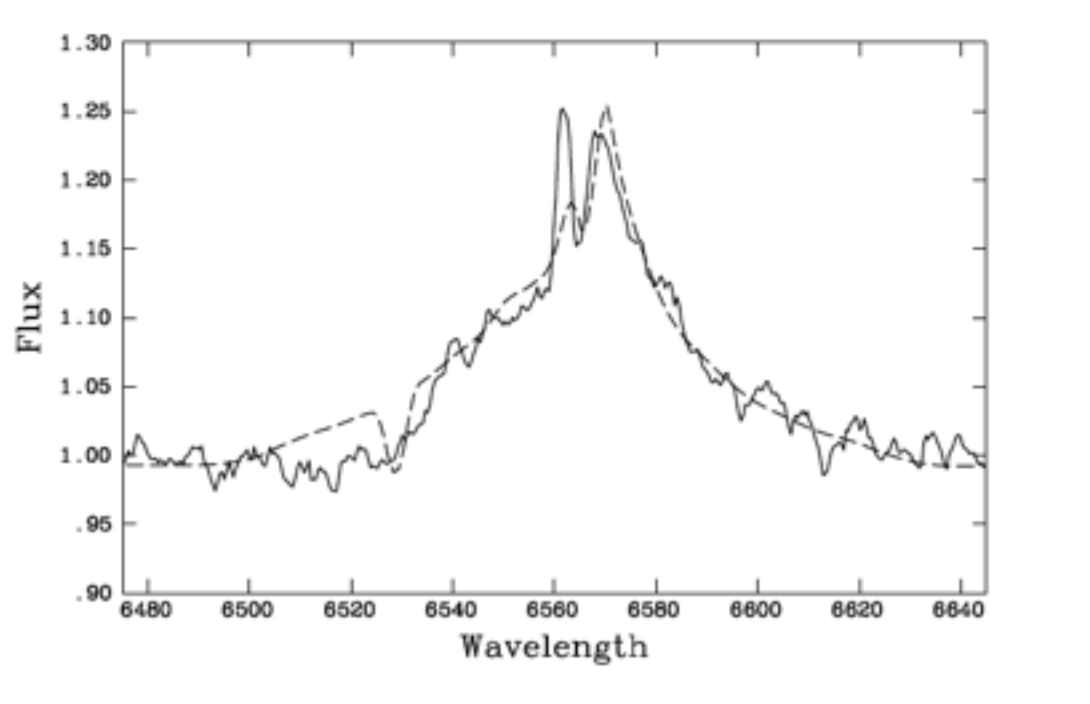

Fig. 13. Observed Hα profile (**solid**) compared with the calculation assuming a mass loss of $18\times10^{-6}\ M_\odot$/yr (dashed). Note that the blue narrow emission peak originates from the H II-region emission.

HD 93129A

Mg XII Lyman-alpha

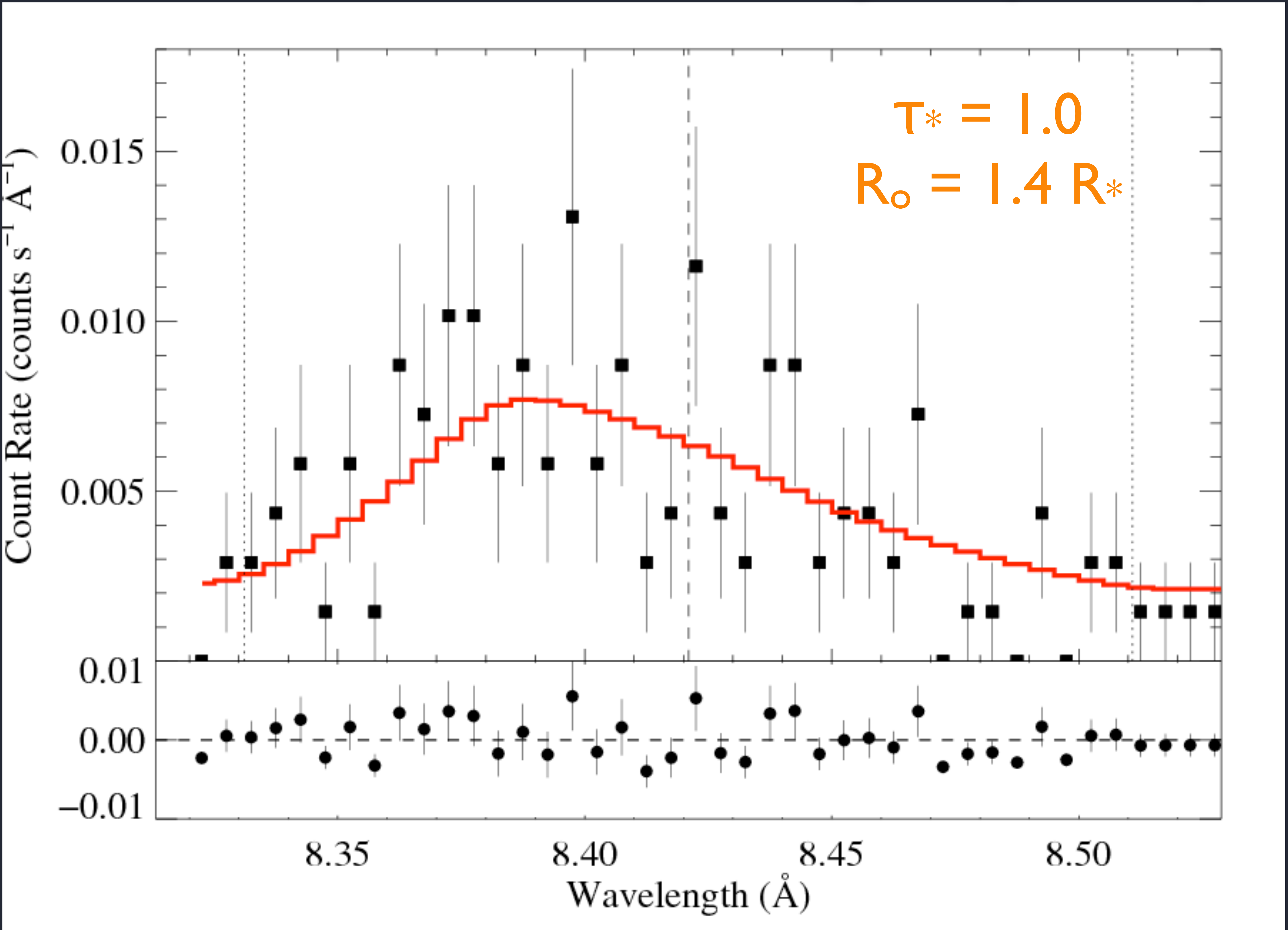

R_o = onset radius of X-ray emission

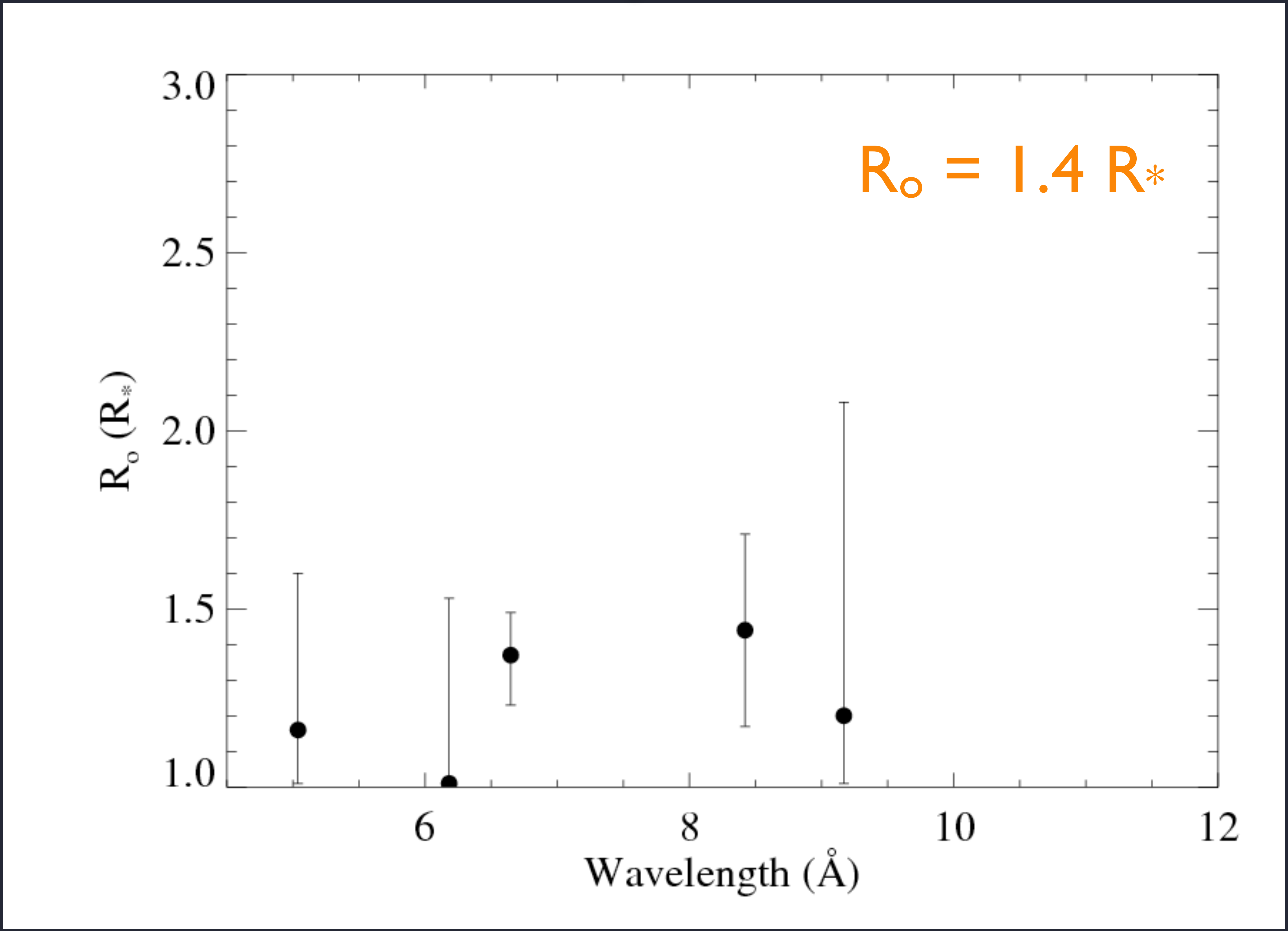

HD 93129A

τ* from five emission lines

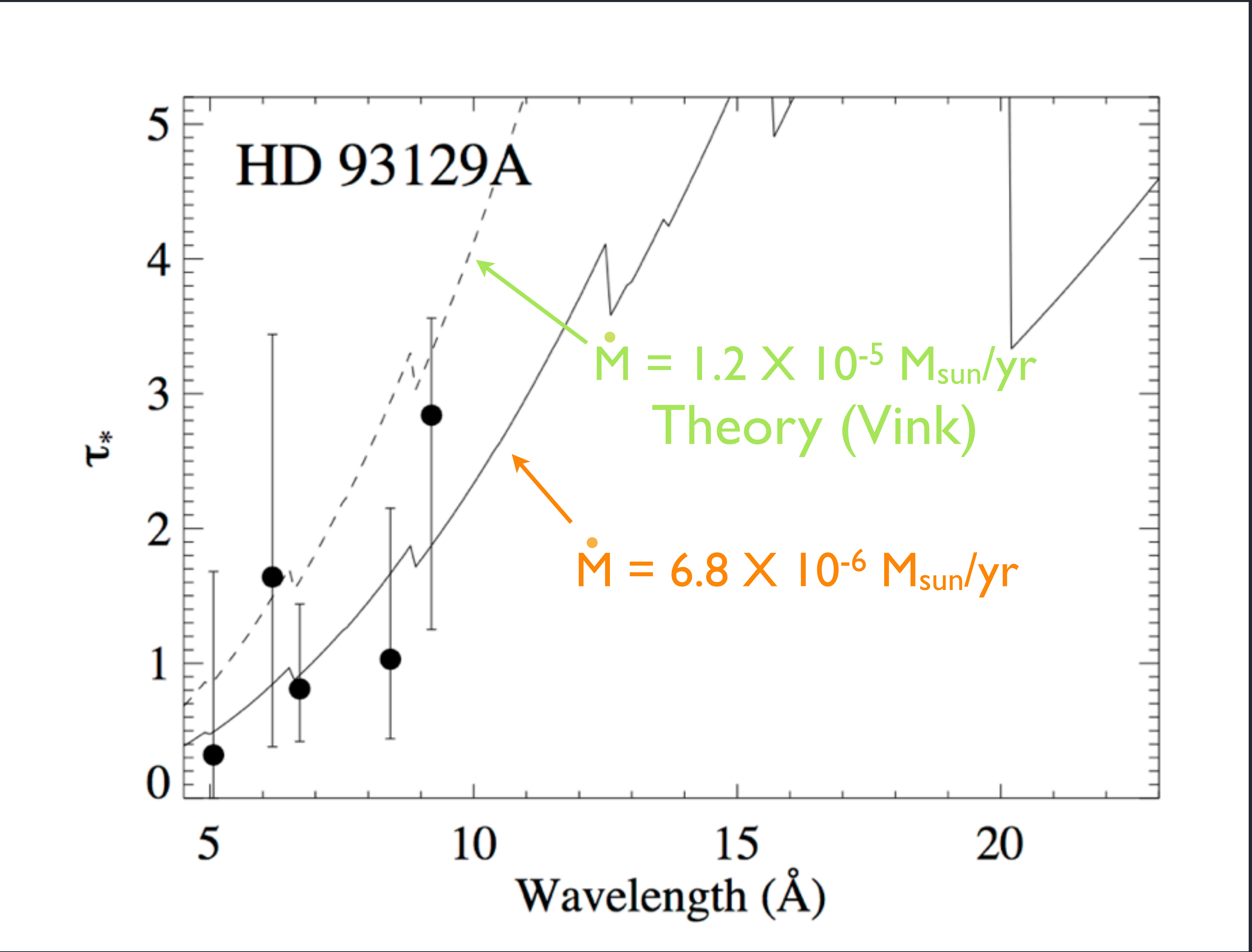

HD 93129A τ* from Chandra CCD spectrum

using *windtabs* wind absorption model (Leutenegger et al. 2010)

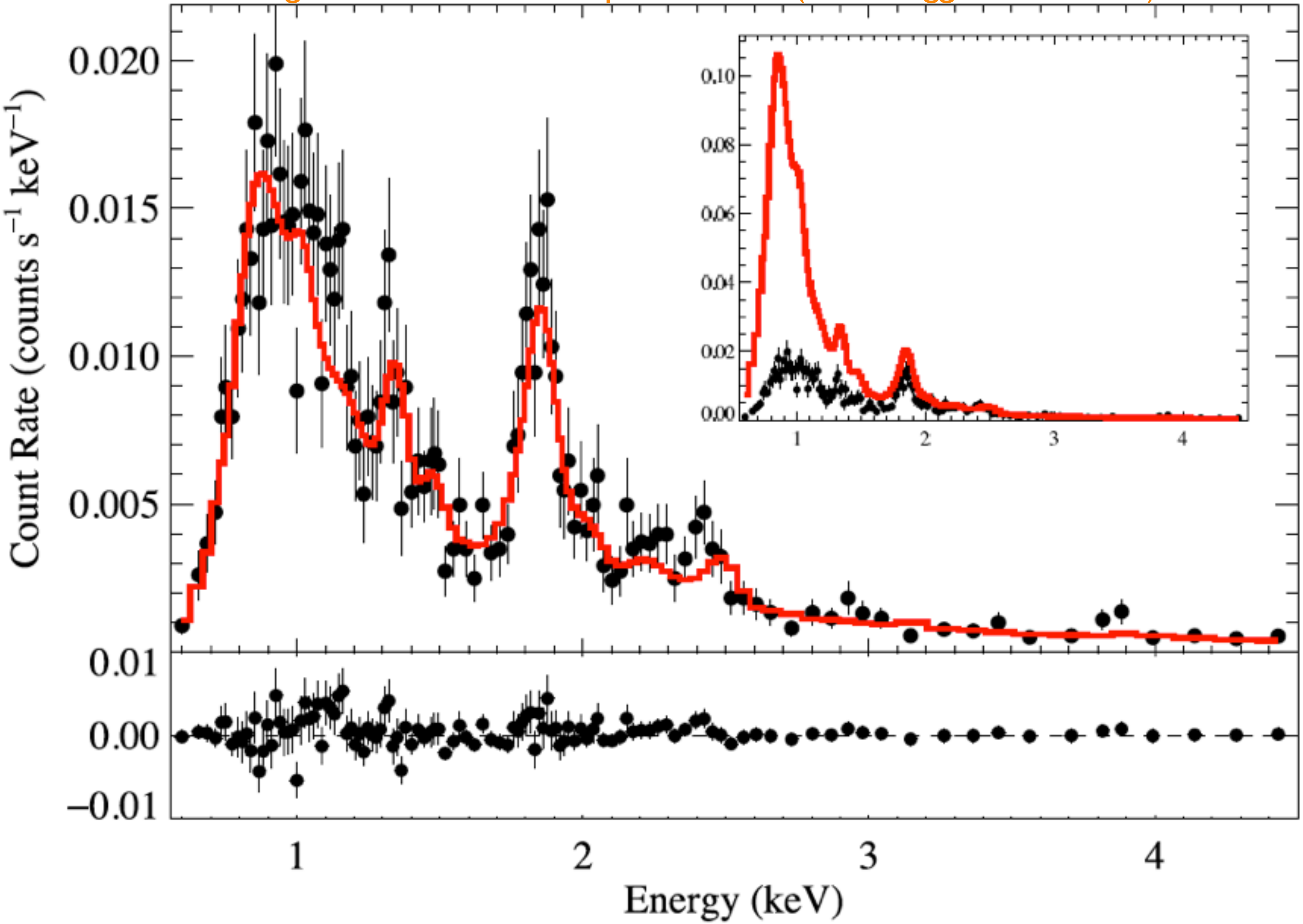

Lower mass-loss rate: consistent with Hα?

Lower mass-loss rate: consistent with Hα?

Yes! With clumping factor of f_{cl} = 12

$\dot{M} = 7 \times 10^{-6}\ M_{sun}/yr$

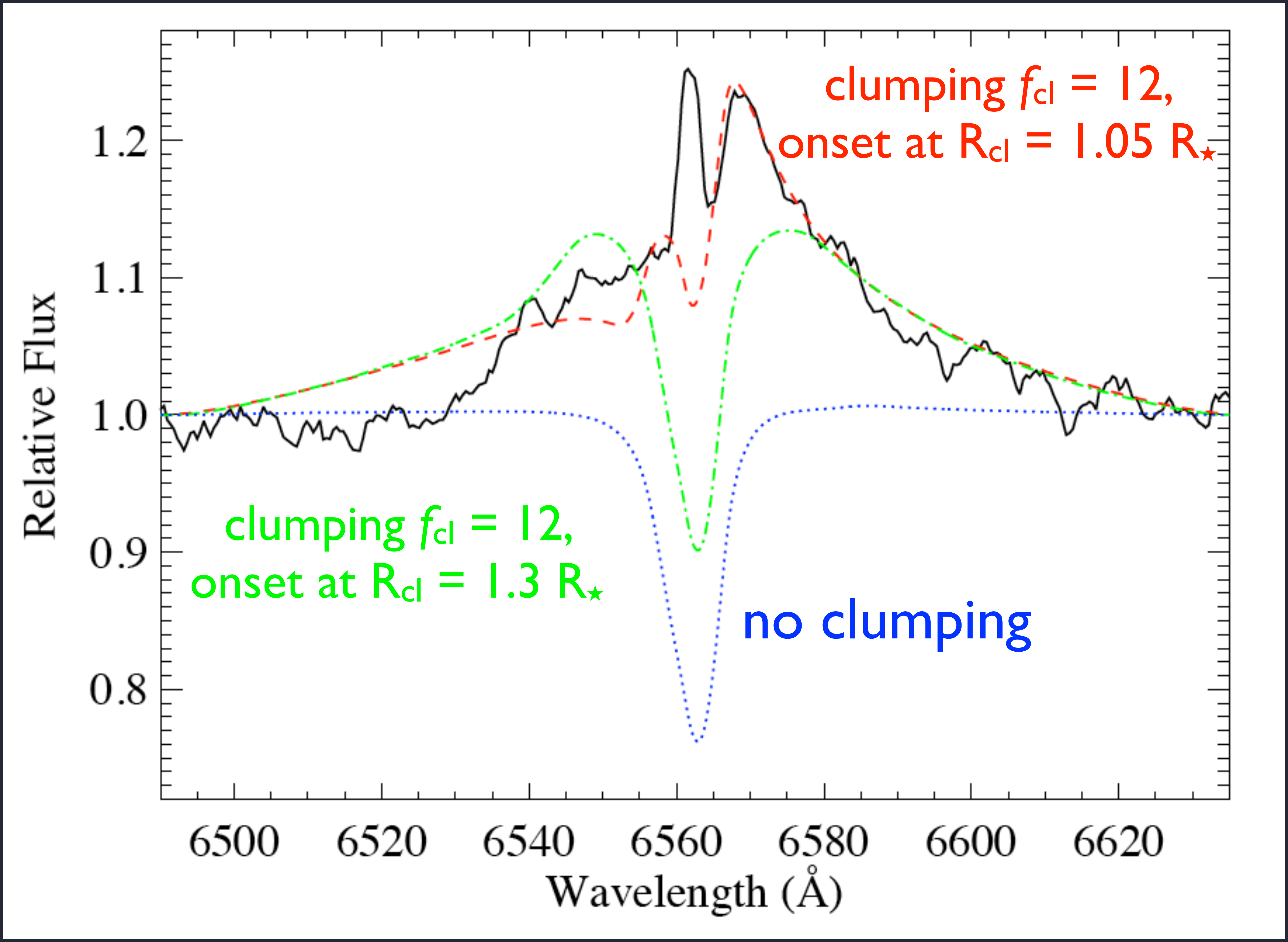

Extension of X-ray profile mass-loss rate diagnostic to other stars

lower mass-loss rates than theory predicts
with clumping factors typically of $f_{cl} \sim 20$

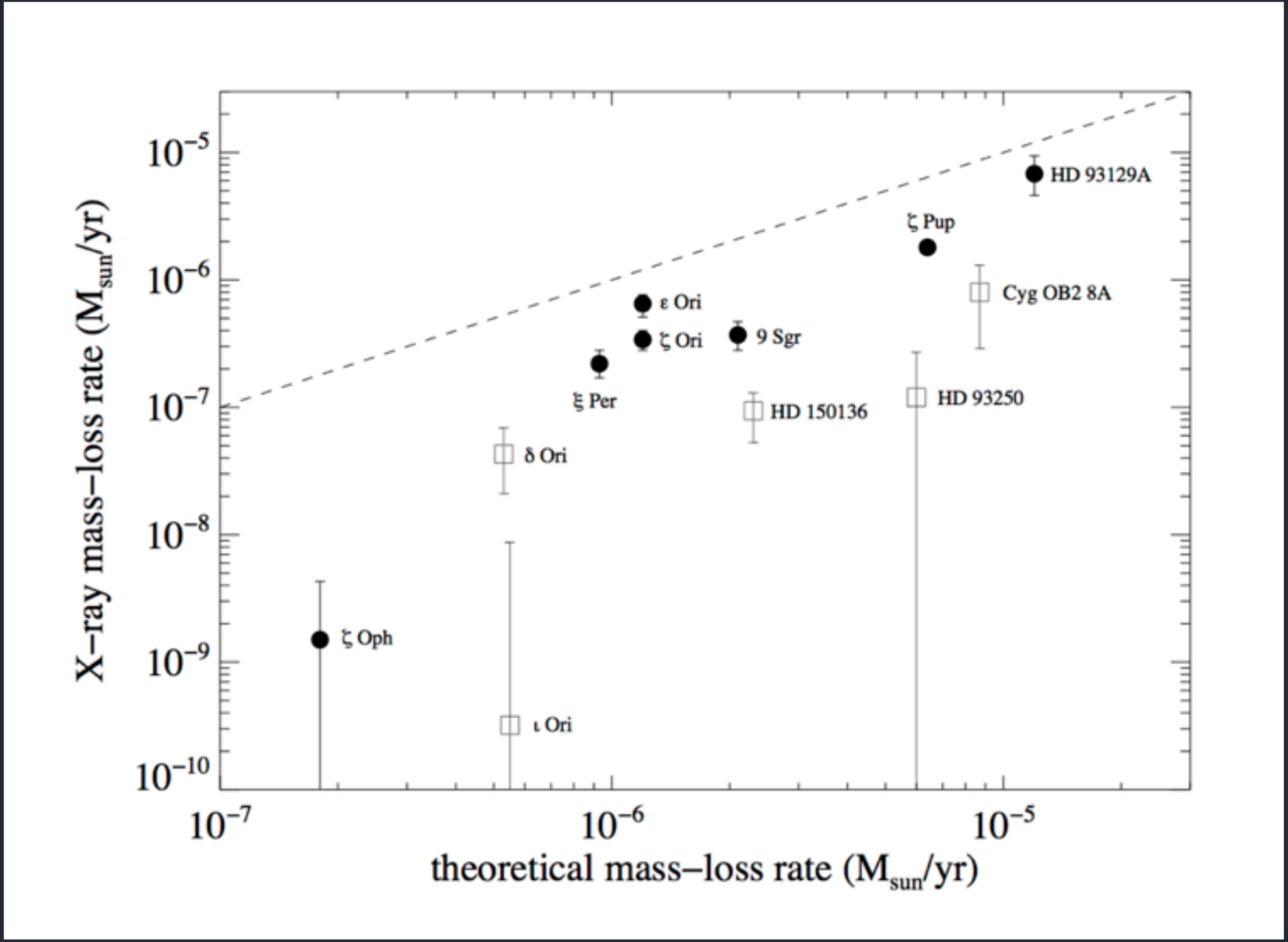

X-ray mass-loss rates: a few times less than theoretical predictions

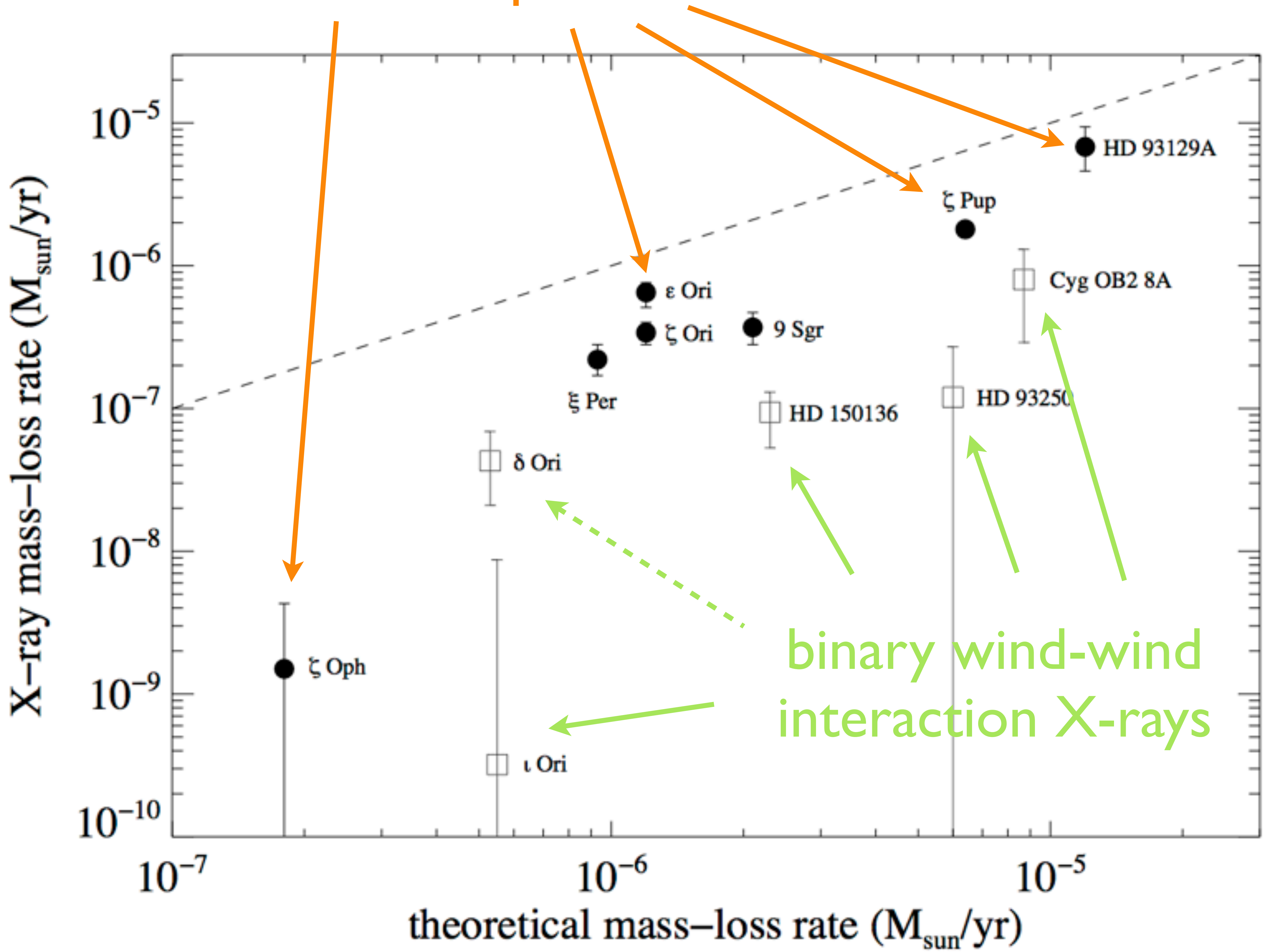

Conclusions

Shocked wind plasma distributed throughout wind, above $R_o \sim 1.5$ R

O supergiant mass-loss rates: a few lower than theoretical predictions

Consistent with Hα, IR/radio if $f_{cl} \sim 15 - 25$

ζ Oph mass-loss rate 100X lower than theory

Quite a few O + O binaries without obvious CWB X-ray emission have profiles that differ from effectively single O stars